1992

Organometallic chemical vapor deposition of copper oxide thin films

Yu-Neng Chang
Iowa State University

Order Number 9234794

Organometallic chemical vapor deposition of copper oxide thin films

Chang, Yu-Neng, Ph.D.

Iowa State University, 1992

U·M·I
300 N. Zeeb Rd.
Ann Arbor, MI 48106

Organometallic chemical vapor deposition of copper oxide thin films

by

Yu-Neng Chang

A Dissertation Submitted to the

Graduate Faculty in Partial Fulfillment of the

Requirements for the Degree of

DOCTOR OF PHILOSOPHY

Department: Chemical Engineering
Major: Chemical Engineering

Approved:

Signature was redacted for privacy.

In Charge of Major Work

Signature was redacted for privacy.

For the Major Department

Signature was redacted for privacy.

For the Graduate College

Iowa State University
Ames, Iowa
1992

TABLE OF CONTENTS

GENERAL INTRODUCTION

Thin solid film fabrication process is one of the most important technical advances contributing to human civilization in this century. Due to their specific material properties, thin films made from semiconductors, insulators, and metals are widely used in modern process industries, electronic devices, optical wave guides, mechanical protection layers, and military communication and detection devices [1]. By definition, thin films are two dimensional materials with film thicknesses less than 1 μm [2]. Early thin film preparation methods include: electron beam evaporation, sputtering, and chemical vapor deposition (CVD) [3]. These techniques have the disadvantages of using high temperatures (above 700^{o}C for CVD using halide precursors) or requiring a vacuum environment.

In 1968, Manasevit first used volatile organometallic compounds as metal precursors and deposited high quality GaAs, GaAlP, and several other III-V compound semiconductor thin films at reduced temperature in an atmospheric pressure CVD reactor [4]. This process vaporizes the group III and group V containing complexes as precursors, uses an inert gas to carry the reactant vapor to the heated substrate surface, activates and reacts precursor molecules over the surface, and deposits thin films as the desired product. Since then, numerous researchers have studied this novel thin film deposition technique, metal-organic chemical vapor deposition (MOCVD) which

is also known as organometallic chemical vapor deposition (OMCVD) [5]. MOCVD processes have several commercial advantages such as producing films with high quality, low operating cost, and high throughput. MOCVD is also particularly competitive for depositing uniform layers on substrates with μm-scale three dimensional geometries. In the 1990s, this capacity is particularly valuable in developing the Ultra Large Scale Integrated Circuit (ULSI) and micromechanical device processes.

However, early MOCVD research was focused only on process development. Without comprehensive understanding of the deposition mechansim, even till the early 1980s, questions related to film purity and interface abruptness still troubled the MOCVD community [6]. In addition to this, there were arguments about whether molecular beam epitaxy (MBE) or organometallic vapor phase epitaxy (OMVPE, a specific type of MOCVD which grows single crystal material) would be the dominant technique for producing compound semiconductor materials for commercial device processing [7]. Stringfellow [8] stated it well in a recent review article:

"It seems we have regarded OMVPE (MOCVD) as an inherently simple technique. Rapid progress was made by putting together a simple apparatus and buying whatever precursors were available from chemical catalogues.....Our primitive understanding of the fundamental aspects of OMVPE was based on the idea that the process basically consisted of pyrolysis of the individual precursors, producing the desired elements, followed by surface processes resulting high-quality semiconductor materials. The approach to optimizing the process was mainly empirical."

More recently, mainly in the past five years, MOCVD has gradually moved from the early, empirical stage to a more mature period of development based on the fundamental understanding of the growth process. Experiments, specifically spectroscopic

methods, designed to probe the growth process have begun to reveal the details of the often complex chemical reactions [8]. Technical obstacles such as graded interface and carbon contamination were eliminated; modern MOCVD process has produced the highest purity InP and GaAs grown by any technique [8]. During this progess, it was realized that the reaction kinetics are strongly dependent on the precursor materials resulting in complicated reaction chemistry; often these precursors are recently developed organic chelate coordinated metal complexes and have not been studied extensively.

Recently, instead of depositing conventional III-V compounds, there are several workers examining the feasibility of using MOCVD to prepare novel oxide films, such as $YBa_2Cu_3O_7$, $BaTiO_3$, and copper oxides [9]. It appears that the deposition process of these novel oxides required the synthesis of new metal precursors, and the deposition reaction is quite different from previous III-V MOCVD processes. For example, the most commonly used copper precursor in superconducting ceramic and copper oxide MOCVD processes, $Cu(acac)_2$, exist as a solid at room temperature [10], while most Ga and In precursors are liquid. In the $Cu(acac)_2$ molecule, copper is coordinated with acac ligands with Cu-O bonding [10], whereas in most group III precursors, the metal atom is chelated by metal-carbon bonding. Also, from the process aspect, oxygen or water is no longer the disaster in III-V MOCVD but a possible co-reactant in oxide MOCVD. It seems that the present stage of oxide MOCVD is the same as the one for III-V MOCVD in the 1970s; there are too many empirical results waiting for some more fundamental investigations to interpret these empirical findings. In this research, a novel oxide MOCVD process was first studied empirically, with the impact of MOCVD processing parameters on film composition

being examined. Then, kinetic experiments were performed to reveal the reaction mechanism in this deposition process. Copper oxides (Cu_2O and CuO), due to their potential applications in opto-electronic devices [11], has been chosen as the material to deposit. $Cu(acac)_2$ is selected as the copper precursor for its wide use in oxide MOCVD and practical value.

This dissertation presents research completed with the intention of adding to the knowledge described above. An atmospheric pressure copper oxide MOCVD process was developed. Specifically, by utilizing modern molecular vibrational or electronic spectroscopic methods and X-ray diffraction techniques, the compositions of MOCVD films were revealed. The work then focuses on the role of $Cu(acac)_2$ precursor decomposition in the MOCVD process. FTIR analyzes the gas phase products from the MOCVD reactor. DSC compares the pyrolysis behaviors of $Cu(acac)_2$ in an inert and an oxidative environment.

The following sections of this dissertation will present a detailed review of literature concerning this work and research completed in this area.

EXPLANATION OF FORMAT

This dissertation contains three papers, each written in a format suitable for publication in a technical journal. A general introduction and literature review have been included to orient the reader to the scientific and industrial relevance of this work. Following these three papers, a general summary is given to provide a comprehensive discussion about research results. A reference list is provided at the end of each paper. References cited in the general introduction are given at the end of the dissertation. The research presented in each paper presents original work conducted by the author.

LITERATURE REVIEW

Due to the fundamental interests and practical applications, oxide MOCVD has become an important research topic recently. Contrary to the abundance of publications on oxide MOCVD process development [12], the understanding about the reaction mechanism of this process is inadequate. For example, it is a general consensus that oxidizers, such as O_2, is necessary for oxide MOCVD process to produce the stoichiometric oxide films with reduced contamination [13], while the basic interaction between the metal precursor and oxygen still remains ambiguous.

In this dissertation, it is intended to both develop a oxide MOCVD process and understand the basic deposition mechanisms. Due to the potential applications of Cu_2O and CuO [11], copper oxides are chosen as the specific materials for MOCVD. Based on the extensively usage of $Cu(acac)_2$ and other metal acetylacetonates as precursors in recent novel oxides MOCVD studies [10], $Cu(acac)_2$ was chosen as the copper precursor. In the following literature reviews, the fundamentals of MOCVD film growth are reviewed first. Previous copper oxide MOCVD studies are then discussed. Since early studies indicated that the MOCVD kinetics are strongly dependent on the precursor decomposition process. The chemical and physical properties of the MOCVD precursor, $Cu(acac)_2$, are discussed in the last section.

Fundamentals of MOCVD Film Growth

To explore the reaction mechanism of oxide MOCVD, basic knowledges about MOCVD are reviewed in this section.

MOCVD Thermodynamics and Kinetics

As pointed out by Spear, for the general CVD system, which include early-stage CVD using halides or hydrides as precursors, and MOCVD using organometallic precursors, the film growth depends on the system thermodynamics, kinetics, and mass transfer of reactants and gaseous products [14]. The first factor, the thermodynamic equilibrium concept, determines the state of a closed system given very long times. By definition, MOCVD processes are open systems, which use gas streams to transport reactant vapors toward substrate and remove gaseous byproducts away; MOCVD are nonequilibrium process [14]. Thus, thermodynamics can define only certain limits for the film growth process: the driving force, maximum growth rate, and number and compositions of the equilibrium phases (including ordered crystalline phases) [14]. In some specific cases, thermodynamics gives valuable information about the CVD process. Bernard used thermodynamic modelings and successfully predicted the deposited phases distribution in chemical vapor transport (CVT) processes, which use metal halides as precursors, and are operated at 900^{o}C in a closed system [15]. On the other hand, as discussed by Vossen [16], thermodynamics is unable to provide information particularly important on the low temperature, nonequilibrium, open system MOCVD, such as

1. exact time required to attain equilibrium,

2. the step involved in the pursuit of the lowest energy state,

3. the rates of the various processes occurring during the transition from the gaseous reactants to the deposited films.

Spectroscopic Methods

To answer these questions, reaction kinetic studies on the MOCVD processes are required. For many III-V MOCVD processes, modern spectroscopic or scattering techniques have been found particularly valuable for studying the MOCVD reaction kinetics [17]. Jensen used Infrared absorption spectroscopy and mass spectrometry to analyze the GaAs MOCVD gas phase species, which include reactive intermediates and decomposition products. From these results, he identified the possible reaction pathways and the most reactive intermediates [18].

In particular, for MOCVD gas phase dynamic analysis, several groups of workers [19] have concluded that Fourier Transform Infrared spectroscopy (FTIR) has several advantages such as :

1. high throughput and responsive for dynamic study,

2. sensitive to most organic compounds, which have strong IR absorption bands,

3. nondestructive to analytes and operable at atmospheric pressure.

Other spectroscopic techniques, such as surface enhanced Raman spectroscopy (SERS) has been used by several groups to study the surface reactions of adsorbed trimethylindium (TMIn) on the GaAs substrate [20]. Since Raman spectroscopy uses an intense and focused laser beam as light source, it has been noted that Raman

technique can be used for the spatial resolving composition analysis in the MOCVD reactor.

Basically, the research methodology for spectrochemical study relies on the investigating of the certain impact of principle MOCVD process parameters, such as temperature (T), reactant partial pressures (Pi), and system total pressure (P_t), on the MOCVD product variables. These MOCVD product variables include film growth rate, film composition, and specifically the composition distribution of the MOCVD gaseous phase byproducts. As pointed out by Jensen [17], analyses of MOCVD gas phase products can reveal as much information as the MOCVD film, but are usually given with less attentions.

Activation Energy

Work done by Shaw and Jackson [21] led to a new approach in MOCVD kinetic study. From compound MOCVD experiments, they concluded that the specific activation energy, which is derived from the reaction rate data of the MOCVD experiment, can be used as a principle index for identification of the reaction controlling mechanism. Shaw suggested that a low activation energy, 3 to 4 kcal/mol, might indicate a diffusion controlled mechanism [21]. An activation energy in the range of 20-30 kcal/mol, indicates a surface reaction (kinetic) controlled mechanism [21]. From MOCVD kinetics studies, primarily the precursor pyrolysis experiments, the activation energy depends on the bond strengths of precursor, the pyrolysis ambient gas, and the rate controlling mechanism involved [22].

Precursor Chemistry

Recently, it has been realized that the precursor decomposition kinetic is critical in determining the film growth rate and film purity in the MOCVD processes. Beach has made a conclusion as [23]:

"For an ideal precursor, it should undergo elimination decomposition un the surface. That is, a low temperature precursor should decompose on the growth surface without incorporating unwanted atoms from the precursor. This is best accomplished by having the unwanted atoms of the precursor eliminated as a stable molecule."

An example is the Mond process, which purifies nickel by the decomposition of nickel tetracarbonyl, $Ni(CO)_4$. In this process, upon heating, the CO ligands were eliminated from precursor and "clean" Ni metal was deposited [23]. This elimination decomposition is also found to be responsible for reduction in carbon incorporation when triethylgallium (TEG) instead of trimethylgallium (TMG) is used to deposit GaAs [23].

According to these literatures, it has been realized that, to discover the fundamental insights of the copper oxide MOCVD process, the kinetic research has to be performed in a comprehensive procedure, which includes:

1. composition analysis of solid MOCVD films,

2. in-situ and ex-situ spectroscopic analyses of gaseous species in the MOCVD reactor; these species include radicals, reactive intermediates, and stable byproducts,

3. the basic decomposition pattern of copper precursor.

Copper Compound MOCVD Processes

To understand previous copper compound MOCVD works and learn the interactions between copper precursor, co-reactant (oxidizer), and processing parameters (deposition temperature), literatures from both Cu MOCVD and copper oxide MOCVD were examined.

Halide CVD

Strictly speaking, technical advances made during the development of copper oxide MOCVD processes depend on the copper precursor these processes used. In the early stage copper oxide CVD process, copper halides was used as the precursor. This halide CVD process has disadvantages of high deposition temperature and contamination. Brewer used CuI as precursor and reacted it with H_2 to deposit copper oxide at 900^{o}C [24]. Gillardeau used CuF_2 as precursor and reduced the deposition temperature to 760^{o}C [25]. Powell used Cu_3Cl_3 to deposit Cu at 500^{o}C [26].

MOCVD

After the recent discovery of ceramic superconductors, several groups of workers used organometallic copper complexes as the precursor to perform MOCVD and reduced both the deposition temperature and sublimation temperature. Zhang used $Cu(C_{11}H_{19}O_3)_2$ as the precursor. He sublimed this precursor at 170^{o}C, and deposited $YBa_2Cu_3O_7$ at 500^{o}C [27]. Because $Cu(acac)_2$ is clean, safe and commercial available, $Cu(acac)_2$ has been used by several groups [28,29] as the copper precursor to deposit copper oxide and superconductor thin films at temperatures from 500^{o}C to 700^{o}C. Primarily, these works were focused on the process development. Based

on these MOCVD studies, Carlsson has proposed a suggestion for depositing metal oxide films with exact stoichiometries is to maintain a high O_2/precursor ratio, which should be much higher than 1 [30].

Deposition Temperature

Deposition temperature is one parameter being extensively studied. Armitage performed MOCVD experiments with air as the carrier gas and deposited CuO film at 480^oC and Cu_2O film at 800^oC [31]. He interpreted this composition distribution as the result of thermodynamics; the thermodynamically stable oxide phase was deposited at the corresponding temperature. Armitage also postulated that the breakage of the copper-ligand bond is the rate controlling step. Holzschuh used a plasma enhanced chemical vapor deposition (PECVD) process, with Ar/O_2 mixture as the carrier gas, and deposited films containing CuO/Cu_2O mixtures at 300^oC, Cu_2O at 400^oC, and Cu at 500^oC [32]. He solved this oxygen deficiencies problem, in the films, by applying an negative bias of 120 V on the substrate holder. Pure CuO films can be deposited at 500^oC by this method. However, SEM results indicated that most MOCVD grown Cu_2O films have a poor film morphology; the deposited film was primarily composed by aggregates of μ size particles.

As reported by Holzschuh; "the film surface is covered by tapered crystallites, 0.1-0.3 μm, and a spacing between them with the same dimension." Practical applications of this film are limited.

$[O_2]$/[Precursor] Ratio

As summarized by Kern and Ban [33], in oxide CVD, the deposition temperature and oxidizer/precursor concentration ratio are the most influential processing parameters affecting film properties. For oxide MOCVD, there exists a specific range for the O_2/precursor ratio to deposit oxide films with desired properties at reasonable deposition rates. In the well studied SiO_2 CVD, the SiO_2 deposition rate decreased as the partial pressure ratio of O_2/SiH_4 was higher than 33 [33]. Ghandhi suggested that O_2 might retard the reaction by being adsorbed on the substrate surface [34], or that a relatively stable intermediate formed in the gas phase and retard the chain reaction. From these reports, the O_2/copper precursor ratio should be controlled carefully during developing the copper oxide MOCVD process.

Self Reduction of Cu(II) in The $Cu(acac)_2$ Precursor

One interesting finding in these $Cu(acac)_2$ using MOCVD studies is the self reduction mechanism of $Cu(II)(acac)_2$. When $Cu(acac)_2$ is thermally decomposed in an inert environment, spectroscopic results indicated that the deposited film can be a mixture of Cu metal (Cu(0), Cu_2O (Cu(I)), and CuO (Cu(II)) [32]. Essentially, the Cu(II) ion in the $Cu(acac)_2$ has been reduced to Cu(I) or Cu(0). From XPS and XRD results, Temple and Reisman found the film they deposited by a MOCVD process at 340^oC, in a pure Ar ambient without using any reducing co-reactant (such as H_2), is copper metal [35]. This self reduction process has resulted in a general agreement that some oxidizers, such as H_2O, O_2 or N_2O, should be added into the MOCVD reactor to prevent this reduction occur [36]. Strictly speaking, the role of oxidizers (O_2) in the $Cu(acac)_2$ using MOCVD process is unclear, because the oxidation state

of copper in $Cu(acac)_2$ precursor is 2+. It might be more appropriate to define the role of oxygen as maintaining the oxidation state of copper during the pyrolysis of $Cu(acac)_2$. Berry tried to thermally decompose $Cu(acac)_2$ in vacuum and received very thin films containing copper with several percent carbon [36].

He made the statement as: "Consequently, we found it necessary to carry out the procedure in an oxygen-rich atmosphere in order to increase the film thickness, reduce the carbon content, and increase the oxygen content in the film."

Therefore, he performed the MOCVD experiment with a carrier gas having an oxygen concentration of 76% (N_2: 150 sccm, O_2: 500 sccm) and deposited CuO/Cu_2O mixture film at 300^oC. Microscopic examination of these dull, black films showed rough, granular surfaces with "feather or whisker-like structure on the order of 10μ and 3μ wide almost perpendicular to the surface"[36].

One lesson learned from Berry's study is that the deposition temperature for producing copper oxide might be reduced by increasing the oxygen concentration, as compared with other deposition results [36].

Copper Oxide Thin Film Analysis

One fact, which should be noted from these MOCVD studies, is that one solid film may contain several phases (CuO or Cu_2O or Cu or their mixtures) and several structures (crystal or amorphous or their combinations); while most MOCVD studies used only one or two kinds of technique and to characterize the film.

Actually, until now, there is no one single technique can reveal all the information required for a complete composition identification. X-ray diffraction (XRD) can detect the crystalline phase by identifying the corresponding crystal planes, but XRD

is unable to identify the amorphous phase. Auger electron spectroscopy (AES) can diagnose the elements in the thin film sample, but AES can't tell which specific compound it is. X-ray photoelectron spectroscopy (XPS) can identify elements and reveal their specific oxidation states, whereas the crystal structure of the film will not be identified. For a comprehensive investigation, it seems that the analysis method should include a combination of XPS, XRD, IR, and AES, which gives the most reliable result.

In summary, from previous copper oxide MOCVD works, it can be realized that:

1. Copper oxides, either CuO or Cu_2O, can be deposited using MOCVD process with $Cu(acac)_2$ and O_2 as the reactants,
2. except Berry's study [36], the lowest temperature to deposit copper oxide is 480^oC,
3. deposition temperature and oxygen concentration are the two most important parameters determining the composition of film.

There are several aspects can be improved:

1. a specific processing range might exist, where copper oxide films can be produced at reduced temperatures, with an improved film morphology,
2. the concept of oxidizer/precursor concentration ratio, which is well adopted in SiO_2 CVD studies, should provide more systematic knowledges and set a comparison standard for the copper oxide MOCVD process development,
3. an integrated spectroscopic/diffraction method, which includes XRD, IR, XPS, and AES should be developed to reveal the real composition of the MOCVD

film.

The first part of this dissertation will summarized the research result for answering these requirements.

Copper(acetylacetonate)$_2$ and Metal Acetylacetonates

In this section, literature related to the molecular properties of the precursor, copper acetylacetonate ($Cu(acac)_2$), and metal acetylacetonates are reviewed to provide fundamental insights for copper oxide MOCVD study.

The chemistry of metal acetylacetonates reflects the different eras in the development of inorganic chemistry, starting with the synthesis of these derivatives for the first time in 1887 [37]. Combes reported the synthesis of acetylacetonates of copper, sodium, beryllium, magnesium, aluminium, lead, iron, nickel, and cobalt [38]. The nature of bonding was soon elucidated by the classical work of Werner [39] followed by studies performed by Morgan and Moss [40], who drew attention to the predominant chelating character of these ligands. These workers suggested that acetylacetonate ligands add 'wings' to the metal atoms, and they also gave a primary idea regarding the stability and structure of metal acetylacetonates. It was suggested that the stability of acetyacetonates of elements with different valences follow the order: univalent $<$ bivalent $<$ tervalent $<$ quadrivalent.

The molecular structure of metal acetyacetonates is of specific importance to understand the reactivity sites in this molecule (Fig. 1). Sarker published the first X-ray crystallographic study on metal acetylacetonates and suggested the presence of four molecules in each cell of aluminum tris(acetylacetonate) which belongs to the C_{2h} space group [41]. On the basis of X-ray measurements and optical properties,

Cox and Webster assumed a specific planar configuration for the 4-coordinated copper(II) acetylacetonate [42]. Finn studied the electric polarization of acetylacetonates of copper, cobalt, chromium ,and zinc, and suggested these derivatives to be polar in character [43].

A new dimension was added to the understanding of the nature of these interesting metal(acetylacetonate)s by Calvin and Wilson [44] who in 1945 suggested the presence of aromaticity in the diketonate ring; this aspect was further pursued by Collman and others [45]. From isotopic labelling experiments, Collman concluded that the chelating from the acetylacetonate ligands were so stable that the central metal ion was "well protected" [45].

Due to the capacity of the acetylacetonate ligands to chelate with metal ions and form inner coordination compounds, metal acetylacetonates have some characteristics of covalent compounds, i.e., solubility in organic solvent and volatility [46]. The latter characteristic was then noticed by MOCVD researchers and employed as the metal precursors.

The precursor ligand, acetylacetone, is capable of keto-enol tautomerism (Fig. 2). The hydrogen atom of the CH_2 group is activated by the adjacent C=O groups, and a conjugate system can arise by a protonic shift. These tautomers exist in equilibrium with each other, and structurally they possess a *cis* configuration and a syn (*cisoid*) conformation. Under appropriate conditions the enolic hydrogen atom of the ligand can be replaced by a metal cation to produce a six-membered chelate ring (Fig. 3) thereby shifting the keto-enol equilibrium in favor of the enol form. From UV [47], IR [47], NMR [48], and deuterium exchange [49] studies, it is generally accepted that the enolic form is favored in non-polar solvents. Simultaneous conjugation and chelation

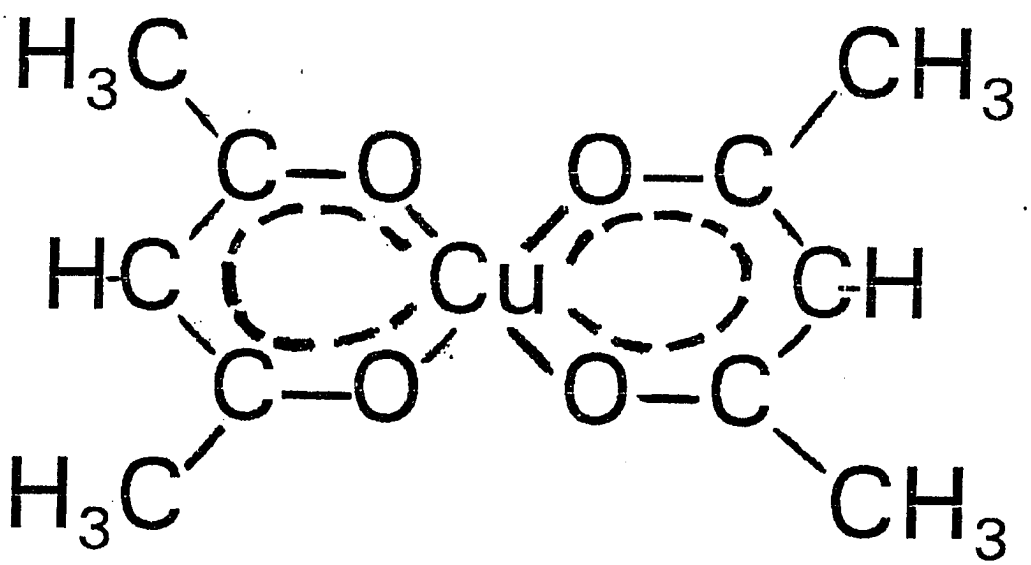

Fig. 1 Molecular structure of copper(acetylacetonate) ($Cu(acac)_2$

through hydrogen bonding is responsible for the stability of the enol tautomers.

The reactivity of the central metal atom in metal(acetylacetonate)$_n$ was limited by the steric effect exerted by the ligands. On the other hand, electrophilic substitution reactions were frequently observed on the outermost CH_3 sites and the C-H sites [50]. These studies of chemical reactions for metal(acetylacetonate)$_n$ was initiated after 1960. Nyholm and coworkers studied the nitration of copper(acetylacetonate)$_2$ with N_2O_4 [51]. The subject has been pursued actively since then and these reactions have implied the possible aromatic behavior of the metal(caetylacetonate)$_n$. A good example is the formation of the 3-carbon substituted products by the attack of a variety of electrophiles on the 3-carbon atom of the six member chelate ring of metal(acetylacetonate)$_n$ bears a close resemblance to substitution reaction in the benzene ring [52]. The polarity of solvent was found to be related to the reaction rate. The reactions appear to be faster in the polar solvent owing to the higher dielectric constants of the media and ease of production of electrophiles.

In addition to the role of solvent, these reactions often depend on three other factors [53]:

1. the central metal atom,
2. the acetylacetonate and its derivative ligands,
3. the halogenating agent.

Volatility, Thermal Decomposition, and Vapor Pressure of Metal Acetylacetonates

The thermal properties of potential MOCVD precursors are important in the feasibility of developing a novel MOCVD process. Precursors which are volatile at low

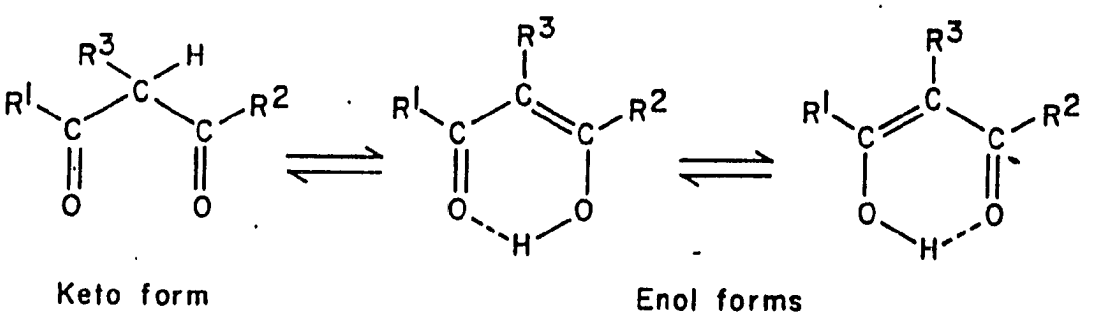

Fig. 2 Keto-enol tautomerism of acetylacetonate

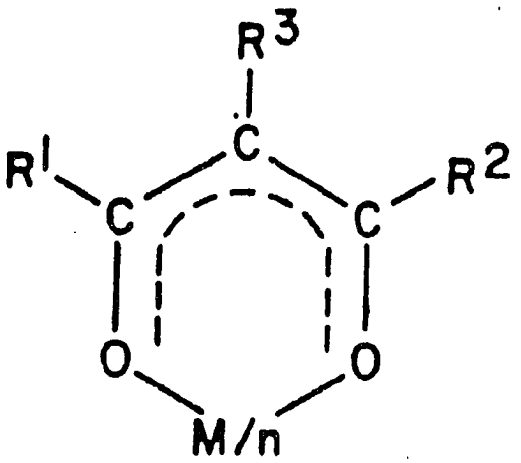

Fig. 3 Six membered chelate ring structure

temperature are favorable because this property can reduce the equipment complexity and cost during designing and manufacturing the MOCVD precursor sublimator. A rule of thumb for metal oxide MOCVD processes operated at atmospheric pressure is, that the metal precursor partial pressure should be no less 0.1 torr to provide appreciable deposition rate [54].

Thermal stability is valued by two factors; the deposition temperature and sublimation temperature. Good precursors should thermally decompose within a specific temperature window determined by the temperature of sublimator (lower limit) and the temperature of the substrate (upper limit). Thermally stable chemicals are unqualified as MOCVD precursors because of the extremely high energies (costs) needed to initiate deposition. Precursors, which decompose at too low a temperature, undergo pre-reaction in the gas phase before reaching the substrate surface during MOCVD process.

Although the volatile nature of some metal acetylacetonates was recognized in 1914 by Morgan and Moss [46], detailed studies have been made since 1950 after discovery of the potential use of acetylacetonates in the separation and analysis of metal by gas chromatography [55,56]. Thermogravimetric analysis has been employed in many cases for rapid determination of the thermal stabilities of these complexes. Some generalizations about the volatility and thermal stability of various metal acetylacetonates are given below:

1. The inert-salt type of acetylacetonates, where both the charge and coordination number of the central metal ions are simultaneously satisfied, such as in $Be(acac)_2$, $Al(acac)_3$, and $Th(acac)_4$, exhibit high thermal stability and volatility.

2. Volatility and thermal stability of most complexes are aceylacetionate ligands.

3. Effective shielding of the metal ions by the ligands enhances their volatility because both the solvation effects and interaction between molecules are lessened.

4. Volatility of metal chelates for a given class of metal with a common ligand increases with a decrease in the radius of central metal atom.

5. Substitution of an aryl group such as furyl, phenyl, or thienyl for a methyl group in an aceylacetone ligand decreases the volatility of metal chelates.

6. Substitution of a group other than hydrogen in the 3-position of the acetylacetonate decreases the volatility and thermal stability of metal chelates.

Chemical stability experiments were mostly performed in aqueous solution. Calvin and Wilson [44] determined the formation constant for copper acetylacetonate and they suggested a completely conjugated six membered ring in the molecular structure. Vapor pressures and heats of vaporization or sublimation of various metal acetylacetonates have been measured by a large number of workers [57,58] by either the isoteniscope or Knudsen effusion method. Berg and Truemper [59] have made a detailed study of the vapor pressure of metal acetylacetonates as a function of temperature. The effect of the structure of the ligand on the volatility of the chelate was evaluated by a systematic substitution of alkyl, fluorinated alkyl, aromatic, and heterocyclic groups in place of R^1 and R^2 on the aceylacetonyl ($R^1COCH_2COR^2$) ligand. It has been suggested that certain molecular factors (symmetry and polarity) are critical with regard to the magnitude of the molar heat of sublimation. From a Clausius-Clapeyron plot, Shulstad indicated that the volatility is strongly dependent on the ligand; chelates with more highly fluorinated ligands are more volatile in

the order: hexafluoroacac (hfac) > tetrafluro-acac (tfac) > fod > acac. It was also observed that the square-planar bis-(fod) chelates of Cu(II) and Pd(II) have higher vapor pressures than the tris-(fod) complexes which were in turn more volatile than the tetra Hf(IV) complexes [60].

Research Objectives

It is the objective of this research to investigate the interaction of MOCVD processing parameters with the copper oxide MOCVD reaction kinetics. By using diffraction and spectroscopic methods, this investigation will attempt to identify the specific processing parametric regions for depositing Cu_2O (cuprous oxide), CuO (cupric oxide), or metallic copper MOCVD films. The possible decomposition mechanism of the MOCVD precursor, $Cu(acac)_2$, will be proposed, based on the deposition result and MOCVD gas phase product distribution observed by FTIR. Fundamental insight into the thermal activated decomposition of $Cu(acac)_2$ will be approached by DSC analysis. Verification of the controlling mechanism responsible for copper oxide MOCVD film deposition is the ultimate goal of this research. This issue is intended to be reached by integrating the knowledge learned from research results of deposition, gas phase IR, and DSC of $Cu(acac)_2$ decomposition studies.

PAPER I.

SPECTROSCOPIC CHARACTERIZATION OF MOCVD COPPER OXIDE AND COPPER THIN FILMS

ABSTRACT

Cu_2O, CuO and Cu films were prepared by metal organic chemical vapor deposition (MOCVD) technique using copper acetylacetonate ($Cu(acac)_2$) as the precursor. Depositions were performed at atmospheric pressure in an oxygen-rich environment. The films were characterized by X-ray diffraction (XRD), X-ray photoelectron spectroscopy(XPS), Auger electron spectroscopy(AES), Fourier transform infrared spectroscopy (FTIR) and scanning electron microscopy(SEM). With a deposition temperature of 360^oC, Cu_2O films could be deposited at an oxygen partial pressure of 150 torr and a copper precursor partial pressure of 0.2 torr. XRD results indicate that the Cu_2O films are polycrystalline, with a preferential [111] orientation. CuO films were deposited at 420^oC with an oxygen partial pressure of 190 torr and a copper pressure of 0.2 torr. The CuO films have crystal grains randomly oriented at [111] and [111] planes. By using water vapor as a co-reactant, copper metal films could be deposited at temperatures above 380^oC, with a water vapor pressure of 15 torr and a copper precursor pressure of 0.20 torr. XRD patterns indicated that most Cu films were polycrystalline and had a preferential orientation at [111] plane. Spectroscopic characterization results indicated the phase distribution in these MOCVD films was determined by the deposition temperature, precursor partial pressures, and co-reactants used (H_2O or O_2).

INTRODUCTION

Transition metal and metal oxide films are valuable materials for optical, microelectronic, and energy related applications[1]. Among these materials, copper metal and its oxides are particularly promising for their applications in microelectronics industry. Copper metal film deposition technique has been extensively studied as a candidate process to replace Al deposition technique for fabricating interconnecting lines used in the Very Large Scale Integrated Circuit (VLSI) technology[2]. Copper oxide (CuO and Cu_2O) films are investigated because of potential uses in solar cells, catalysts, and related superconductors [3]. Due to the specific electronic properties, such as the unique band structure and exciton nature, copper oxide is one of the earliest examined semiconductor materials [4]. Cuprous oxide (Cu_2O) has a simple cubic structure, with four copper atoms tetrahedrally coordinated to each oxygen atom and two oxygen atoms linearly bridged by a copper atom. There are several difficulties encountered in preparation of Cu_2O. Cu_2O is thermodynamically unstable in ambient environment and temperatures for conventional crystal growth technologies [5]. Cu_2O is highly reactive at temperatures above 1000^oC both in solid and in the molten state (melting point of Cu_2O is 1125^oC) [6]. Bulk Cu_2O crystals have been grown by high temperature (higher than 700^oC) processes, such as hydrothermal growth, melt growth, and floating zone methods, with growth ambient under

careful controlled. A high density of crystal imperfections, such as cation vacancy and precipitate of impurities, was frequently observed in these bulk crystal growth products [7].

On the other hand, copper oxide crystals grown by thin film processes could be prepared at much lower temperatures, with much lesser crystal defects [8-10]. Copper oxide films have been prepared by conventional processes such as thermal oxidation [8], electrodeposition [9], and reactive sputtering [10]. Compared to these methods, metal organic chemical vapor deposition (MOCVD) technique is more promising because MOCVD can operate at low processing temperature, grow films almost free from carbon contamination and deposit on a wider selection of substrate materials. Due to the high device density requirement (line width less than 0.2 μm) for future Ultra Large Scale Integrated Circuit (ULSI) processes, MOCVD is more competitive than other thin film process for its unique capability to layout uniform deposition layers on substrates with three dimensional geometries. In this research project, we developed an MOCVD process to deposit copper and copper oxide films and characterized the MOCVD films using spectroscopic techniques.

Copper acetylacetonate ($Cu(CH_3COCHCOCH_3)_2$), the most commonly used copper precursor in ceramic superconductor MOCVD processes [11-13], was employed as the precursor. $Cu(acac)_2$ is a chelate coordinated organometallic complex, which is volatile at moderate temperatures (its vapor pressure of about 0.2 torr at 200^oC). This complex is commercially available and less toxic than other β-dikentonate derivatives. Previous research with metal acetylactonate–MOCVD processes has established that oxidizing gases are necessary to deposit films with certain stoichiometries [14,15]. Ajayi reported that the hydrocarbon ligands liberated

from $Cu(acac)_2$ were responsible for the reduction of the surface of CuO films[14]. Armitage also reported that less carbon and fluorides were present in the film, if the deposition was performed in 760 torr of air[15]. As a general rule in oxide MOCVD process, the oxidizer/precursor ratio should be much higher than 1. In this study, the $O_2/Cu(acac)_2$ partial pressure ratio will be calculated to examine this rule. On the other hand, previous studies also indicated that, by using different co-reactants, such as H_2 or H_2O, the final stoichiometry of films might change. From a computer simulated deposition calculation, Carlsson indicated that, for MOCVD using $Cu(acac)_2$ and water as the reactants, the primary phase in deposited film was metal copper [16]. The feasibility to deposit copper compound films by using water vapor as the co-reactant is explored in this research.

Multi-phase stoichiometry and coexistence of crystalline and amorphous structures is a general characteristic of many oxide MOCVD films. Copper containing films, with possible combinations of Cu^0, Cu^{1+}, and Cu^{2+} in the sample film, appears to be a challenge for composition study. The research methodology is developed as follow: Because AES has the sensitivity to analyze low atomic weight elements, specifically carbon, AES is first used to analyze the elements contained in the MOCVD film. The possible compounds in the MOCVD film is analyzed by XRD, which revealed the specific diffraction peaks corresponding to the crystal planes of compounds. The possible compounds are the result of every possible combinations of the elements found by AES. For example, if AES find Cu and O in the film, the XRD result should be compared with standard powder diffraction pattern of Cu, CuO, and Cu_2O. In principle, XRD has the advantages as nondestructive and efficient accessing of data, but also suffers on the limitation for just capable of revealing

crystalline phases. From monitoring the change of the kinetic energy of X-ray photoelectron, XPS can detect the variations in the electronic environment; XPS works as a powerful technique to identify the oxidation state of copper, regardless of the material structure. To focus on the detection of possible carbon contamination, the molecular vibrational spectroscopy, IR, is employed. IR is particularly sensitive to organic compounds, even the material is in the amorphous state.

In this study, depositions were performed to identify the range of processing parameters which yield Cu_2O, CuO and Cu films (identified by XRD). Extensive film characterizations were applied to reveal the complete compositional information of copper and copper oxide films.

EXPERIMENTAL PROCEDURE

MOCVD Film Deposition

The deposition experiments were conducted in a tubular quartz reactor. $Cu(acac)_2$ (Aldrich, purity 99%) was sublimed with He (Air products) as the carrier gas. This stream was mixed with O_2 (Air products) and He to obtain the desired partial pressure of oxygen. Partial pressure of copper precursor was derived from the mass balance equation according to the weight loss of precursor and precursor collected downstream. Oxygen partial pressure was calculated based on the mass balance between the flow rates. Water vapor was supplied by bubbling He stream through a sealed quartz container holding 100 ml deionized distilled water. Water vapor pressure was calculated by the saturated vapor pressure value and checked with weight loss of water in the container after experiment. The depositions were performed on cut Si(100) wafers (p-type, Unisil corp.). Each film was deposited with 10 minutes. Deposition and sublimation temperatures were measured by K-type thermocouples.

Diffraction, Spectroscopic, and Microscopic Characterizations of MOCVD Films

X-ray diffraction (XRD)

XRD patterns were taken at room temperature and ambient atmosphere. A Siemen D-500 X-ray diffractrometer, using a Cu K_α radiation source was used to analyze MOCVD films. The sample diffraction pattern were obtained using a $0.05^o/2\theta$ step size with a one-second counting time per step. The diffractrometer detector signal was interfaced to a Digital Equipment Corporation DPD 11/23 computer using Siemen's Diffract V version 2.0 software to process data.

X-ray Photoelectron Spectroscopy (XPS), X-ray Induced Auger Electron spectroscopy (XAES), and Auger Electron Spectroscopy (AES)

Deposited films were analyzed by AES with a Perkin Elmer PHI 600 Scanning Auger Microscope. The AES results were recorded in the derivative mode (peak-to-peak modulation of 1 eV) with a cylindrical mirror analyzer. The electron probe beam energy and current density are 3 kV and 4 mA/cm^2, respectively.

The XPS and XAES results were obtained by using an AEI 200B Spectrometer equipped with an Al K_α radiation. A Nicolet 1100 computer was used for signal averaging and storage. All AES, XPS, and XAES experiments were performed at ultra high vacuum (10^{-10}torr) and room temperature.

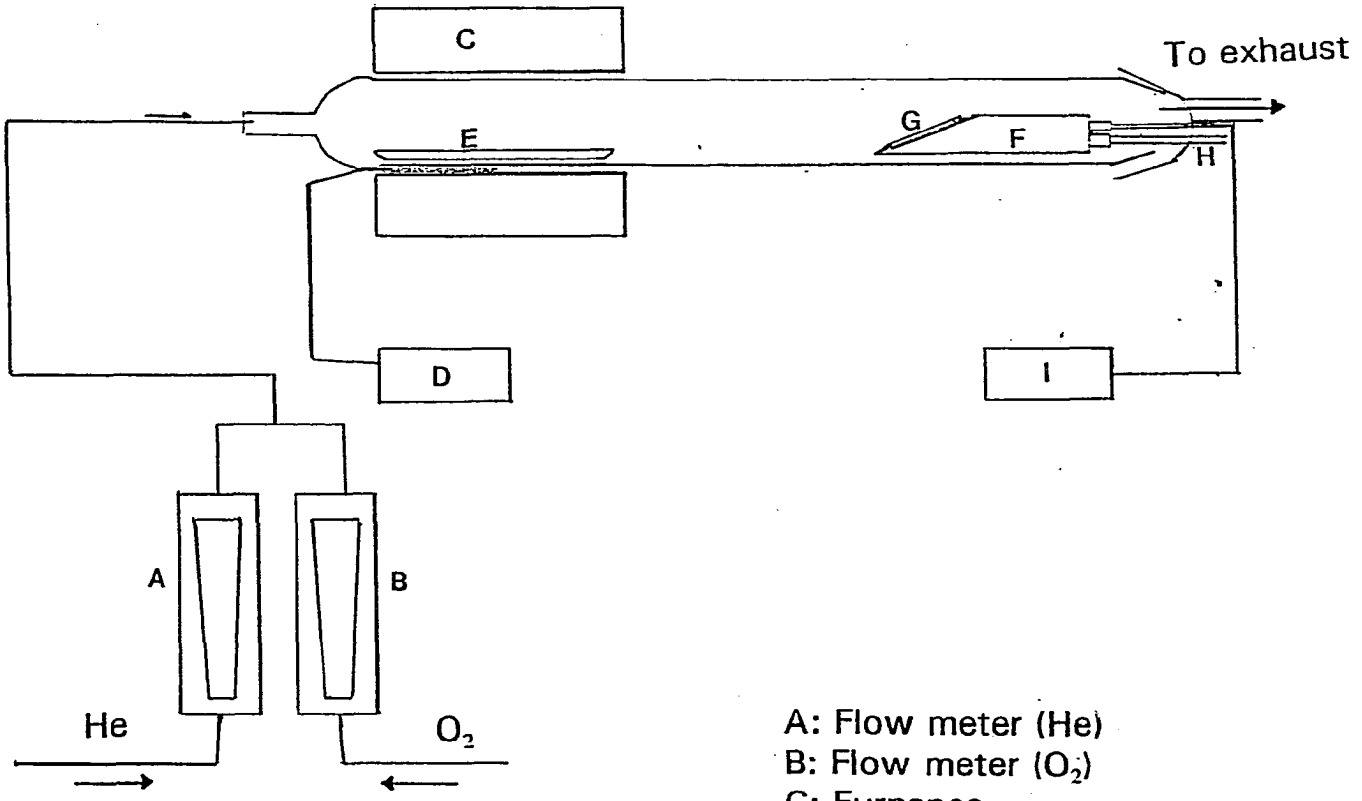

A: Flow meter (He)
B: Flow meter (O_2)
C: Furnance
D: Thermocouple ($T_{sublime}$)
E: Sublimator
F: Susceptor
G: Si Substrate
H: Power feedthrough
I : Thermocouple ($T_{deposition}$)

Fig. 1 MOCVD Reactor System Set-up

Fourier Transform Infrared Spectroscopy (FTIR)

Infrared spectra of MOCVD thin films were obtained by using a Nicolet 60SX spectrometer equipped with a water-cooled glowbar source and a mercury-cadmium-telluride (MCT) detector. Transmission IR spectra of MOCVD films were collected with a resolution of 4 cm^{-1} at wavenumber ranging from 400 cm^{-1} to 4000 cm^{-1}. The spectra of films were obtained by ratioing collected sample spectra with background Fourier transformed interferogram of a Si wafer. All transmission IR spectra were taken at room temperature the sample compartment, which was purged with dry air .

Scanning Electron Microscopy (SEM)

The scanning electron micrographs were taken from a SEM(Cambridge S-200) with magnifications from 4,000 to 30,000 by a low energy electron beam with an acceleration voltage of 15-18 kV. Electron micrographs were taken at high vacuum (10^{-6} torr) and room temperature.

EXPERIMENTAL RESULTS

The MOCVD experimental results are organized as follow:

1. Defining the specific processing parameters to produce Cu_2O, CuO, and Cu films

2. Diffraction, spectroscopic, and microscopic characterization results of Cu_2O, CuO, and Cu MOCVD films

MOCVD Process Study

The influence of carrier gas flow rate (Q_t) on the process was examined. Initially, depositions were carried with a low carrier gas flow rate, 100 sccm, with the other deposition parameters fixed at: T=360^{o}C, P_{total}=760 torr, P_{O2}=150 torr, and P_{cu}=0.20 torr. From SEM observations (Fig. 2), films deposited at such conditions show a discontinuous morphology, with island like deposits among uncoated substrate surface. The spherical shape of deposited particles suggested that these solids were formed in the gas phase by homogenous nucleation. This poor film morphology could be improved by increasing the carrier gas flow rate. Continuous films with smooth surfaces were deposited with a carrier gas flow rate above 600 sccm.

Processing Conditions for Depositing MOCVD Films

The following sections discuss the MOCVD processing conditions which yield Cu_2O, CuO, and Cu films. XRD was used to scan-survey and map out the specific phases in each MOCVD film.

Cu_2O Films

With both P_t (760 torr) and Q_t (750 sccm) kept constant, depositions using a variety of reactant concentrations and substrate temperatures were performed. The films were analyzed by XRD, which could identify the crystalline phases, such as oxides, metals, or impurities in the films. On Table 1, the processing conditions for films containing crystalline Cu_2O, CuO and Cu phases were listed. Table 2 lists the d-spacings for possible copper compounds. For a limited range of processing parameters, the crystalline Cu_2O phase was the only crystalline phase in the films. With an oxygen partial pressure of 150 torr, at low precursor concentration (P_{Cu}=0.20 torr), Cu_2O film was deposited at a narrow temperature range (360^oC). As indicated above, the P_{O2}/P_{Cu} is 750, far exceeding 1. At higher precursor concentration (Pcu=0.25 torr), the temperature range to deposit Cu_2O films is broader (340 to 380^oC). At a P_{Cu} of 0.36 torr, Cu_2O could be deposited at 420^oC.

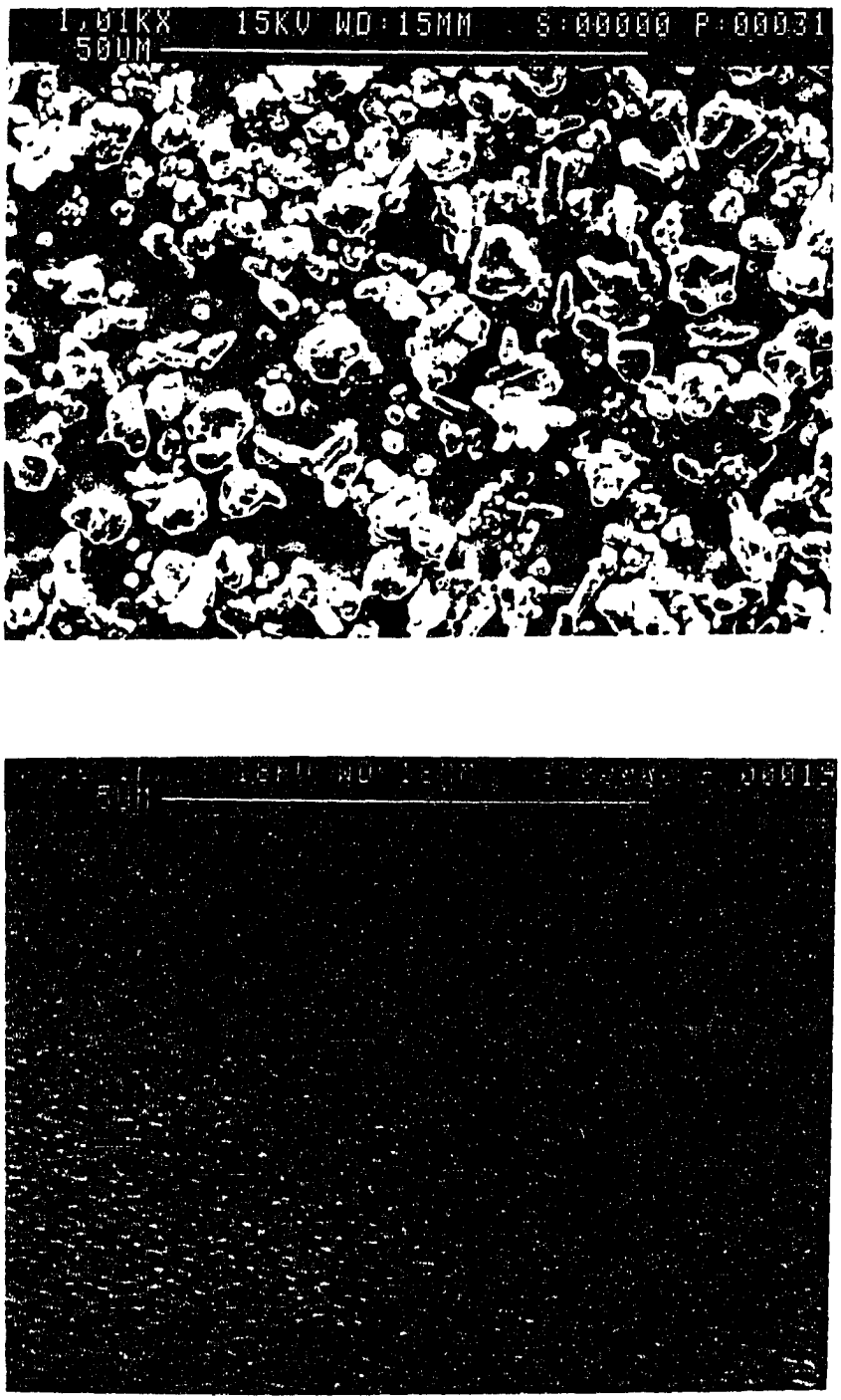

Fig. 2 SEM of MOCVD films, deposited at 360°C, P_{O2}= 150 torr, P_{Cu}=0.20 torr. and (A) Q_t= 100 sccm, or (B) Q_t= 600 sccm

Table 1: MOCVD processing condition for preparing primarily Cu_2O films

$T_{dep}(^oC)$	P_{O2}(torr)	P_{Cu}(torr)	P_t(torr)	Q_t(sccm)	XRD (Å)
340	150	0.20	760	750	2.08, 2.46
360	150	0.20	760	750	2.46
380	150	0.20	760	750	2.32, 2.46, 2.53
400	150	0.20	760	750	2.32, 2.53
340	150	0.25	760	750	2.46
360	150	0.25	760	750	2.46
380	150	0.25	760	750	2.46
400	150	0.25	760	750	2.32, 2.46, 2.53

Table 2: *d*-spacings for crystal planes of reference compounds

compound	plane	d-spacing (Å)	intensity(%)
Cu	(111)	2.08	100
.	(200)	1.81	78
Cu_2O	(110)	2.53	34
.	(111)	2.46	100
.	(200)	2.32	23
.	(211)	2.14	17
CuO	(110)	2.75	12
.	(002)	2.53	49
.	(111)	2.52	100
.	(111)	2.32	96
.	(200)	2.31	31

CuO Films

Three processing parameters; deposition temperature, partial pressures of copper precursor and oxygen, were examined to deposit CuO films. According to XRD map surveying results, CuO film depositions were achieved by either enhancing deposition temperature or increasing oxygen pressure or decreasing copper precursor pressure. Increasing deposition temperature is the most efficient way. Increasing oxygen partial pressures causes poor film morphology; from SEM observations, films deposited with oxygen partial pressures higher than 300 torr have discontinuous surfaces and irregular thicknesses. With an oxygen pressure of 190 torr, and a precursor pressure of 0.20 torr, CuO phase predominated MOCVD film were deposited at temperatures above 380^{o}C. For a P_{Cu}=0.25 torr, CuO was deposited at temperatures higher than 420^{o}C. As shown on Table 3, all these diffraction peaks (d=2.32$\AA$, 2.53$\AA$) were assigned to the crystal planes of CuO. For deposition temperatures above 600^{o}C, carbon contamination becomes significant. The P_{O2}/P_{Cu} ratio, 950 in the requirement to deposit CuO film, was much larger than 1.

Cu Films

Cu metal films were deposited, after some exploratory studies. Water vapor was found to be a efficient reactant for depositing Cu(0). With an water vapor pressure of 15 torr, Cu films were deposited at a precursor pressure of 0.20 torr and deposition temperatures above 380^{o}C. As found by XRD patterns, these crystal grains in the Cu films were primarily oriented on the [111] orientation. Below 340^{o}C, deposits were composed of primarily amorphous copper oxides as revealed by transmission IR and the broadened XRD peaks. Above 550^{o}C, the deposited films were plagued by severe

Table 3: MOCVD processing condition for preparing primarily CuO films

$T_{dep}(^oC)$	P_{O2}(torr)	P_{Cu}(torr)	P_t(torr)	Q_t(sccm)	XRD (Å)
380	190	0.20	760	750	2.32, 2.46, 2.52
400	190	0.20	760	750	2.32, 2.52
420	190	0.20	760	750	2.32, 2.52
440	190	0.20	760	750	2.32, 2.52
380	190	0.25	760	750	2.46
400	190	0.25	760	750	2.32, 2.46, 2.52
420	190	0.25	760	750	2.32, 2.52
460	190	0.25	760	750	2.32, 2.52

carbon contamination, presumably originating from the undesirable carbon-carbon bond cleavage of the acetylacetone ligand, which was liberated from $Cu(acac)_2$, on the surface. As shown on Table 4, the P_{H2O}/PCu ratio to deposit Cu film is 75.

Diffraction and Spectroscopic Characterizations of MOCVD Films

Cu_2O Films

XRD, AES, XPS, and IR were used to analyze the films. Results of a film deposited at 360^{o}C, using a carrier gas flow rate of 750 sccm, with a precursor pressure and oxygen pressure being 0.20 torr and 150 torr were listed in the following sections.

The XRD pattern, as shown in Figure 3, contains only one strong diffraction peak at d=2.464Å. From the computer search of structure diffraction patterns for all Cu-O compounds, this peak is assigned to the Cu_2O (111) plane. Another weak peak

Table 4: MOCVD processing condition for preparing primarily Cu films

$T_{dep}(^oC)$	P_{H2O}(torr)	P_{Cu}(torr)	P_t(torr)	Q_t(sccm)	XRD (Å)
340	15	0.20	760	750	2.33, 2.46
380	15	0.20	760	750	2.08, 1.81
400	15	0.20	760	750	2.08, 1.81
420	15	0.20	760	750	2.08
380	15	0.25	760	750	2.08, 1.81
400	15	0.25	760	750	2.08, 1.81
420	15	0.25	760	750	2.08
460	15	0.25	760	750	2.08

at d=2.714Å originates from Si(200) plane of the substrate. This (111) preferential orientation pattern was also found in other Cu_2O crystalline phase dominated films.

AES was used to reveal the elemental information of the film. By recording the peak-to-peak ratio(dN/dE) of the O(KLL) line at 510 eV, C(KLL) line at 271 eV, Cu(MNN) line at 58 eV, and Cu(LMM) line at 918 eV, the Auger depth profile spectrum, as shown in Figure 4, indicates that there are two compositional zones in the film. On the top surface layer (20Å thick), copper, oxygen, and carbon were the major elements. The concentration of carbon dropped to below 1 % under the surface layer. Beneath the surface layer, the film volume is primarily composed of Cu and O.

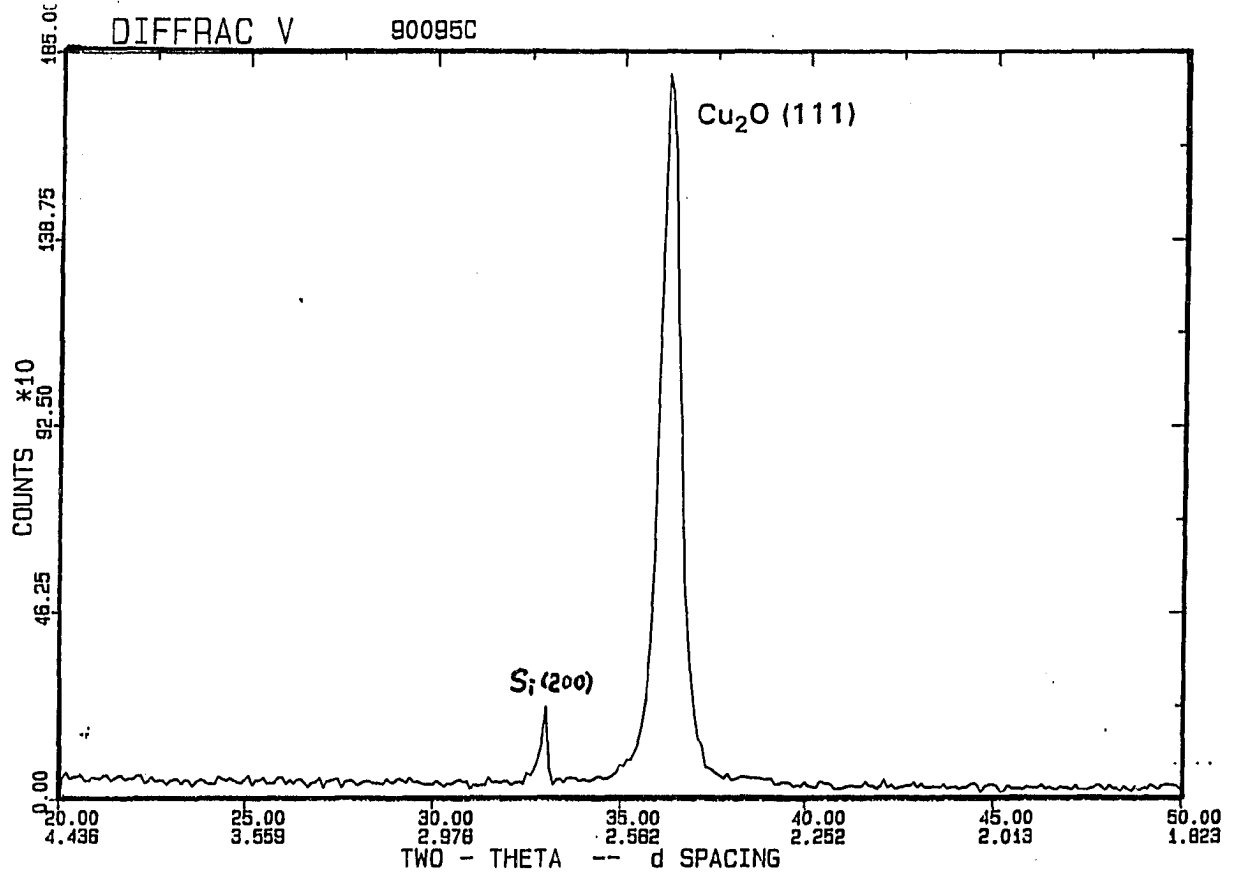

Fig. 3 XRD pattern of Cu_2O MOCVD film

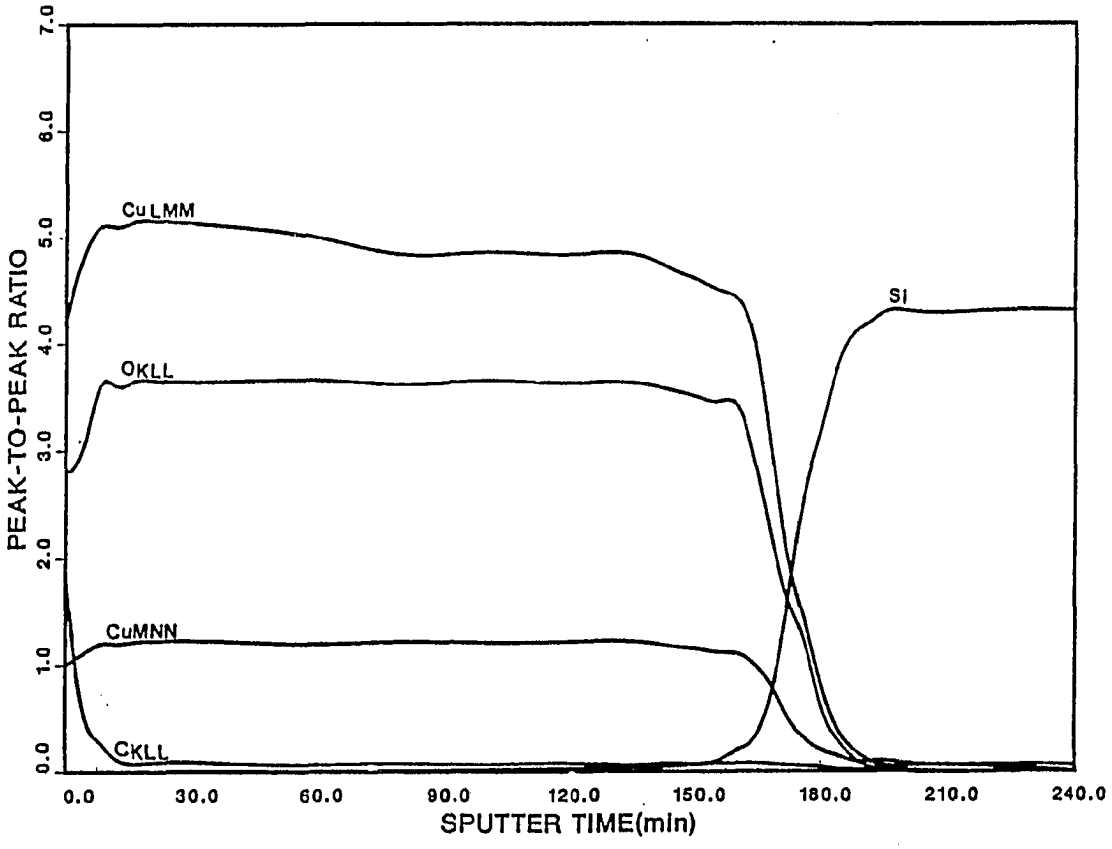

Fig. 4 Depth profile Auger diagram of Cu_2O MOCVD film

The possibility of other amorphous phase was analyzed by depth profile XPS. After the surface layer was sputtered off, the film was analyzed by XPS. The XPS spectrum of Cu2p core electrons of this film, as shown in Figure 5, shows two peaks at 932.7 eV (Cu2p3/2) and 953 eV (Cu2p1/2). The width (FWHM) of the Cu2p3/2 peak is 1.8 eV. The distance between the Cu2p3/2 peak and the Cu2p1/2 peak is 20.3 eV. This XPS spectrum corresponds to the Cu2p electrons from Cu^{o} or Cu^{+1}. As shown on the Table 5, these values can not be assigned to the peaks for copper carbonates ($CuCO_3$) or hydroxides ($Cu(OH)_2$). Also, the absence of Cu2p satellite peaks rule out the possibility of Cu^{2+} compound, such as CuO. The only possible compounds are Cu_2O or metal copper. By comparing the X-ray induced AES (XAES) peak position of the Cu(LMM) in the spectrum, 916.1 eV, with the XAES value for Cu, 918.4 eV, and Cu_2O, 916 eV [8], we conclude that the only detectable phase is Cu_2O.

In the transmission IR spectrum of this MOCVD film (Fig. 6), only one absorption band at 610 cm^{-1} was observed. This low wavenumber IR band was assigned to the first order sublattice mode (F_{1u}) of Cu_2O molecule. The thickness of the film limited IR observations of much weaker secondary IR modes of Cu_2O. Periodic interference fringes were another characteristic in the IR spectrum, which was attributed to the uniform thickness of Cu_2O layer and large difference in refractive indexes between Si and Cu_2O. These two factors cause an enhanced internal reflection when IR beam transmitted through the film.

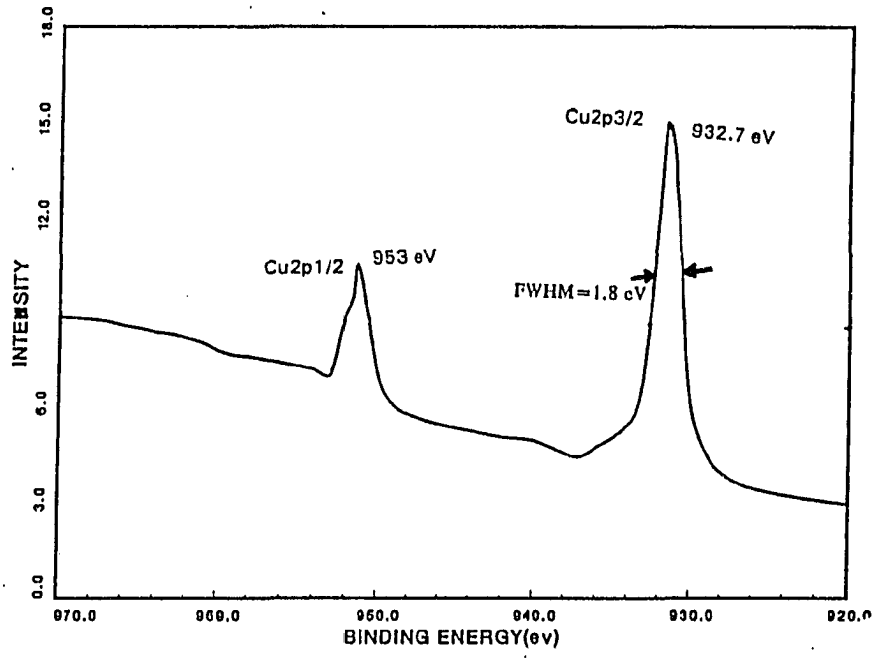

Fig. 5 XPS of Cu_{2p} electrons from MOCVD film

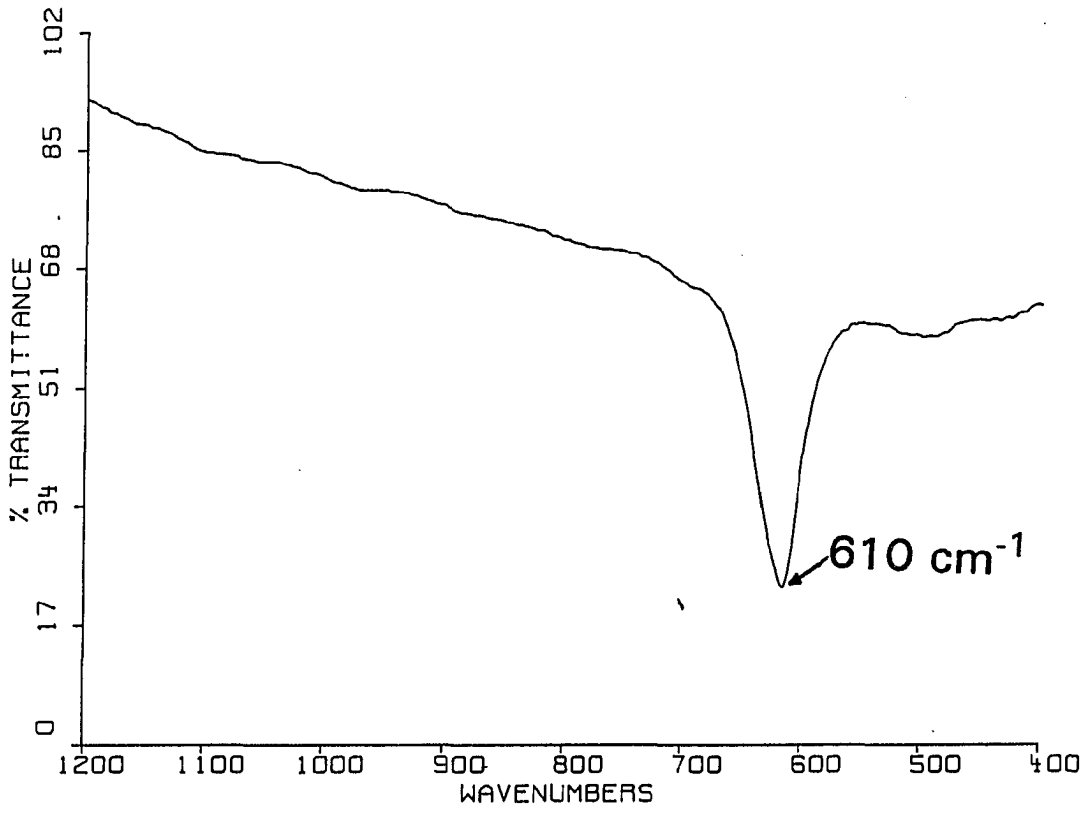

Fig. 6 Transmission IR spcetrum of Cu_2O MOCVD film

Table 5: XPS and XAES results of Cu_2O MOCVD film and standard values of reference compounds

XPS parameters (eV)	MOCVD film	Cu(II)	Cu(I)	Cu(0)	$CuCO_3$
Cu2p3/2	932.7	933.8	932.7	932.8	934.6
Cu2p3/2(FWHM)	1.8	4.0	1.8	1.9	4.0
CuXAES(LMM)	916.1	917.8	916.0	918.4	916.5
α_{Au}	1848.8	1851.6	1848.7	1851.2	1851.1
O1s	530.5	529.6	530.4	NA	530.2

CuO Films

Spectroscopic results of XRD identified CuO films were acquired following the same procedure discussed in last section. Experimental results of a film deposited at 420^oC, using a carrier gas flow rate of 750 sccm, with a precursor pressure and oxygen pressure of 0.2 torr and 190 torr respectively, are described. In Fig. 7, the XRD pattern indicated that the CuO film has crystal grains randomly oriented at [111] and [111]. Wide scan XPS (Fig. 8) revealed that the CuO film surface contained Cu, O, and C elements. After sputtering the top surface layer (20Å), carbon concentration dropped significantly. In the narrow scan XPS spectrum of the Cu2p electrons from the MOCVD film (Fig. 9), the presence of two satellite peaks (at B.E.=944 eV and 964 eV) and the broad width of the cu2p3/2 peak (4.1 eV) are strong evidence for the presence of Cu^{2+} ions. Table 6 shows the kinetic energy of the X-ray induced Auger electron of copper (Cu(KLL)), which is 916 eV. This value is relatively closed to the standard value of the kinetic energy of the electron from Cu(II)(KLL). In Fig. 10, depth profile XPS results of Cu2p, O1s, and CuAuger (XAES) were recorded. The coherences in peak heights, shapes, and positions indicated that the CuO film had a uniform composition distribution in the film volume. Transmission IR spectroscopy

Table 6: XPS and XAES results of CuO MOCVD film and standard values of reference compounds

XPS parameters (eV)	MOCVD film	Cu(II)	Cu(I)	Cu(0)	$CuCO_3$
Cu2p3/2	933.7	933.8	932.7	932.8	934.6
Cu2p3/2(FWHM)	4.1	4.0	1.8	1.9	4.0
CuXAES(LMM)	917.6	917.8	916.0	918.4	916.5
α_{Au}	1851.3	1851.6	1848.7	1851.2	1851.1
O1s	530.4	529.6	530.4		530.2

provided more compelling evidence of the dominating CuO phase. The IR spectrum shows a strong absorption band at 480 cm^{-1}, accompanied by two shoulders at 440 and 540 cm^{-1}, which were assigned to the first order lattice modes of the CuO crystal. The overall results indicate a generally consistent agreement between XPS/XAES, XRD, and IR.

Cu films

The spectroscopic characterization results of an MOCVD film deposited at 400^{o}C, with a P_{Cu} of 0.20 torr and P_{H2O} of 15 torr are discussed. Except IR, which displayed zero transmission due to the low transmittance of copper metal film, all the other spectroscopic characterization results indicated conclusive information supporting the presence of metal copper phase. The sharp Cu(111) and Cu(200) diffraction peaks observed in the XRD (Fig. 12) suggested that the Cu films have a well ordered crystal structure and larger crystal grains. Compared with standard powder diffraction pattern of copper, the XRD pattern of the MOCVD Cu film indicated a preferential [111] orientation in the film structure.

Compared to the standard values of reference compounds, the XPS data from Cu2p electrons and Auger parameters of Cu from the MOCVD film suggested a

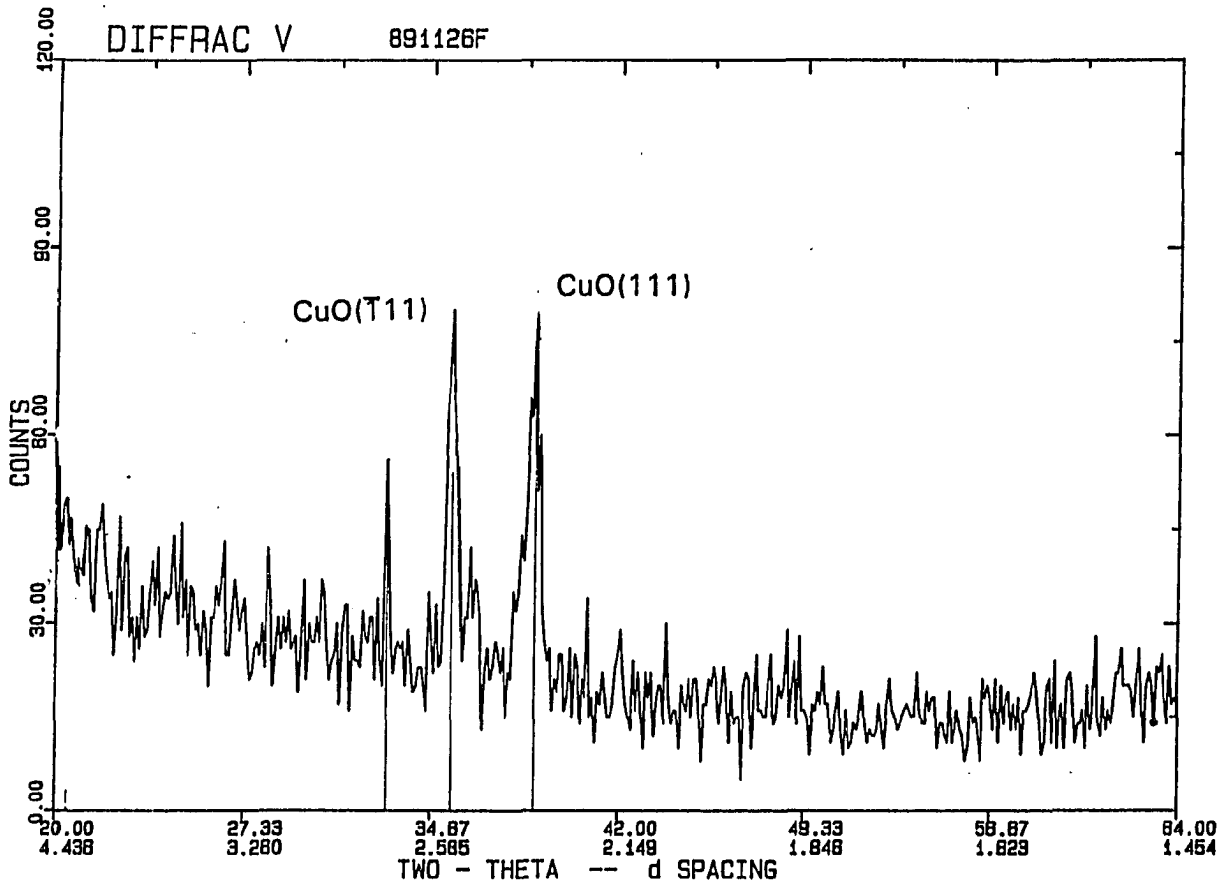

Fig. 7 XRD pattern of CuO MOCVD film

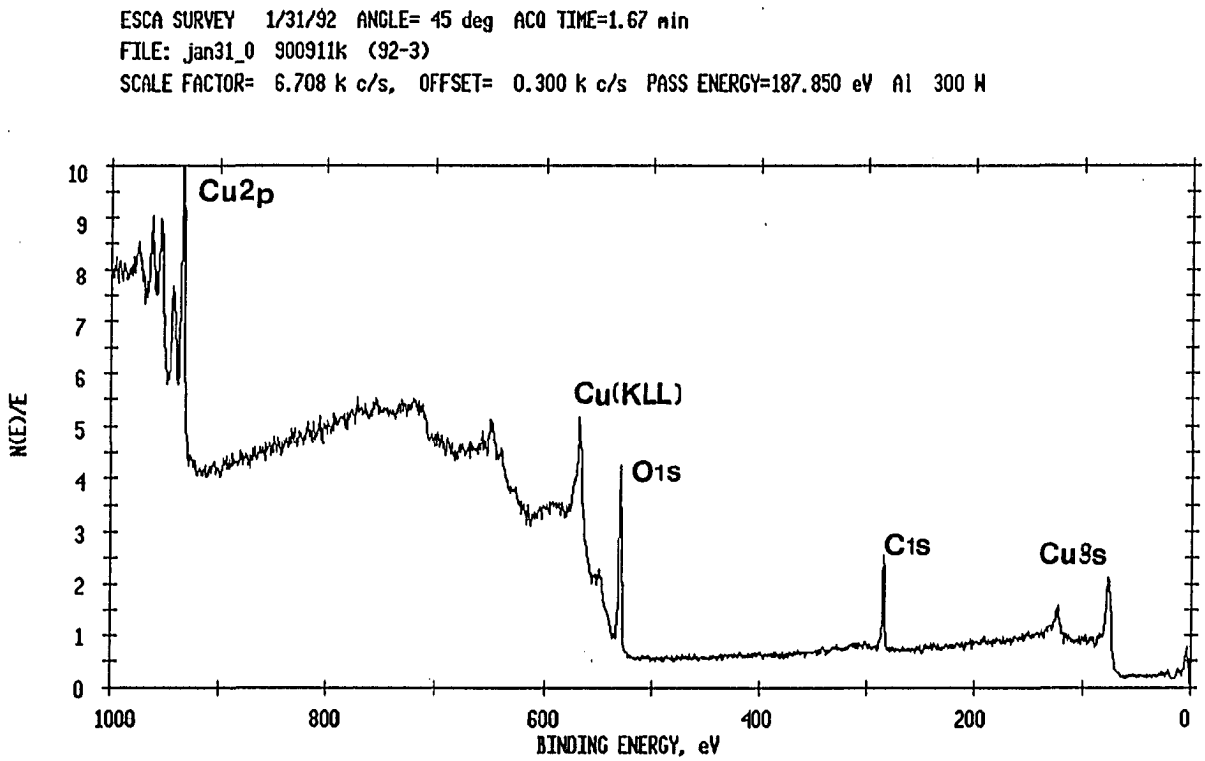

Fig. 8 Wide scan X-ray photoelectron spectrum of CuO MOCVD film (unsputterred)

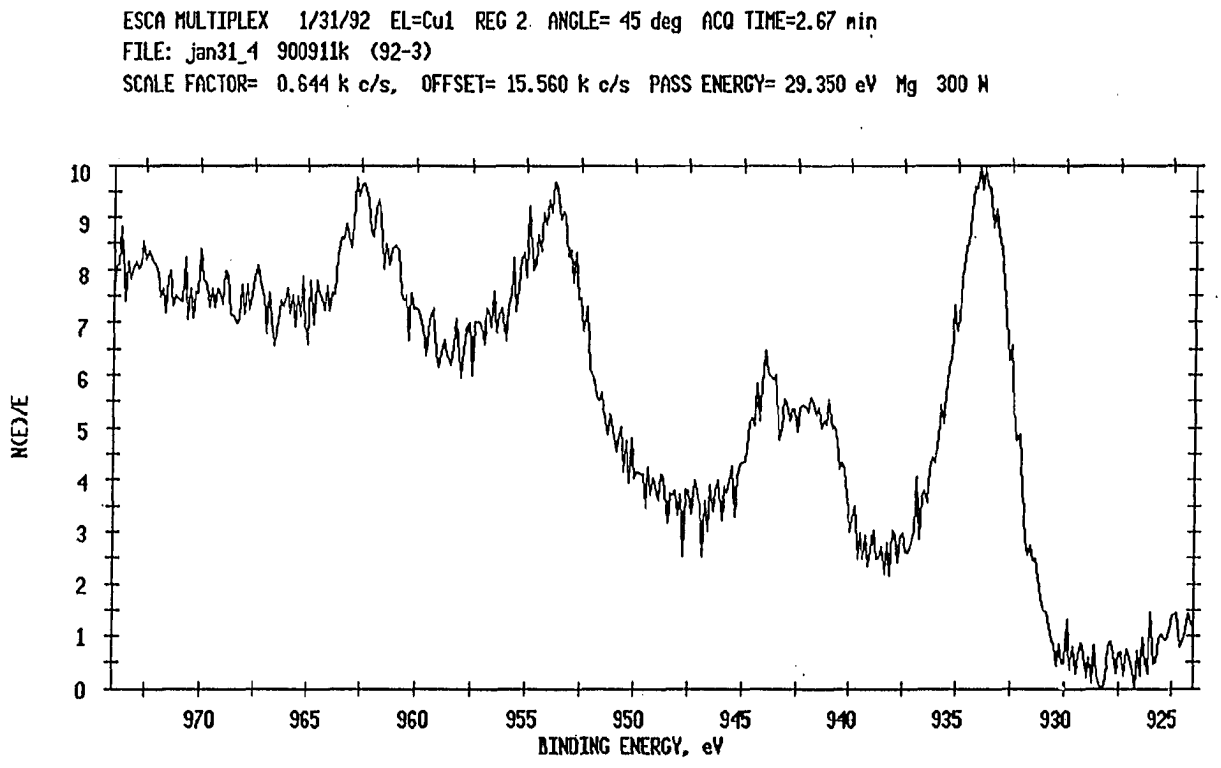

Fig. 9 Narrow scan X-ray photoelectron spectrum of Cu2p electrons from CuO MOCVD film (sputterred)

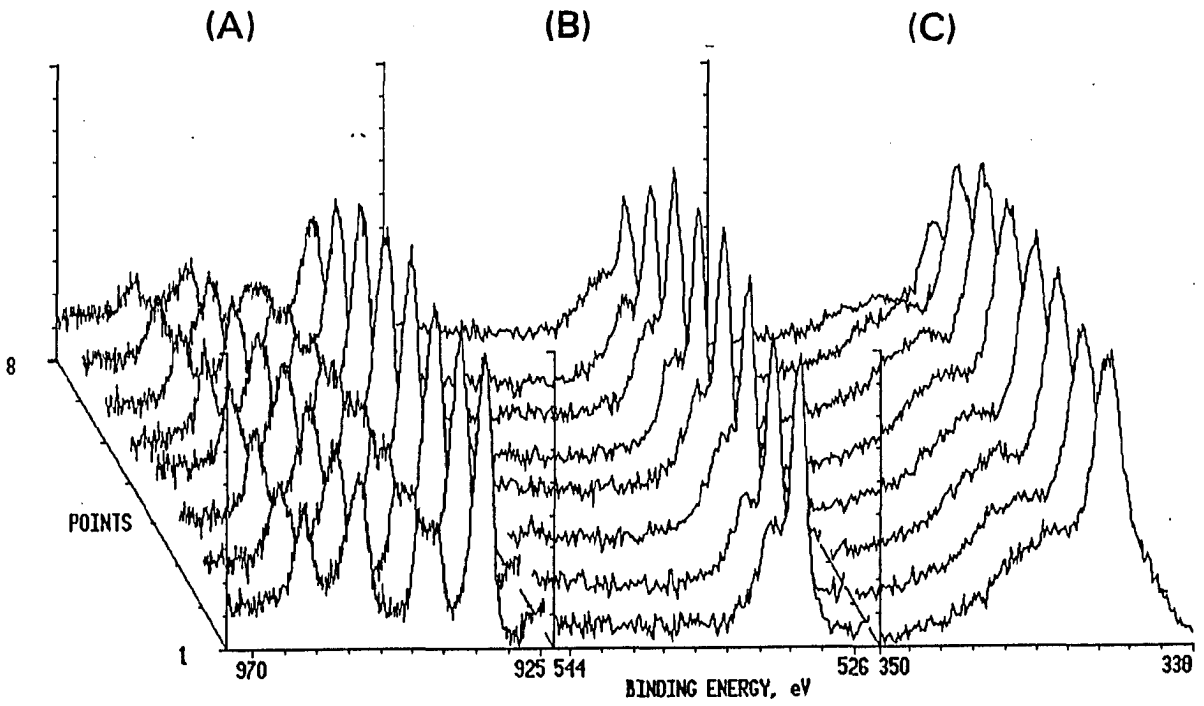

Fig. 10 Depth profile X-ray photoelectron spectra of (a) Cu2p, (b) Cu (AES) and (c) O1s from the copper oxide MOCVD film

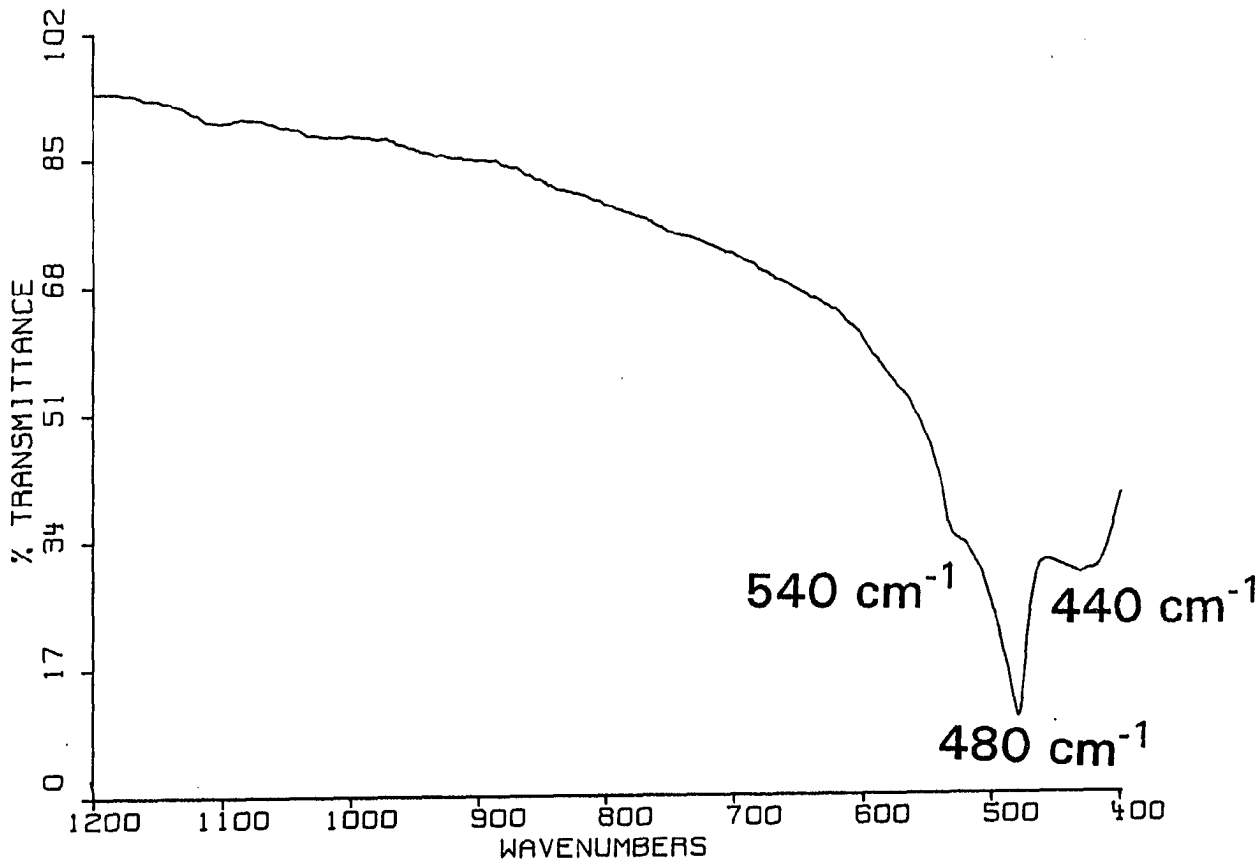

Fig. 11 Transmission IR spectrum of CuO MOCVD film

Table 7: XPS and XAES results of Cu MOCVD film and standard values of reference compounds

XPS parameters (eV)	MOCVD film	Cu(II)	Cu(I)	Cu(0)	$CuCO_3$
Cu2p3/2	932.9	933.8	932.7	932.8	934.6
Cu2p3/2(FWHM)	1.9	4.0	1.8	1.9	4.0
CuXAES(LMM)	918.3	917.8	916.0	918.4	916.5
α_{Au}	1851.2	1851.6	1848.7	1851.2	1851.1
O1s	NA	529.6	530.4	.	530.2

high concentration of Cu(0) (Table 7). The XPS results and depth profile AES data suggested that the MOCVD film is primarily composed by metal copper, with insignificant amounts of oxygen and carbon.

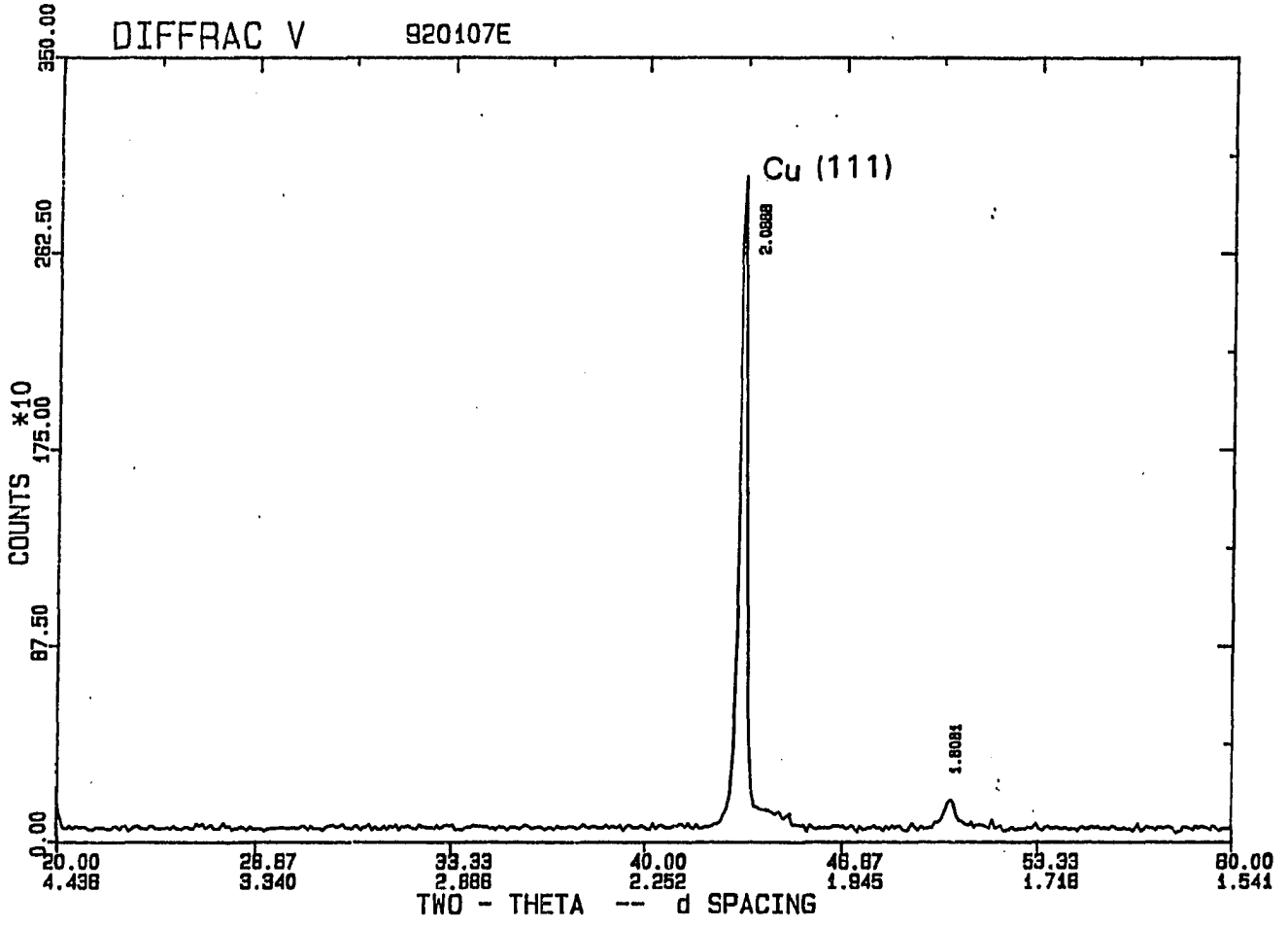

Fig. 12 XRD of Cu MOCVD film

DISCUSSION

Compared with previous copper oxide and copper MOCVD studies, this research has made some technical improvements in the following aspects:

(1) by increasing the carrier gas flow rate, copper oxide films with improved morphology were prepared and homogeneous nucleation were retarded.

(2) an integrated method, which used XRD, XPS, XAES, AES, and IR, was employed to analyze copper oxide MOCVD films.

(3) by using water vapor reacted with sublimed $Cu(acac)_2$ vapor, copper metal MOCVD films were prepared.

From the MOCVD film characterization results (IR and XRD), it was noted that the film stoichiometry could be controlled by regulating specific process parameters. Among these parameters, the deposition temperature and reactant partial pressures were the most important. According to XRD results (Table 1 and Table 2), Cu_2O films were deposited at lower temperatures and CuO films were deposited at higher temperatures, in the MOCVD processes using $Cu(acac)_2$ and O_2 as reactants. The XRD results also indicated that, at intermediate temperatures (380^0C for P_{Cu}=0.20 torr and P_{O2}= 150 torr), MOCVD films containing Cu_2O and CuO mixtures were deposited.

Depending on the specific co-reactant is added with $Cu(acac)_2$ vapor, oxygen or

water vapor, at high temperature, above 370^{o}C, the deposition product is different. By using 190 torr of oxygen and 0.20 torr of Cu(acac)$_2$, CuO was deposited at 400^{0}C. By using 15 torr of water vapor and 0.20 torr of Cu(acac)$_2$, Cu metal was deposited at 400^{o}C. It seems that, at high temperatures, the decomposition pathway for Cu(acac)$_2$ is strongly dependent on the particular secondary reactant is using. At low temperature, below 360^{o}C, both oxygen and water vapor using MOCVD produced Cu_2O phase predominated films.

The oxidation state of Cu in Cu(acac)$_2$ vapor is Cu(2+). According to XPS results from the MOCVD films deposited, at 360^{o}C (with P_{O2}= 150 torr, P_{Cu}=0.20 torr), this value change from 2+ in the Cu(acac)$_2$ vapor to Cu(1+) in Cu_2O solid. The reduction of Cu ions is probably related to McDonald's mass spectrometric study [17]. In his experiment, it was observed that the Cu(II)(acac)$_2$ molecule became a Cu(I)(acac) radical, when one acetylacetonyl (acac) ligand was liberated from the Cu(acac)$_2$ molecule. Since the MOCVD reactor is operated at 340^{o}c, with an oxygen partial pressure of 150 torr, it is recognized that Cu(acac)$_2$ has a strong tendency to has the Cu(II) reduced, when the decomposition of Cu(acac)$_2$ occur. The actual role of O_2 gas in the MOCVD reaction is suggested to oxidize the fragmented hydrocarbon radicals and prevent further reduction of the Cu(I). At higher temperatures ($>$ 420^{o}C), oxygen may react more actively, and Cu(II) will not be reduced to Cu(I) when Cu(acac)$_2$ decomposes; CuO is deposited.

There might be a interrelation between the deposition temperature and reactant concentrations. As revealed by XRD, if the partial pressure of Cu(acac)$_2$ is 0.36 torr, with oxygen partial pressure fixed at 150 torr, Cu_2O films can be deposited at 420^{o}C. This might indicate, if the P_{O2}/P_{Cu} ratio is too low (410 in this case), even high

temperature won't prevent the reduction of Cu(II) in $Cu(acac)_2$ occur.

The experimental results of the P_{O2}/P_{Cu} ratio ranges from 600 to 1000. This evidence probably indicated that the P_{O2}/P_{Cu} ratio is a workable concept in oxide MOCVD process development.

All MOCVD films were polycrystalline, with Cu and Cu_2O films tend to have a preferential orientation. IR and XPS have been proven as a surface sensitive probe especially for detecting noncrystalline phase in the MOCVD films, such as surface carbonates.

Both the deposition temperature and the oxidizer were identified critical factors on film stoichiometry. Based on free radical reaction theory, a primitive model of O_2 assisted $Cu(acac)_2$ pyrolysis process is proposed. By comparing the bond strengths in $Cu(acac)_2$, which ranging from 48 kcal/mol (Cu-O bond) to 100 kcal/mol (C-H bond), to the bond strength of O_2, which has a strong double bond, 119 kcal/mol. This comparison implies that $Cu(acac)_2$ is more fragile than O_2. It is suggested that the decomposition of $Cu(acac)_2$ with formations of reactive radicals is the initiation of the entire reaction.

Overall, the deposition results suggest that both thermal energy (moderate deposition temperature) and oxygen are necessities for depositing copper oxide film. Deposition temperature above a critical value is needed to overcome the energy barrier of $Cu(acac)_2$ pyrolysis. Addition of O_2 may oxidize those decomposed hydrocarbon radicals which may contaminate or reduce the deposited oxide film.

CONCLUSION

According to spectroscopic results, Cu_2O films were deposited by the MOCVD process using $Cu(acac)_2$ as the precursor. The film composition was measured by AES, XPS, and XRD. It seems the Cu_2O (111) oriented grains are the primary phase. CuO films were prepared by MOCVD with temperatures above 420^oC. CuO films have no preferential orientation in the structure. Cu films were prepared by MOCVD process using $Cu(acac)_2$ and water vapor as the reactants. The phase distribution in MOCVD films depend on processing condition, mostly deposition temperature and reactant concentrations.

ACKNOWLEDGEMENTS

The author would like to thank Dr. Andreg for his assistance in XPS measurement and Dr. Belvolo for his assistance in carrying out AES measurement.

REFERENCES CITED

1. W.M. Sears, and E. Fortin, Thin Solid Films, 103, 303 (1983).

2. H.J. Pauwels, and G. Vanhoutte, J. Phys., D11, 649 (1978).

3. S. Nakahara, Thin Solid Films, 102, 345 (1983).

4. H.S. Potda, and A. Mitra, Solar Energy Matl., 4, 291 (1981).

5. G. Beensh-Marchwicka, and M. Slaby, Thin Solid Films, 88, 33 (1982).

6. S.R. Kurtz, Thin Sold Films, 147,,167 (1987)

7. C.M. Jackson, Surface Science, 6, 171 (1967)

8. T. Karsson, Solar energy Matl., 10, 105 (1984)

9. D. Kachieve, J. Cryst. Growth., 40, 29 (1977)

10. M.H. Grabow, J. Appl. Phys., 98, 561 (1988)

11. S. J. Poston, R.K. Reisman, J. Electron. Matl., 18, 553 (1989)

12. A. Scherer, Solar Energy Matl., 9, 139 (1989)

13. K. Zhang, Appl. Phys. Let., 54, 380 (1989)

14. O.B. Ajayi, M.S. Akanni, and J.N. Lambi, Thin Solid Films, 185, 123 (1990).

15. D.N. Armitrage, N.I. Dunhill, R.H. West, and J.O. Williams, J. Cryst. Grow., 108, 683 (1991)

16. J. O. Carlsson, personal communication (1992)

17. J.V. Mcdonald, R.G. Charles, and W.M. Hickam, J.Am. Chem. Soc., 62, 1098 (1958)

PAPER II.

GAS PHASE PRODUCT ANALYSIS OF THE COPPER OXIDE MOCVD PROCESS STUDIED BY TRANSMISSION FOURIER TRANSFORM INFRARED SPECTROSCOPY

ABSTRACT

The vapor phase product distribution of the copper oxide MOCVD reaction was analyzed by transmission Fourier transform infrared spectroscopy (FTIR). In the atmospheric pressure MOCVD reactor, 0.20 torr of copper precursor vapor, Cu(acetylacetonate)$_2$ (Cu(acac)$_2$), was transported by a He/oxygen mixture stream and reacted over the heated substrate surface. After deposition, the effluent stream was introduced into a gas phase IR cell, where infrared (IR) spectra were collected, from 400 cm^{-1} to 4000 cm^{-1}. The impact of deposition temperature on the MOCVD gas phase product distribution was examined. The IR results indicated that two factors, steric effect from the chelating ligands, and the bond strength sequence in the Cu(acac)$_2$ molecule, affect the MOCVD gas phase product distribution. For Cu(acac)$_2$ being heated at low temperature, IR absorption bands of water vapor and CO_2 (presumed oxidation products from the CH_3 groups in Cu(acac)$_2$) were observed. Above 300^{o}C, the IR absorption bands of acetylacetone (acac), the chelate ligand in the Cu(acac)$_2$ molecule, appeared. Above 350^{o}C, the IR absorption bands of acetone at 1214, 1363, and 1732 cm^{-1} were observed. At higher temperatures, the intensities of CO_2 bands also increased. Basic decomposition mechanism was proposed, based on the relative bond strengths and the kinetics of free radical reaction.

INTRODUCTION

Due to fundamental interests and practical applications, chemical vapor deposition (CVD) of copper oxide films become an important research topic recently [1-10]. In CVD processes, precursor selection is a critical issue ensuring reliable film quality, high throughput rate, and low operation cost. Among developed copper precursors, such as copper acetylacetonate ($Cu(acac)_2$) [3], copper hexafluoroacetylacetonate ($Cu(hfac)_2$) [4], copper halides [5], and copper(I) *tert*-butoxide ($Cu(O\text{-}t\text{-}Bu)_4$) [6], $Cu(acac)_2$ ($Cu(CH_3COCHCOCH_3)_2$) is especially promising because $Cu(acac)_2$ is safe, cheap, commercial available and capable of producing high quality copper oxide films [7]. Since 1988, $Cu(acac)_2$ has been used as the precursor to prepare copper oxide and copper films by low pressure CVD, plasma CVD, and atmospheric pressure CVD [8-10].

For the $Cu(acac)_2$ using MOCVD process, film stoichiometry was affected by certain specific processing parameters, such as deposition temperature and oxygen partial pressure [8]. Based on deposition studies, researchers have recognized that this behavior might be related to the decomposition mechanism of the $Cu(acac)_2$ precursor in the MOCVD [8-10]. Principally, the decomposition pattern of organometallic complexes, such as $Cu(acac)_2$, depends on the reaction environment. However, contrary to the large number of processing technique studies, very limited amount

of work have been performed on the $Cu(acac)_2$ based MOCVD mechanism, which is complicated by the multiple phases (gas and solid) and multiple reactants ($Cu(acac)_2$ and O_2) involved.

On the other hand, in the much simplified vacuum environment, studies [11-14] indicated that $Cu(acac)_2$ tended to decompose or react by two principal routes. For homogenous pyrolysis (or in the absence of oxidizing agent), the sequence of bond strength in the $Cu(acac)_2$ molecule itself may be the determining factor. Usually, the weakest bond in this organometallic molecule should break first [12-14].

If there are another reactant participates (such as the oxygen involving MOCVD), steric factor (the second parameter) will be significant [15,16]. For example, MOCVD workers have long acknowledged that copper oxide film growth can only be accomplished by breakage of Cu-ligand bonds in the $Cu(acac)_2$ structure. Copper atom must be liberated from the acetylacetonyl ligand cage to form copper oxide. In the $Cu(acac)_2$ molecule, there are four oxygen atoms coordinating to the central copper atom.

Stereochemistry argument have suggested that this square planar structure of $Cu(acac)_2$ acts as a structural hindrance against nucleophilic oxidizer's attack to the central copper atom[15]. Collman has provided supporting evidence with isotopic labelling experiments [16]. In a series of room temperature solution study, Collman characterized the structures of activated $Cu(acac)_2$ complexes and concluded that the most active sites in the $Cu(acac)_2$ were on the "ring" C-H and the branch CH_3 groups. That is, copper is essentially well "protected" and inert[16]. The reaction of oxidizing agent with center copper is inhibited, unless the $Cu(acac)_2$ molecule itself breaks up.

The behavior of $Cu(acac)_2$ decomposition in inert or vacuum environment primarily followed the bond strength model [12-14]. Based on mass spectrometry results, Mc Donald proposed two competing routes for $Cu(acac)_2$ decomposition: one through successively losing of the CH_3 on the acac ring and followed by complete fracture of the remain body. The other favored liberating the whole acetylacetonyl at once [12]. Also using mass spectroscopic analysis, Charles [13] studied the impact of temperature on $Cu(acac)_2$ decomposition in a vacuum environment. Charles found that, above 200^oC, $Cu(acac)_2$ began to release heavier fragments. Acetylacetone was found from 200^oC to 250 ^oC. Acetone, acetic acid, and CO_2 were found from 250^oC to 350^oC. Recently, Richardson used Fourier transform mass spectrometry to study $Cu(acac)_2$ decomposition and confirmed earlier findings [14]. Richardson also discussed the extensive proton exchange phenomena between acetylacetonly radicals and acetylacetone vapor molecule [17]. Among these experiments, acetylacetone seemed to be a generally observed products for $Cu(acac)_2$ pyrolyzed in inert environment, where the intra-molecular bond strength was assumed to be the determining factor.

However, these studies were all performed in idealized UHV environments, without oxidizing agent involved. It was also assumed that there was no surface reaction (a homogeneous state). On the other hand, copper oxide MOCVD processes operate at atmospheric pressure, with a significant concentration of oxygen; both homogeneous reaction and heterogeneous reaction are significant.

Research challenges for copper oxide MOCVD are presented in two aspects. First, ambiguity regarding whether bond strengths or stereochemical factor is the determining factor for $Cu(acac)_2$ decomposition in the MOCVD reactor. Based on

the methodology discussed above, analysis of the gaseous product distribution from the MOCVD reactor seems to be a feasible approach. The relative distribution of vapor phase products might reflect the specific controlling parameter. For instance, if a large amount of heavier compounds, such as acetylacetone, were observed in the effluent vapor, it might indicate the breakage of Cu-O bond, the weakest bond in $Cu(acac)_2$, occur. That is, the bond strength factor determines how $Cu(acac)_2$ pyrolyzes.

The second challenge exists on the technical aspect. The MOCVD vapor analysis should be performed with instrument owning on line measurement capability, at atmospheric pressure and without distorting the actual information. Among analytical instrument available, gas phase transmission IR spectrometry seems to be an impressive candidate. IR owns the advantages of: accuracy on monitoring concentration of gas phase species, sensitivity on the wavenumber shifts of specific functional groups, and nondestructive diagnosis nature [17]. However, transmission IR has never been applied to the study of pyrolysis $Cu(acac)_2$ before. In our group, the IR gas phase analysis has been a well developed technique on catalysis research [18]. We modified this IR analysis technology and attempted to use it for MOCVD gaseous product stream analysis.

In this preliminary study, essential gaseous products from decomposed $Cu(acac)_2$ vapor in oxygen enriched environment were identified by transmission FTIR. The impact of temperature was examined.

EXPERIMENTAL PROCEDURE

Depending on the specific temperature ranges studied, the experiments were performed in three stages with three different experimental set-ups. For $Cu(acac)_2$ pyrolysis experiment in the temperature range from room temperature to 150^oC, a in-situ experimental set up was used (Fig. 1). 10 mg of $Cu(acac)_2$ was placed in a sample pan made of Al foil and pyrolyzed in a IR cell, where IR spectra were collected. This IR cell, which was made by modifying an gas IR cell used for catalysis research, was pre-filled with He/O_2 (4:1) mixture gas. After the temperature of pan reached the designated temperature for 10 minutes, IR spectra were collected with an accumulation of 400 scans.

This gas IR cell, with a optical transmission length of 8 cm, is composed by a quartz tube and two 38 mm diameter, 6 mm thick KBr windows. The cell wall temperature was maintained at 150^oC, by resistive heating to prevent condensation of vapor. Both KBr windows were water cooled to prevent thermal cracking due to difference between the thermal expansion coefficients of KBr and copper rings.

The second stage of experiment, with temperature range from 150^oC to 280^oC, was performed in an ex-situ IR/$Cu(acac)_2$ set up (Fig. 2). This system was composed by a subliming/decomposing flask containing $Cu(acac)_2$ and a gas IR cell used in stage I. 2 grams of $Cu(acac)_2$ was loaded in a 250 ml flask, which was situated on

a programed heated hot plate. A steam of He/O_2 mixture, with a total flow rate of 125 ml/min, transported both sublimed $Cu(acac)_2$ vapor and decomposed fragments into the IR cell, where IR spectra were collected as described above.

In the final stage, the ex-situ MOCVD-IR experiment (Fig. 3) was conducted in the MOCVD operating temperature range, from 280^oC to 400^oC. MOCVD experiments were performed in a horizontal quartz tube reactor as described before [10]. The ex-situ MOCVD gas phase products analysis was conducted by introducing exhaust gas from the MOCVD reactor into the IR cell.

In all three stages of experiments, the gas IR cell was installed in the sample compartment of a Nicolet 60SX FTIR spectrometer, which is computer interfaced and can perform automatic spectral scanning. Every IR spectra was collected with a resolution of 4 cm^{-1}, by averaged over 400 scans. Each scan took 1 second. The spectrum of each sample was the ratio between the collected file and the background file, which was collected from the empty IR cell with carrier gas flowing through it.

In the MOCVD reactor, the $Cu(acac)_2$ (as received Aldrich, purity 99%) was sublimed with He (Air products) as the carrier gas. This stream was mixed with He and oxygen to obtain the desired partial pressure of precursor vapor. The depositions were performed on Si(100) (p-type, Unisil corp.).

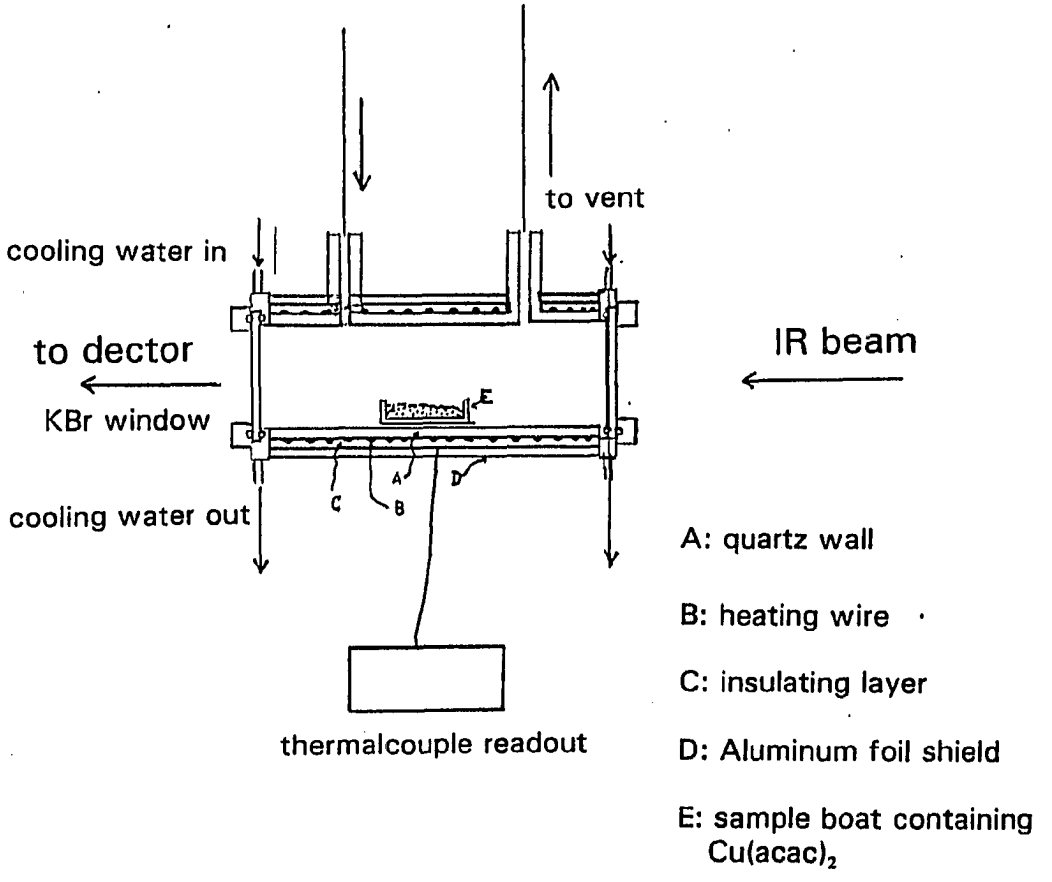

Fig. 1 In-situ $Cu(acac)_2$ pyrolysis–IR analysis cell

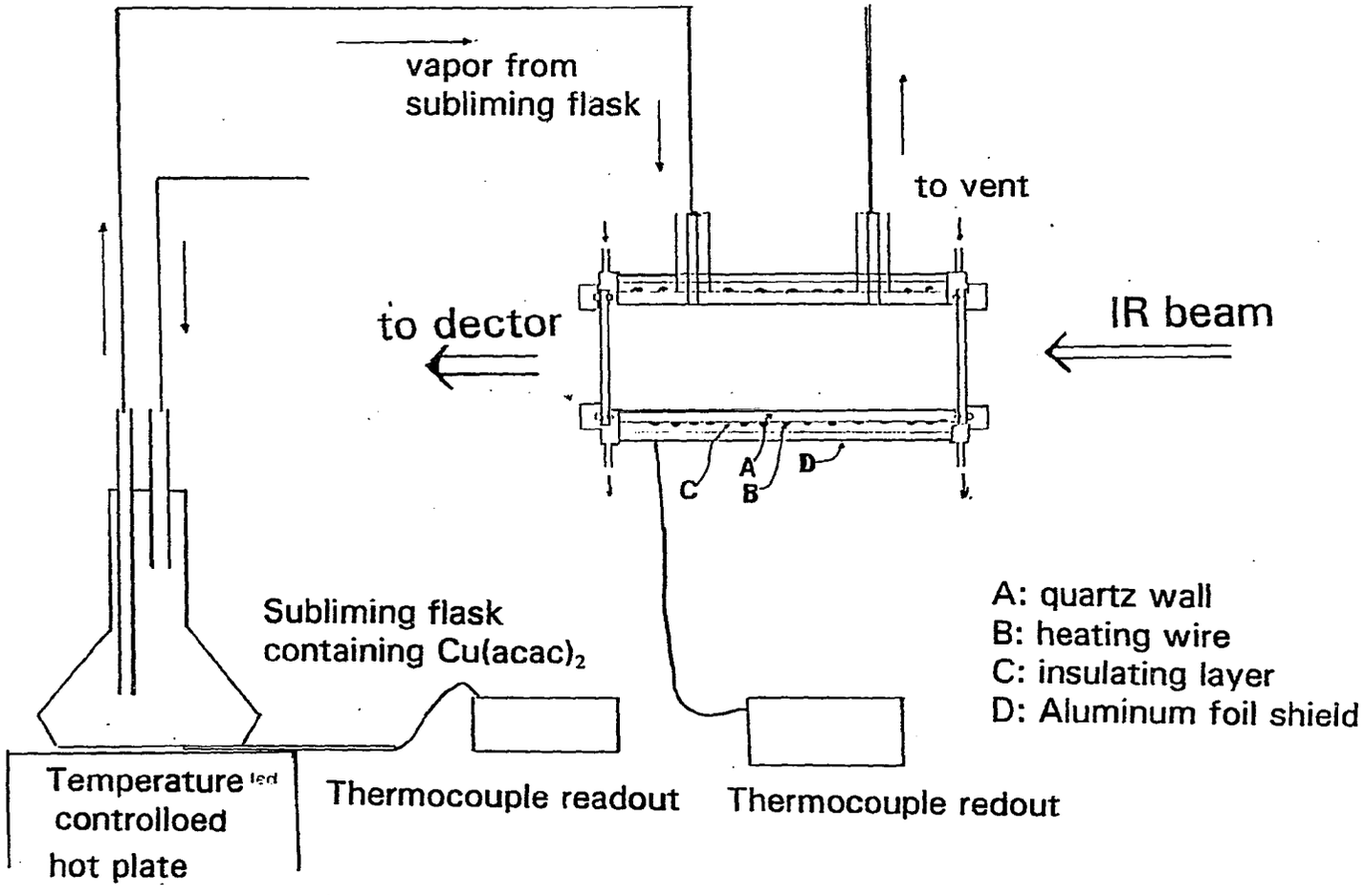

Fig. 2 Ex-situ $Cu(acac)_2$ pyrolysis–IR analysis set-up

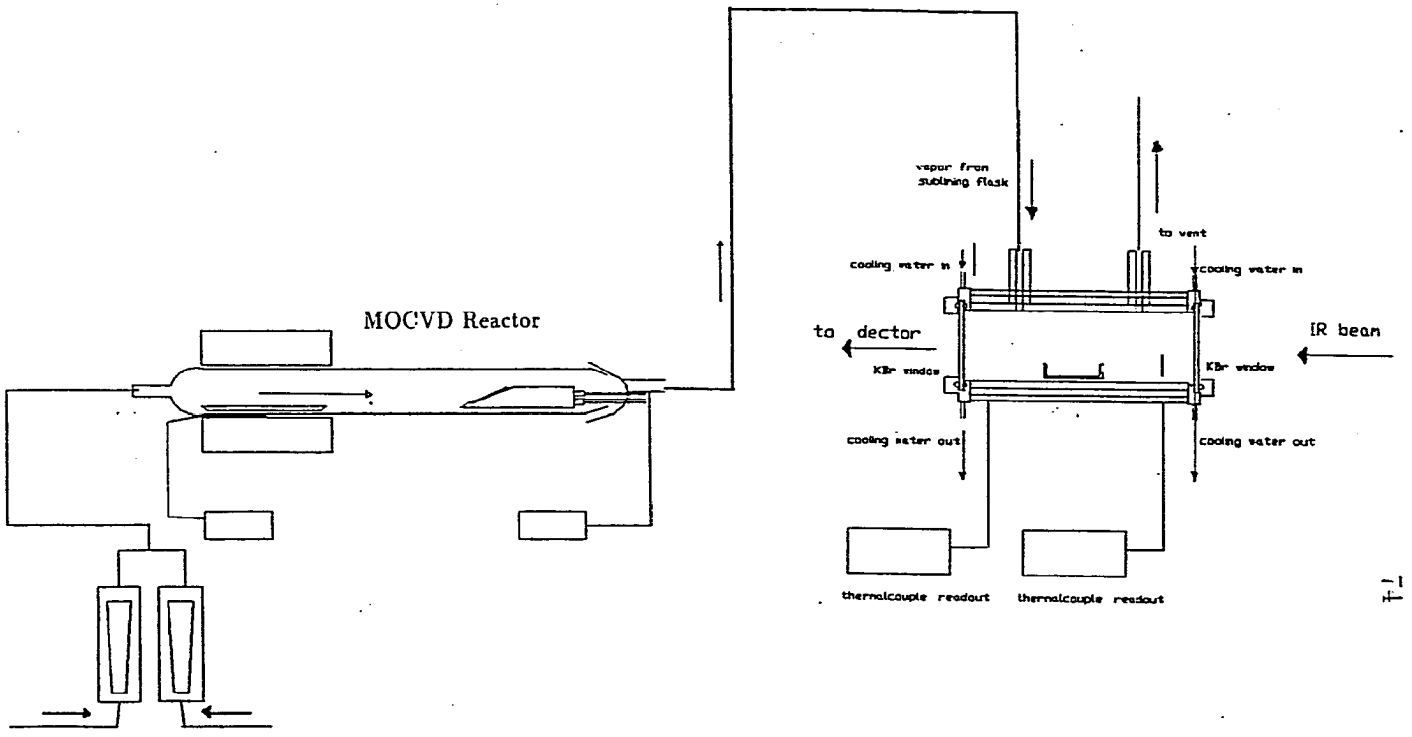

Fig. 3 Ex-situ MOCVD–IR analysis set-up

EXPERIMENTAL RESULTS

IR Spectrum of $Cu(acac)_2$

To both identify the purity of $Cu(acac)_2$ purchased (Aldrich co.) and establish reference bands of $Cu(acac)_2$ for comparison with IR spectra from the MOCVD exhaust gas stream, IR spectrum of a solid standard $Cu(acac)_2$ (0.01g)/KBr (0.5g) disk was collected. The IR bands observed in the spectrum, as shown on Fig. 4, were compared with values in literature[19] (Table 1). Essentially, the three characteristic bands of $Cu(acac)_2$ at carbonyl related 1500cm^{-1} zone(1529, 1552, and 1577 cm^{-1}), which are the unique IR band feature of diketonate coordinated organometallic compounds [20], were used to identify $Cu(acac)_2$.

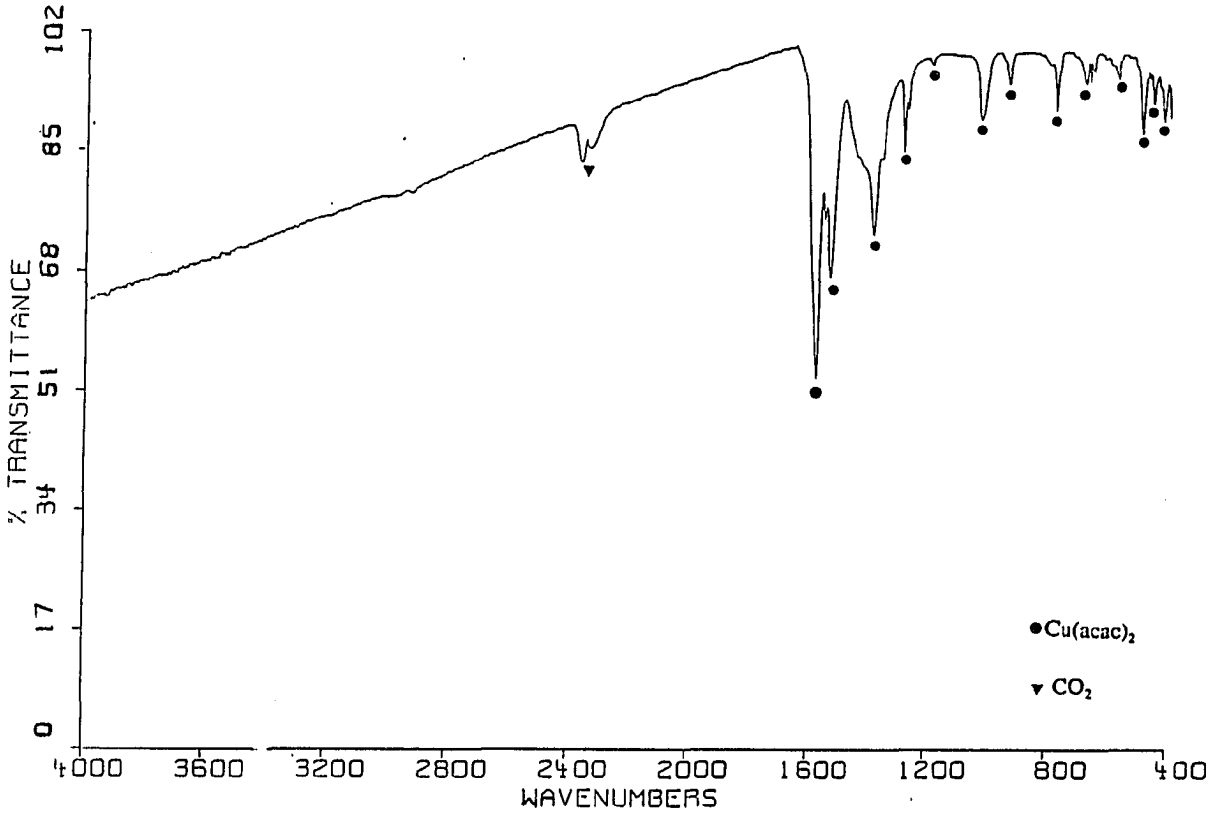

Fig. 4 IR spectrum of $Cu(acac)_2$/KBr wafer

Table 1: IR bands found in $Cu(acac)_2$/KBr wafer and reference bands positions (cm^{-1})(Nakamoto [19])

Experimental values	Nakamoto	Band assignment
1579	1577	v(C-C) + v (C-C)
1550	1552	combination
1530	1529	v(C-O) + v(C-C)
1459	1461	$\delta_d(CH_3)$
1353	1353	$\delta_s(CH_3)$
1274	1275	v(C-CH_3) + v(C-C)
1189	1189	ρ_δ(CH) + v(C-CH_3)
1018	1018	$\delta_r(CH_3)$
936	936	v(C-C) + v(C-O)
780	780	π(CH)
684	684	v(C-CH_3)+ring deformation
.	.	+v(Cu-O)
653	653	$\pi(CH_3$-C)
611	611	ring deformation + v (Cu-O)
452	452	v(Cu-O) + v (C-CH_3)

In-Situ $Cu(acac)_2$ Pyrolysis-IR Study

To study the impact of temperature on $Cu(acca)_2$ pyrolysis products, IR experiment was first performed with $Cu(acac)_2$ pyrolyzed in the temperature range from room temperature to 250^oC. This experiment was aimed to investigate (a) the possibility of pre-decomposition of $Cu(acac)_2$ vapor in the MOCVD reactor (b) possible decomposition mechanism, and (c) potential contaminating products to MOCVD film growth.

To observe the trace amount of initial oxidative decomposition products from $Cu(acac)_2$, the first experiment was carried in an in-situ IR-pyrolysis cell (Fig. 1). $Cu(acac)_2$ was pyrolyzed in an ambient pre-filled with He/O_2 (4:1) mixture. Below 80^oC, no IR band was observed. From 80^oC to 120^oC, the collected IR spectra revealed that only $Cu(acac)_2$ vapor was present in the gas phase.

The next experiment was performed with 10 mg of $Cu(acac)_2$ pyrolyzed in an IR cell, which was continuously purged with a He/O_2 (4:1) mixture stream (125 ml/min).

The IR spectra were shown on Figure 5, Below 150^oC, only the IR bands of $Cu(acac)_2$ vapor were observed. Above 160^oC, two groups of IR bands, one from 1300 to 1800 cm^{-1} and the other from 3300 to 3800 cm^{-1}, were observed. These bands were assigned to the O-H banding modes and O-H stretching modes of water vapor. Above 230^oC, $Cu(acac)_2$ condensed on the windows and deterred further experiment. Subsequent experiments were conducted with an ex-situ IR pyrolysis set up (Fig. 2). Gas phase species from decomposed $Cu(acac)_2$ were then transported by 100 ml/min of He and 25 mil/min of O_2 into the IR cell. The IR results again indicated that water was the lowest temperature decomposition product of $Cu(acac)_2$

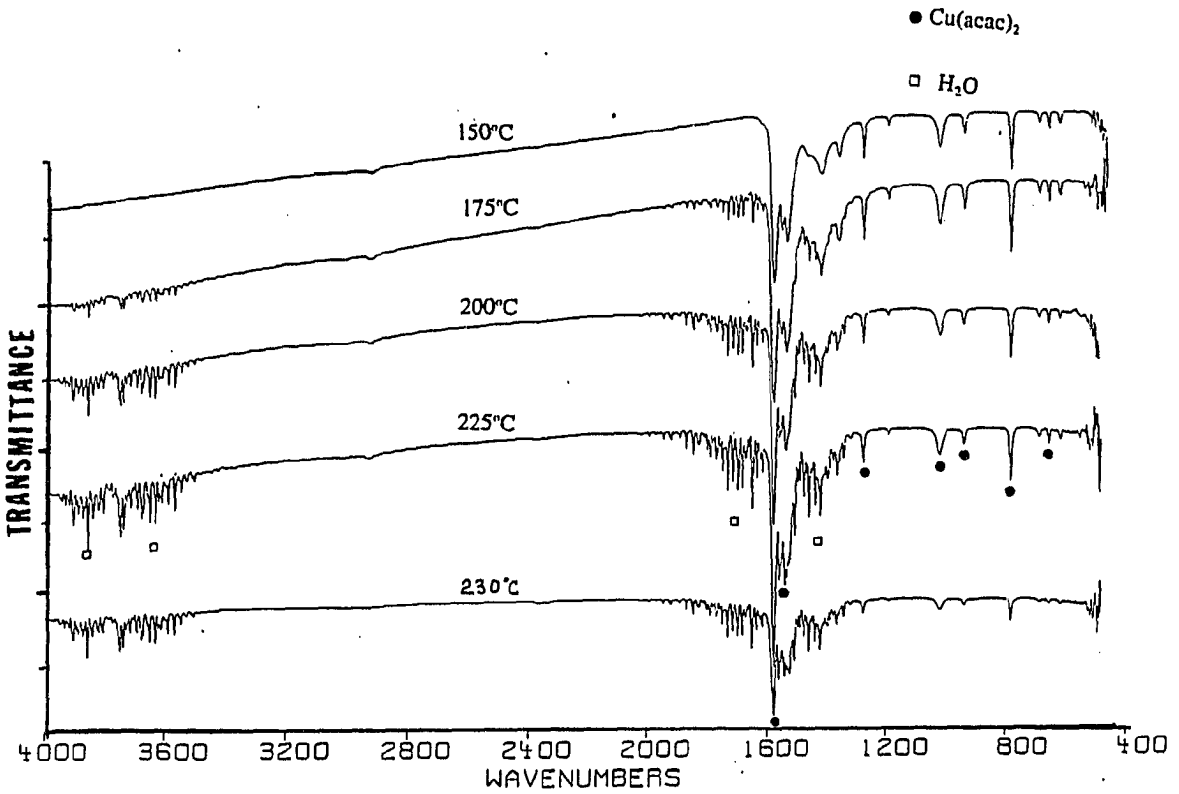

Fig. 5 IR spectra of gas phase products from Cu(acac)$_2$ pyrolysis with temperatures from 150^{o}C to 230^{o}C

(from 160 to 190 ^{o}C). Above 275^{o}C, CO_2, with its strong IR stretching mode at 2330 cm^{-1} and 2359 cm^{-1}, and weak IR bending mode at 668 cm^{-1}, was found (Fig. 6).

The final experiments were conducted by directly introducing the effluent gas from the MOCVD reactor into the IR cell (Fig. 3). The IR spectra were similar to the flask sublimed results; only CO_2 and H_2O were found in the temperatures from 150^{o}C to 280^{o}C.

Ex-situ MOCVD-IR Gas Phase Analysis

Above 300^{o}C, IR spectra of the effluent gas from the subliming flask revealed intense bands of $Cu(acac)_2$. These IR bands from $Cu(acac)_2$ are so intense that the IR bands from other species, particularly in the carbonyl region (1200-1700 cm^{-1}), were masked out. This phenomena implies that, in the flask, above 300^{o}C, the $Cu(acac)_2$ evaporation rate (which generated $Cu(acac)_2$ vapor) exceeded the $Cu(acac)_2$ decomposition rate (which produced vapors of decomposed fragments). Based on this fact, the flask set-up was unsatisfactory for high temperature study.

To acquire $Cu(acac)_2$ pyrolysis data at temperature above 300^{o}C, the IR spectra have to be taken directly from exhaust gas of the MOCVD reactor, which sublimes $Cu(acac)_2$ solid and decomposes $Cu(acac)_2$ vapor separately (Fig. 3). Based on the ex-situ MOCVD-IR results, both deposition temperature and presence of oxygen are the most important factors determining the gaseous pyrolysis product distribution of $Cu(acac)_2$.

Above 300^{o}C, with using He/O_2 (4:1) mixture as the carrier gas, the IR spectra (Fig. 7) of the MOCVD gas products revealed additional absorption bands from

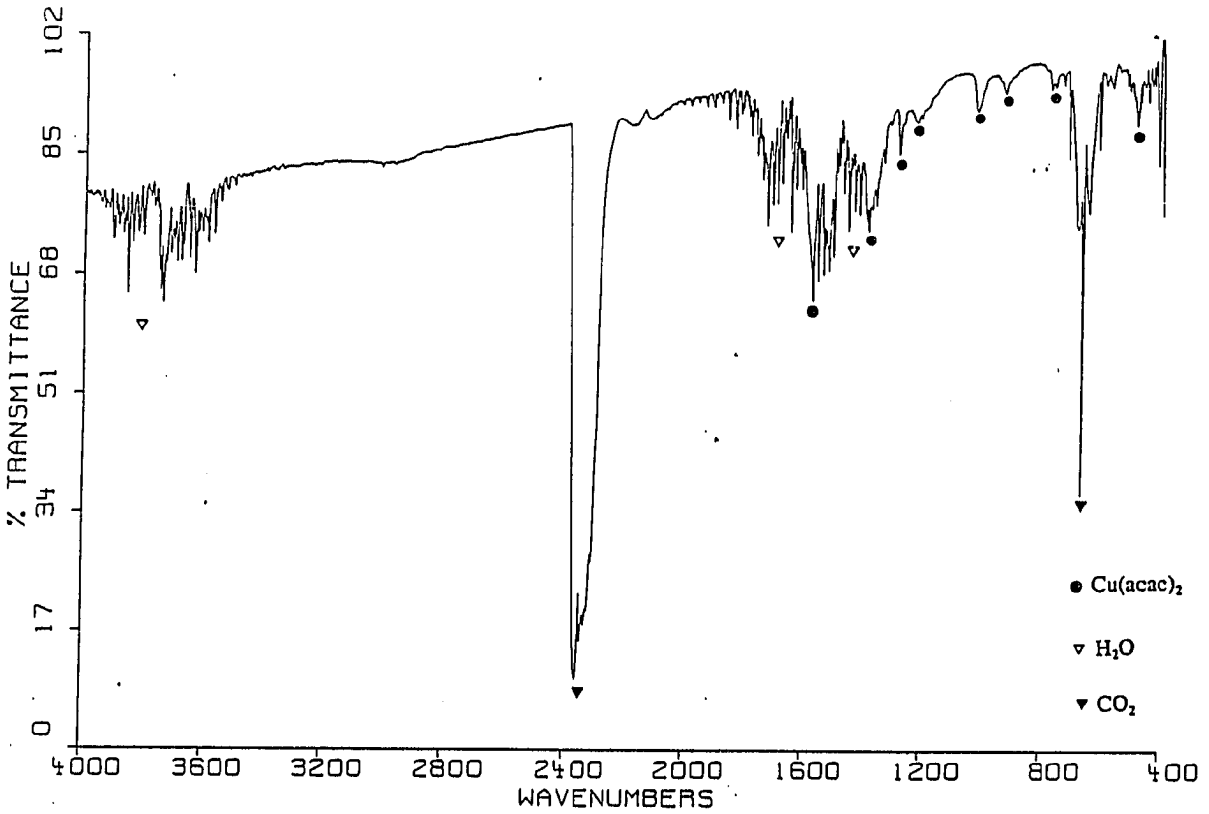

Fig. 6 IR spectrum of gas phase products from $Cu(acac)_2$ pyrolysis (temperature at 280^oC

organic vapor molecules, with higher molecular weight. One significant C=O vibrational band appeared at 1623 cm^{-1} was assigned to the cyclized enol form of acetlyacetone (acac) (Fig. 8), which has the strongest carbonyl peak at 1623 cm^{-1}) [21]. Due to thermodynamics, the vapor phase acac usually favors to exist in the enol form (more than 96%) [22]. The other bands of acac were also identified, as shown on Fig. 7. However, due to the similarity in symmetry with acac ligands in $Cu(acac)_2$, the positions of these bands were very near to the corresponding bands of $Cu(acac)_2$. It was found that the 1623 cm^{-1} band was the most compelling evidence for identification of acac in the $Cu(acac)_2$/acac vapor mixture. Characteristic bands of $Cu(acac)_2$ at 1532, 1552, and 1574 cm^{-1} were also identified. The small wavenumber shifts might be attributed to the temperature effect on the $Cu(acac)_2$ vapor. In addition to acac and $Cu(acac)_2$, IR bands of methane, with weak intensity at 1300 cm^{-1} and 3000 cm^{-1}, and acetone which has main peaks at 1214 cm^{-1}, 1363cm^{-1}, and 1732 cm^{-1}, were found [23, 24]. Overall, as temperature rose from 300^{o}C to 340^{o}C, the intensities of IR bands from CO_2 and water both grew up, with acetylacetone as the primary heavy-molecular-weight specie in the vapor phase.

For MOCVD operated with deposition temperature above 350^{o}C, acac, acetone, and $Cu(acac)_2$ are the primary species found in IR (Fig. 9), while the concentration (intensities of IR bands) sequence changed. Acetone, noticed by its three equivalent strong bands at 1214, 1363, and 1732 cm^{-1}, became the major decomposed fragment in the gas phase. Also, the intensities of the O-H bands and C=O bands increased significantly, indicating more CO_2 and H_2 were produced. A supporting evidence for the presence of acetone by identification of its characteristic C-H bands at 2947, 2970, and 3010 cm^{-1}. The unique vibrational-rotational transition band structure

due to the free motion of vapor molecule was also noted (Fig. 10).

For MOCVD operated at temperatures from 350^{o}C to 400^{o}C, the IR bands of acetone became more intense than the IR bands of acac. In this He:O_2 (4:1) mixture gas using MOCVD environment, acetone has the strongest IR bands among 1200 to 1700 cm^{-1}. In this temperature range, temperature increasing caused the intensities of the CO_2 and H_2O IR bands increased.

Overall, at low temperature, from 150^{o}C to 250 ^{o}C, CO_2 and H_2O were observed as the only thermal oxidative dissociation products from Cu(acac)$_2$. Heavier decomposed fragments, such as acetylaceton and acetone, were found at temperature above 270 to 280^{o}C. The location of these lowest temperature seemly weren't affected by the system oxygen concentration. Overall, in the MOCVD processing condition, the primary fragments in the gas phase were acetone and acetylacetone. Especially , the vapor phase concentration of acetone increased enormously as deposition temperature increased from 340^{o}C to 390^{o}C, where the primary composition phase of deposition product was found to transit from Cu_2O to CuO.

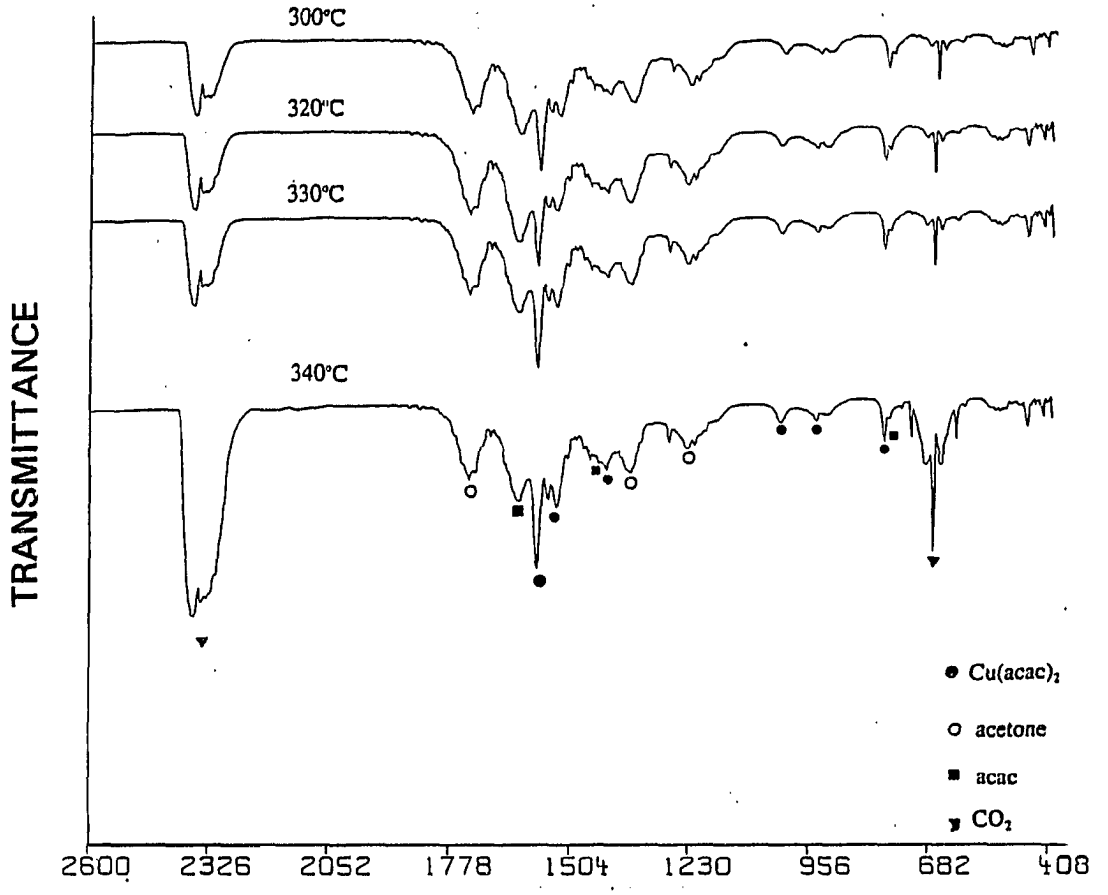

Fig. 7 IR spectra of gas phase products from the copper oxide MOCVD reactor (T_{dep}= 300 - 340^{o}C, Q_{He}:Q_{O2} = 4 :1)

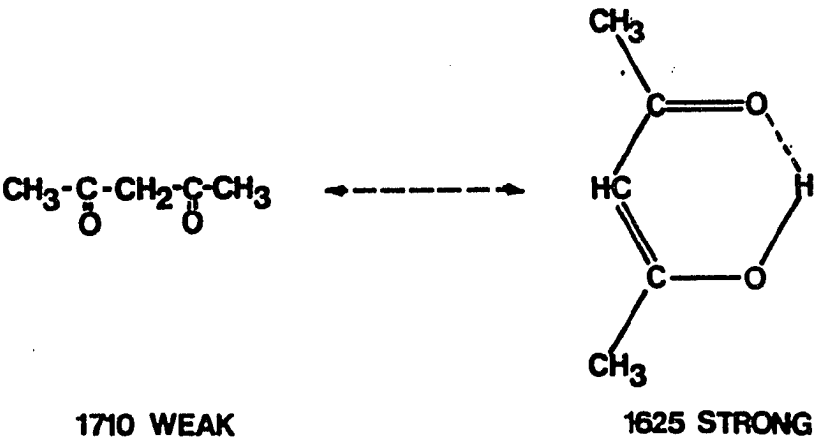

Fig. 8 Vapor phase Keto-Enol transformation of acetylacetonate

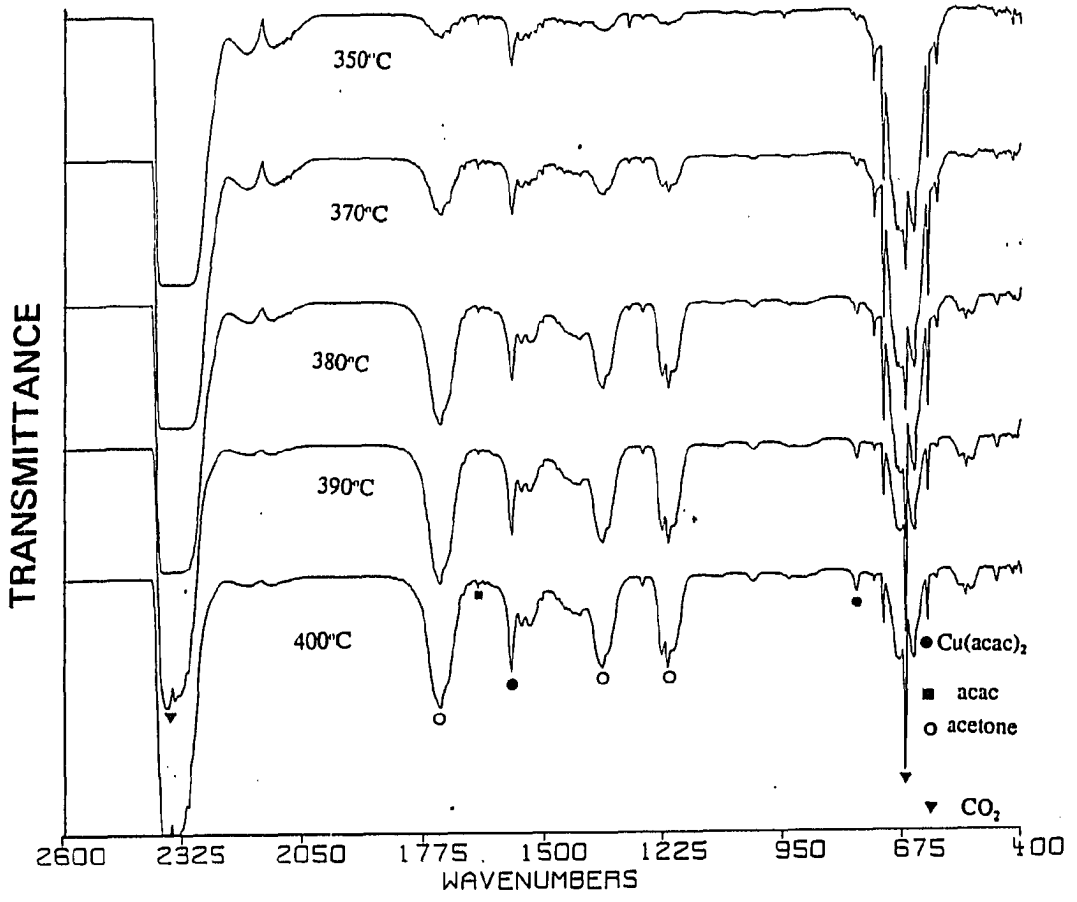

Fig. 9 IR spectra of gas phase products from copper oxide MOCVD reactor (T_{dep}= 350-400°C, $Q_{He} : Q_{O2}$ =4 : 1)

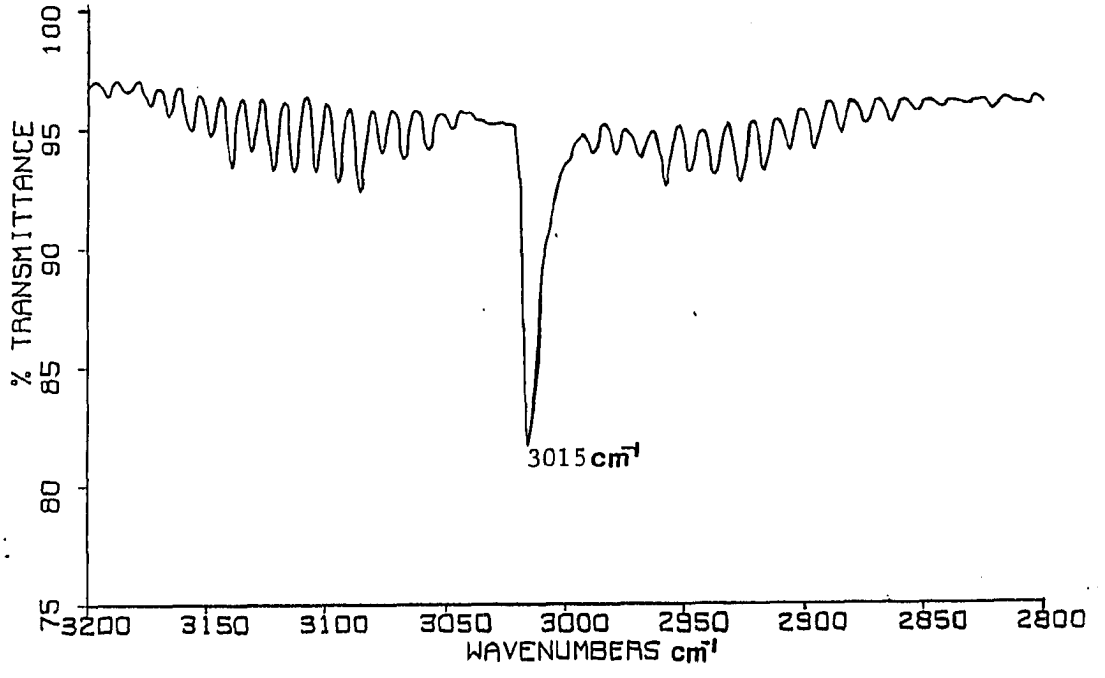

Fig. 10 IR spectrum of the C-H rotational-vibrational transition band

DISCUSSION

Based on reaction kinetics, the key components determining the deposition rate of the copper oxide MOCVD process should be the reactive intermediates, copper carrying radicals. These radicals are liberated from dissociated $Cu(acac)_2$ molecules and can further decompose to leave copper atoms onto the substrate surface. Because these radicals are unstable, they are unable to be observed by IR directly. However, through observing the stable gaseous products from the MOCVD reactor, IR results can be used to interpret some kinetic aspects of the MOCVD process.

As an empirical model, the overall IR observation can be interpreted according to the competition between two factors, the molecular steric effect and relative bond strength. From IR results, each factor determines the product distribution at one specific processing condition. At low temperatures (150^oC to 280^oC), due to the steric effect, the CH_3 groups, which are the preferential groups on the $Cu(acac)_2$ molecules, are oxidized first with CO_2 and H_2O produced(Fig. 5,6). Since at such a low degree of thermal activation, thermal energy is insufficient to break any bond in the $Cu(acac)_2$. In this temperature range, $Cu(acac)_2$ itself doesn't dissociate, or undergoes any unimolecular decomposition. In this circumstance, the relative bond strength factor is not important. In the $Cu(acac)_2$ molecule, only the outermost CH_3 groups experience the least steric hindrance and are oxidized by ambient oxy-

gen. When the deposition temperature reached 300^{o}C, IR spectra indicated that acetylacetone molecules were in the gas phase. These heavier decomposed fragments were resulted from the breakage of the weakest Cu-O bonds in $Cu(acac)_2$. This is a strong indication that the bond strength sequence factor, which has a strong dependence on the thermal activation energy, resulted in this phenomena.

It is reasonable to assume that the low temperature products, CO_2 and H_2O, were resulted from the oxidation of methyl radicals (CH_3) on the ligand rings of the $Cu(acac)_2$. This assumption is supported by previous studies of the $Cu(acac)_2$ molecular structure; the specific carbon-carbon bond between C-CH_3 has the second lowest bonding strength in the $Cu(acac)_2$ molecule: 2.6X10^{5}dyne/cm [19]. Mass spectra of $Cu(acac)_2$ fragmentation also implied that the ion peaks particularly at m/e=247 and 232, the molecular weights of $Cu(acac)_2$-CH_3 radical and $Cu(acac)_2$-2(CH_3), were of high intensities [13]. From deposition results in part I, it seems this CH_3 oxidation reaction will not initiate the solid film deposition. One reason might be that the Cu-ligand structure in the remained fragment is not dissociated; this copper carrying species is stable and resists to liberate copper.

Previous $Cu(acac)_2$ decomposition experiments indicate that the acetone vapor, which is observed in Fig. 9, originates from the decomposition of acetylacetone [25-30]. Mass spectrometric studies [12] indicated that decomposition of $Cu(acac)_2$ never produces acetone, but the decomposition of acetylacetone produces acetone [25]. From IR study, it indicated that acetone was the primary decomposition product at the high temperature region, 350^{o}C to 400^{o}C. This is consistent with the Charles's observation that the $Cu(acac)_2$ pyrolysis reaction proceed more extensively at high temperature, and acetone was found at temperatures above 350^{o}C [13].

As discussed in part I, in the MOCVD process, $Cu(acac)_2$ undergoes a reduction reaction for deposition temperatures below 380^oC. McDonald noted that Cu ion in the $Cu(II)(aca)_2$ molecule is redu when $Cu(acac)_2$ decomposes into Cu(acac) and acac radicals [13]. In the IR experiments performed at temperature from 300^oC to 340^oC, acetylacetone vapor was observed. This observation indicates that a reaction (as similar to what McDonald observed in mass spectra) which produces Cu(I)(acac) radicals, may take place in the MOCVD reactor.

Based on IR results, we hypothesized a simplified model account for the MOCVD kinetics (Fig. 11). First, there are two factors acting on the reaction kinetics of $Cu(acac)_2$ molecule, the steric effect exerted by four CH_3 and electrostatic repulsion force by four oxygen atoms, and the bond strength sequence. The bond strength sequence is a strong function of energy, the activation energy, or the temperature of the system (thermal energy). On the other hand, steric effect, in the isobaric gas phase system, doesn't seem to be affected by the system temperature. Therefore, when deposition temperature increases, the relative importance of these two factors may change. According to IR results, in the low temperature experiments, thermal energy is not enough to provide substantial amount of reactive activated radicals. Steric effect is the influential factor. At high temperature, thermal energy is enough to provide a large amount of reactive activated complexes, so that the weakest Cu-O bonds break first and form acetylacetone molecules and Cu(acac) radicals in the gas phase. This step might be the initial step of film deposition. It might be speculate that the Cu(acac) radical is the most abundant reactive intermediates in the MOCVD gas phase. This Cu(acac) radical is supposed to have a much higher reactivity with oxygen, and the interactions between $Cu(acac)_2$ radicals and O_2 composed the prop-

agation step in the film deposition process. The concentration of Cu(acac) radicals might depend on the deposition temperature and oxygen concentration, which are determinative to the composition of deposited films.

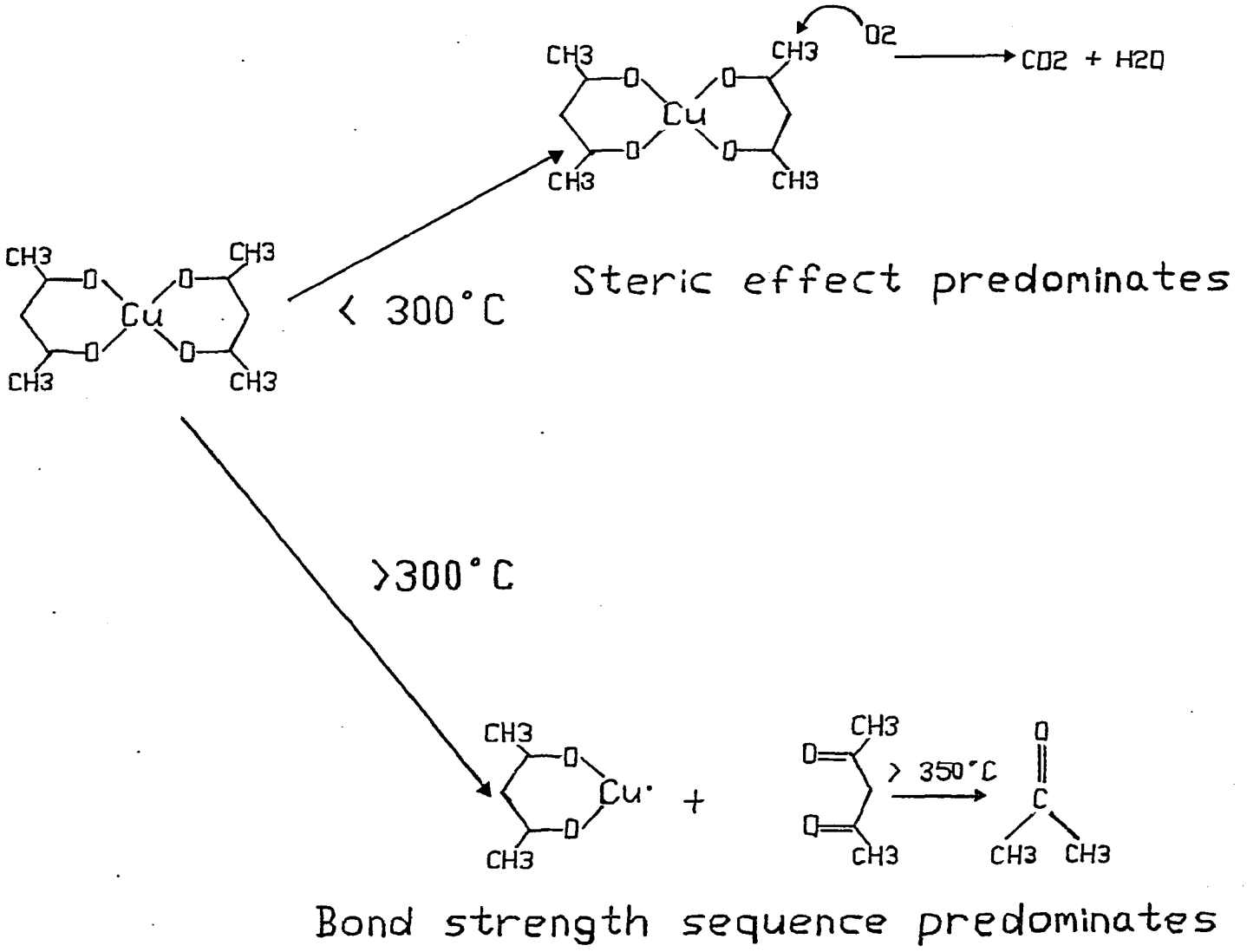

Fig. 11 Suggested decomposition mechanism of $Cu(acac)_2$ in the MOCVD condition (P= 1atm, P_{O2}= 0.2 atm

CONCLUSION

Gaseous products from the copper oxide MOCVD process were analyzed by FTIR in an atmospheric pressure condition. The results indicated that the decomposition product distribution of $Cu(acac)_2$ in the MOCVD reactor was influenced by thermal energy and the presence of oxidizer. Acetylacetone, acetone, CO_2, and water vapor were the primary products observed by IR.

Stereo hindrance is the determining factor at low temperatures. Due to steric factor, oxygen can not approach the central copper, but can oxidize the outermost CH_3 groups in the ligand of $Cu(acac)_2$ and produces H_2O and CO_2. The bond strength sequence factor, or the unimolecular decomposition of $Cu(acac)_2$ becomes important as temperature reaches 300^oC. Due to the breakage of Cu-O bonds in $Cu(acac)_2$, acetylacetone ligand was liberated and further decomposed into acetone in the oxidative environment (above 380^oC). Copper is liberated at this temperature region and the MOCVD processing range is directly related to this mechanism. Higher temperature causes more acetone molecules produced and promotes the $Cu(acac)_2$—$Cu(acac)$+acac reaction toward the irreversible right side. This action favors production of more copper carrying radicals and deposition rate is increased.

REFERENCES CITED

1. W.M. Sears, and E. Fortin, Thin Solid Films, 103, 303 (1983).

2. H.J. Pauwels, and G. Vanhoutte, J. Phys., D11, 649 (1978).

3. S. Zhang, and H.C. Lu, Appl. Phys. Lett., 52, 1974 (1988).

4. D.N. Armitrage, N.I. Dunhill, R.H. West, and J.O. Williams, J. Cryst. Grow., 108, 683 (1991)

5. L. Brewer, and A. C. Loonam, J. Am. Chem. Soc., 72, 3038 (1950)

6. M.E. Gross, J. Electrochem. Soc., 138, 2422 (1991).

7. P.J. Gellings, MRS Fall meeting, 168, 125 (1990)

8. Y.N. Chang and G.L. Schrader, MRS Proceeding, vol. 250, (1990)

9. H. Holzschuh and H. Suhr, Appl. Phys. A 51, 486, (1990)

10. H. Suhr, and F. Schmaderer, Physica C, 151, 784 (1988).

11. M.M. Jones, Inorg. Chem., 1, 166 (1962).

12. R.G. Charles, J.V. Hoene, and W.M. Hickman, J. Phys. Chem., 62, 1098, (1958).

13. C.G. Macdonald, and J.S. Shannon, Aust. J. Chem., 19, 1545 (1966)

14. P. Sharpe, and D.E. Richardson, J. Am. Chem. Soc., 113, 8339 (1991)

15. J.P. Collman, and D.A. Buckingham, J. Am. Chem. Soc., 85, 3039 (1963)

16. J.P. Collman, and W.L. Young, Inorg. Syn., 7, 187 (1963)

17. B.S. Sywe, J.R. Schlup, and J.H. Edgar, Chemistry of Materials, 3, 737 (1991)

18. R.W. Wenig, and G.L. Schrader, Ind. Eng. Chem. Fund., 25, 612 (1986)

19. K. Nakamoto, P.L. McCarthy, and A. Martell, J. Am. Chem. Soc., 83, 1272 (1961)

20. M. Mikami, I. Nakagawa, and T. Shimanouchi, Spcetrochimica. Acta, 23A, 1037 (1967)

21. V.R. Mecke, and E. Funck, Zeischrift fur Elektrochemie, 60, 1124 (1956)

22. S. Sasaki, Y. Itagaki, T. Kurokawa, and K. Nakanicshi, Bull. of Chem. Japan, 40, 76 (1967)

23. P.F. Krause, B.G. Glagola, and J.E. Katon, J. Chem. Phys., 61, 5331 (1974)

24. D.C. McKean, Spectrochimica Acta, 31A, 861 (1975)

25. R.G. Charles, W.M. Hickman, and J.V. Hoene, J. Phys. Chem., 63, 1243 (1959)

26. M.J. Lacey, and J.S. Shannon, Organ. Mass. Spect., 6, 931 (1972)

27. C. Reichert, and J.B. Westmore, Cand. J. Chem., 48, 3213 (1970)

28. H.F. Holtzclaw, H.E. Baumgamter, L.L. Lintedt, andP.F. Roger, J. Am. Chem. Soc., 91, 3774 (1969)

29. M.J. Lacey, C.G. McDonald, and J.S..Shannon, Aust. J. Chem., 25, 2559 (1972)

30. C. Reichert, G.M. Bancroft, and J.B. Westmore, Cand. J. Chem., 48, 1362 (1970)

PAPER III.

THERMAL DECOMPOSITION OF MOCVD PRECURSOR, COPPER(ACETYLACETONATE), STUDIED BY DIFFERENTIAL SCANNING CALORIMETRY (DSC)

ABSTRACT

Thermal decomposition of the copper oxide MOCVD precursor, copper acetylacetonate ($Cu(acac)_2$), was studied by differential scanning calorimetry (DSC) at atmospheric pressure, in an ambient with reactive gas concentration simulated as the standard processing condition used in copper oxide MOCVD. In each dynamic DSC experiment, 10 mg of $Cu(acac)_2$ sample was programed heated at a constant heating rate in a temperature range from 25^oC to 400^oC. In the collected thermograms, energy exchanges between system and environment were recorded with respect to the specific temperature. In each experiment, either an inert (He, N_2) or reactive (air, $He+O_2$) gas stream was purged into the sample chamber with a constant flow rate of 36 ml/min. According to DSC results, thermal dissociation of $Cu(acac)_2$ starts at 200^oC, and ends by 350^oC. Experimental data indicated that the pyrolysis pattern of $Cu(acac)_2$ was influenced by the deposition temperature and chemical nature of gas ambient. Particularly, the oxygen concentration in the ambient has a specific impact on the exothermic DSC peak. As the oxygen partial pressure in the purge gas stream increased, the peak height for the DSC exothermic peak also increased. Increasing of heating rate caused the DSC peak to shift toward high temperatures. This phenomena is due to the activation energy involved in such a particular transition. These DSC data were analyzed by the Kissinger equation to estimate the activation

energies for the endothermic step and exothermic step, which were 30 kcal/mol and 20 kcal/mol, respectively. From experimental results, the nature of DSC peaks were assigned, and a simplified model was proposed to interpret the DSC observations.

INTRODUCTION

Cu(acetylacetoante)$_2$ is a primary copper precursor used in MOCVD techniques [1-10]. High quality CuO, Cu_2O, and Cu films could be prepared by thermal CVD, LPCVD, PECVD, and LACVD using Cu(acac)$_2$ as the copper precursor [10]. In the MOCVD literature, most research has been focussed on process development, i.e., the optimization of MOCVD processing parameters to improve film quality. However, the fundamental portion of MOCVD knowledge, the reaction mechanism, has remained untouched. Recently, we have used FTIR to analyze the gas phase products for copper acetylacetonate decomposition [(Cu($CH_3COCHCOCH_3$)$_2$, Cu(acac)$_2$)] during MOCVD process[11] and attempted to propose a primitive kinetic model.

From both deposition [10] and IR studies [11], these results indicated that the pyrolysis of Cu(acac)$_2$ in the MOCVD reactor was determined primarily by the deposition temperature and the chemical nature of the environment, and this precursor decomposition kinetics played an active role in the final stoichiometry of deposited MOCVD films. Also, since MOCVD processes are operated at low temperature, with film growing front (the vapor/solid interface) in a highly nonequilibrium stage, reaction kinetics seems to be the principle factor needed for considering.

As pointed out by Stringfellow; "For the low temperature MOCVD, which uses organometallic complexes as precursors, the deposited phase distribution of

the MOCVD reaction is strongly dependent on the precursor decomposition behavior[12]".

It is in this paper that we have determined to study the decomposition kinetics of MOCVD precursor, $Cu(acac)_2$, with specific emphasis on the energetic and reactive aspects.

For material thermal decomposition studies, modern thermal analysis has advantages such as:

1. capable of surveying a broad temperature range,
2. using a variety of programed heating rates to perform dynamic study,
3. accuracy in locating the specific phase transition temperature,
4. monitoring the reaction rate exactly.

These thermal analysis techniques include thermogravimetric analysis (TGA), differential thermal analysis (DTA), and differential scanning calorimetry (DSC). Previous thermal analysis of $Cu(acac)_2$ has been studied by using TGA [13], DTA [13,14], and mass spec (MS) [15]. Glavas first used DTA and TGA to study $Cu(acac)_2$ pyrolysis with a sample weight of 100 mg and a heating rate of 5^oC/min in open air ambient [13]. From TGA results, the sample weight decreased through a smooth curve which started at 150^oC, passed through a deflection point at 200^oC, and ended by 270^oC. From DTA experiments in air, two exothermic peaks were observed at 230^oC and 385^oC, with an endothermic peak at 255^oC. Glava's data indicated that there are some exothermic reactions corresponding to $Cu(acac)_2$ pyrolysis in air. However, in modern thermal analyses, the sample weight is required to be less than 20 mg to avoid large temperature inhomogeneity in the sample. This indicated that the Glava's sample might be too large and the experimental data may be unreliable

for research reference. Using DTA, Yoshida studied the $Cu(acac)_2$ pyrolysis in air and N_2[14]. For $Cu(acac)_2$ pyrolyzed in air, three peaks were found in the temperature range from 250^oC to 350^oC. Yoshida's result implied that the presence of oxygen in gas ambient may cause the exothermic reaction for $Cu(acac)_2$ pyrolysis. Later, both Radhakrishnan [15] and Patnaik [16] used TGA to study the pyrolysis of $Cu(acac)_2$ in N_2. They found that $Cu(acac)_2$ decomposition started at 463^ok, reached the rate maximum at 524^ok, and ended by 538^ok. This reaction had an activation energy of 144.15 kJ/mol [15]. These results were obtained from TGA, which can monitor weight loss, but is unable to differentiate the weight loss of sample caused by evaporation or decomposition. These data are not conclusive and more experiments seem necessary for revealing the identity of these data.

In the last five years, the advantages of DTA and a more advanced technique, differential scanning calorimetry (DSC) have been realized by MOCVD researchers and used for precursor decomposition study. Monscinkhoft used DSC to study the decomposition of $Al(OH)_3$, an Al MOCVD precursor [17]. Poston and Reisman used DTA to investigate the pyrolysis of $Rh(acac)_3$, a metal MOCVD precursor [18]. They found that thermal analysis data were useful for identification of fundamental precursor properties and valuable for MOCVD process development.

In principle, the recently developed DSC technique is superior to TGA and DTA for reaction kinetic study. DSC records the specific energy required to establish a zero temperature difference between a substance and a reference material versus either time or temperature; these two species are subjected to identical temperature regions in an environment heated at a constant rate. DSC is more sensitive to phase transition temperature (with a precision of 0.01^oC) and is capable of directly monitoring the

exact rate of energy exchange (or reaction rate). These factors seem to be especially promising for studying the kinetic aspect of $Cu(acac)_2$ pyrolysis.

It has been long argued that DTA is unable to monitor the maximum reaction rate accurately because when the maximum temperature difference between sample and environment is reached, the maximum reaction rate have already occurred [19]. On the other hand, DSC peaks directly correspond to the maximum reaction rates, which can be used for kinetic mechanism identification. Reliable DSC instruments became commercially available only after 1970 [20]. No DSC study on the reactive decomposition of $Cu(acac)_2$ has been done to date. To study the processing condition used in MOCVD, the particular interests for DSC study will emphasize the impacts of temperature, oxygen concentration, and heating rate on the pyrolysis of $Cu(acac)_2$.

In addition to studying the processing parameters, DSC data is used to estimate the specific activation energy for the corresponding transition step. Based on absolute kinetic theory, Kissinger has formulated a mathematical equation, the Kissinger equation [21]. By analyzing the dynamic DSC results at various heating rates, the Kissinger equation can estimate the activation energy for a specific phase transition step. In Kissinger's model, the relationship between peak temperature and programed heating rate yields the respective activation energy. Due to its practical assumption, the Kissinger model has been found particularly useful in predicting the activation energy for decomposition reactions with the liberation of gas involved [21-23].

This study will first investigate the nature of $Cu(acac)_2$ decomposition, and determine the key parameters influencing DSC curves. Then, dynamic Kissinger analysis of the heating rate vs. peak temperature results will be performed. The impact of the oxidizing environment on the precursor pyrolysis was also examined.

EXPERIMENTAL PROCEDURE

DSC experiments were performed in a TA Instrument 2910 thermal analyzer (Fig. 1), which was interfaced to a microprocessor (Thermal analyst 2100) capable of automatically programmed heating. The basic operating principle of DSC is depicted in Fig. 2. In the DSC cell, the sample and reference pans were kept at the same temperature, while the difference in energy flow rates (dH/dt) used to maintain such temperature balance was recorded against time (or temperature, in the case of a constant heating rate). A disk type thermocouple made of constantan serves as both the major path of heat transfer to the two pans and the temperature monitoring device. The Alumel wires and Chromel wires, attached to the raised indentations beneath each pan, formed the other half of the differential thermocouple system.

Each DSC experiment was performed in three-steps. In the first step, a baseline calibration, as referenced with the melting point of Indium, was performed with the specific heating rate and the purge gas composition. The second step repeated the baseline calibration with two additional Pt pans situated in the DSC chamber. In the final step, 10 mg of $Cu(acac)_2$ was placed in one Pt pan, with a diameter of 3 mm and a depth of 2 mm. This Pt pan was then installed with another empty Pt pan in the chamber, as shown on Fig. 2. Air, He, N_2 and O_2/He mixture gases were used as the purge gases.

The gas flow rates were measured by calibrated rotameters (Shorate, Brooks Instrument), with a precision of 0.1 ml/min. Usually, a flow rate of 36 ml/min at 1 atm was used. In the inert environment experiment, the $Cu(acac)_2$ (Aldrich, purity 99%) was heated within He or nitrogen (Air products) gas purged ambient. The oxidizing-environment experiments were performed in ambients purged with air or a mixed stream of He and oxygen. The flow rates of oxygen and He were controlled by rotameters to obtain the desired partial pressures.

Heating rates were controlled and monitored by the Du Pont Thermal Analyst 2100, which uses a IBM Personal System /2 Model 70386 computer as the control module. The value of heating rate (r) ranged from 5^oC to 50^oC/min.

According to the Kissinger equation, the slope of the line drawn by the nature log of heating rate (r) divided by the square of peak temperature (Tp) versus the inverse of peak temperature (1/Tp) is equal to the negative of the activation energy (Ea) divided by the gas constant (R, 1.987 cal/mol k).

$$d(\ln(r/Tp_2)/d(1/Tp) = -(Ea/R)$$

In each experiment, the temperature where the maximum heat flow rate occurred (Tp) was recorded against the heating rate used (r). A PC installed software , ENERGRAPH, was used to perform the linear regression calculation with $\ln(r/Tp^2)$ against 1/Tp.

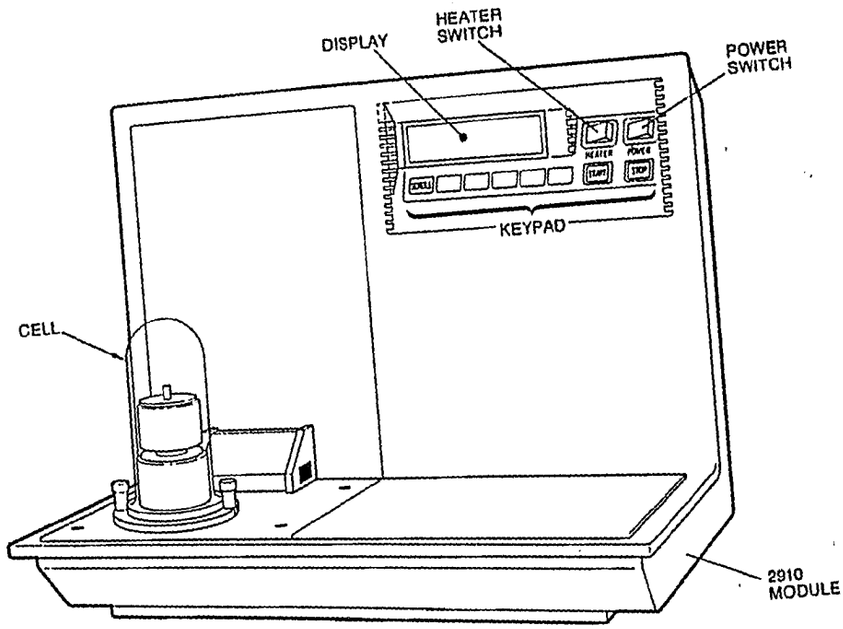

Fig. 1 DSC 2910 Thermal Analyzer

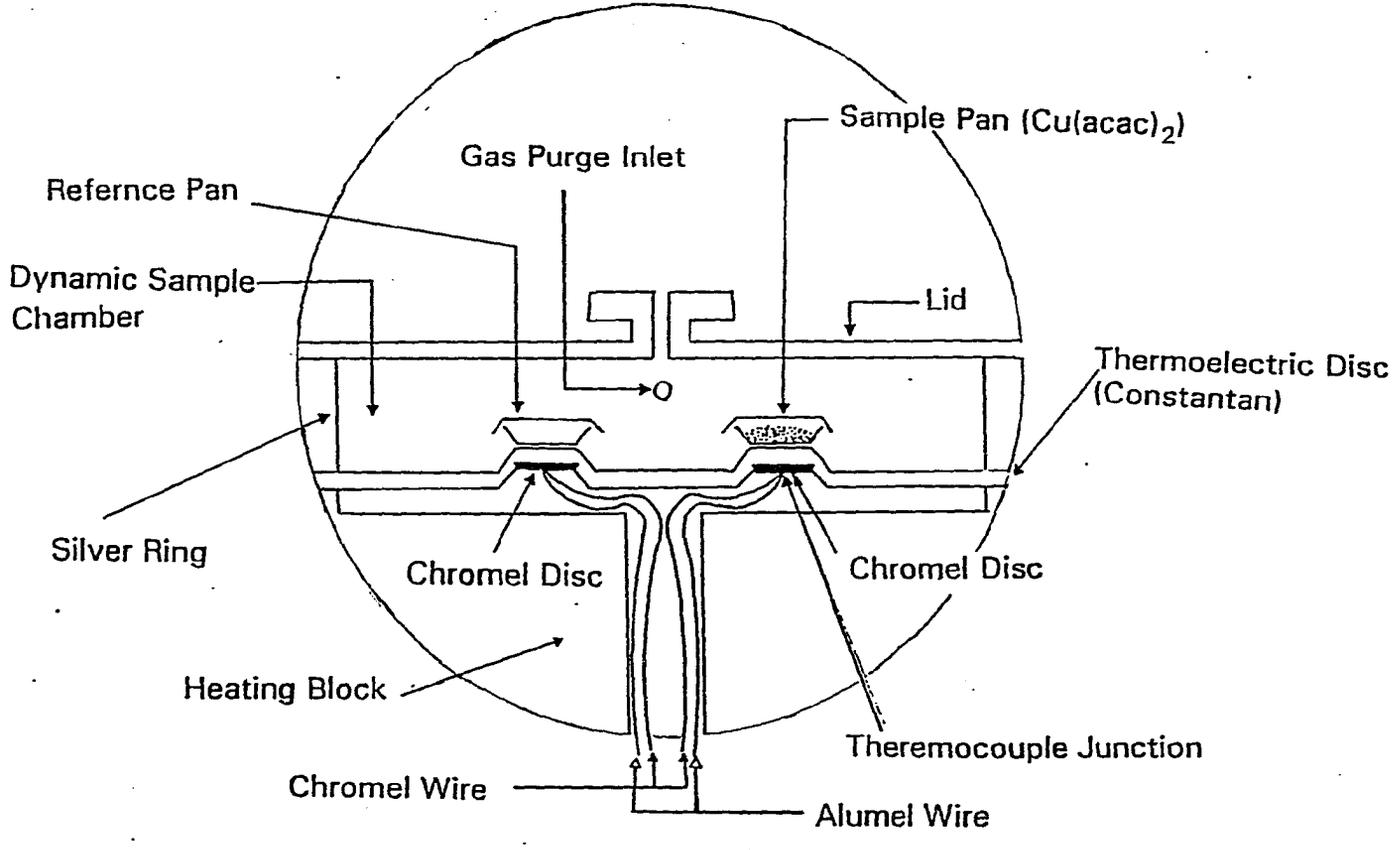

Fig. 2 Cross section diagram of the DSC cell

EXPERIMENTAL RESULTS

The DSC results are described as in the following order:

1. DSC of $Cu(acac)_2$ in Inert Ambient
2. DSC of $Cu(acac)_2$ in Oxygen Containing Ambient
3. DSC of $Cu(acac)_2$ in Ambient Gas with Different Molecular Weights
4. DSC of $Cu(acac)_2$ with Different Heating Rates

DSC Patterns of $Cu(acac)_2$ Pyrolyzed in Inert Ambient

The effect of temperature on pyrolysis of $Cu(acac)_2$ in an inert gas was examined first. A DSC diagram for $Cu(acac)_2$ pyrolyzed in He, with a heating rate of 5^oC/min, was shown in Fig. 3. One endothermic reaction started at 190^oC and reached the maximum reaction rate (Q_{max}=0.8 mW) at 234^oC. This endothermic reaction was then followed by a broad exothermic plateau, which was assumed to be composed of several consecutive exothermic reactions, in the range from 260^oC to 330^oC. It was suggested either an evaporation process or a endothermic decomposition was responsible for this endothermic step.

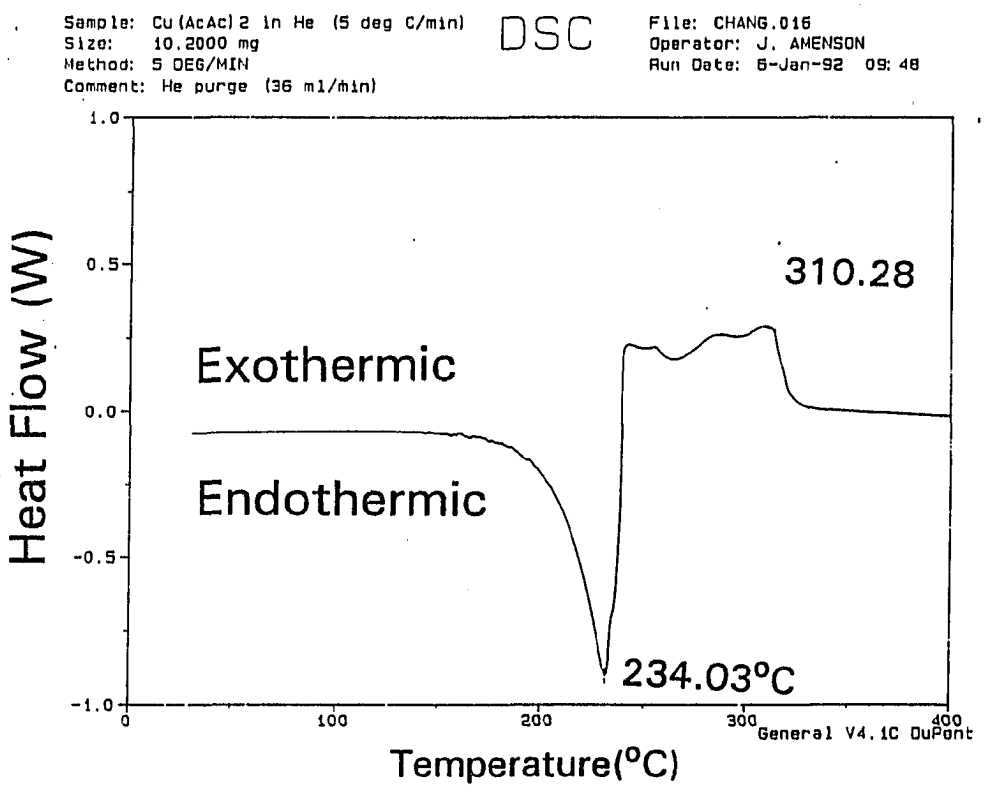

Fig. 3 DSC of $Cu(acac)_2$ pyrolyzed in He

DSC Patterns of $Cu(acac)_2$ Pyrolyzed in Oxidizing Ambient

The impact of oxygen on $Cu(acac)_2$ pyrolysis was then studied by performing DSC experiments in a He stream containing 20% oxygen, with a heating rate of 5^oC/min (Fig. 4). Compared with DSC performed in a pure He ambient(Fig. 3), the endothermic peak for DSC in He/O_2 mixture was still located at almost the same position, 234^oC, while the following exothermic reactions developed into a much simpler pattern. The exothermic reaction in the lower temperature region grew into one sharp exothermic peak at 246^oC, with a peak height two times higher than the one in He. The growth of the 246^oC peak seems to be accompanied by the diminishing of the exothermic peak at 307^oC (Fig. 3,4). The results for identical experiments performed at a faster heating rate, 10^oC/min) are presented in Fig. 5A and Fig. 5B. The addition of oxygen again caused the exothermic reactions (Fig. 5) to develope into a single exothermic step (Fig. 5). From both experiments, oxygen addition has altered the exothermic decomposition pattern of $Cu(acac)_2$ significantly in the low temperature region (from 200-240^oC). The presence of oxygen appear to cause the original high temperature reaction (above 270^oC) to occur earlier at low temperature (Below 260^oC).

Oxygen Concentration Effect

To further investigate the effect of oxygen, a series of DSC experiments were performed with the same heating rate, 10^oC/min, but with different oxygen concentrations, 20%, 25%, and 50% (Fig. 7A, Fig. 7B, and Fig. 7C) in the purge gas stream. Comparison of these DSC patterns shows the first endothermic step

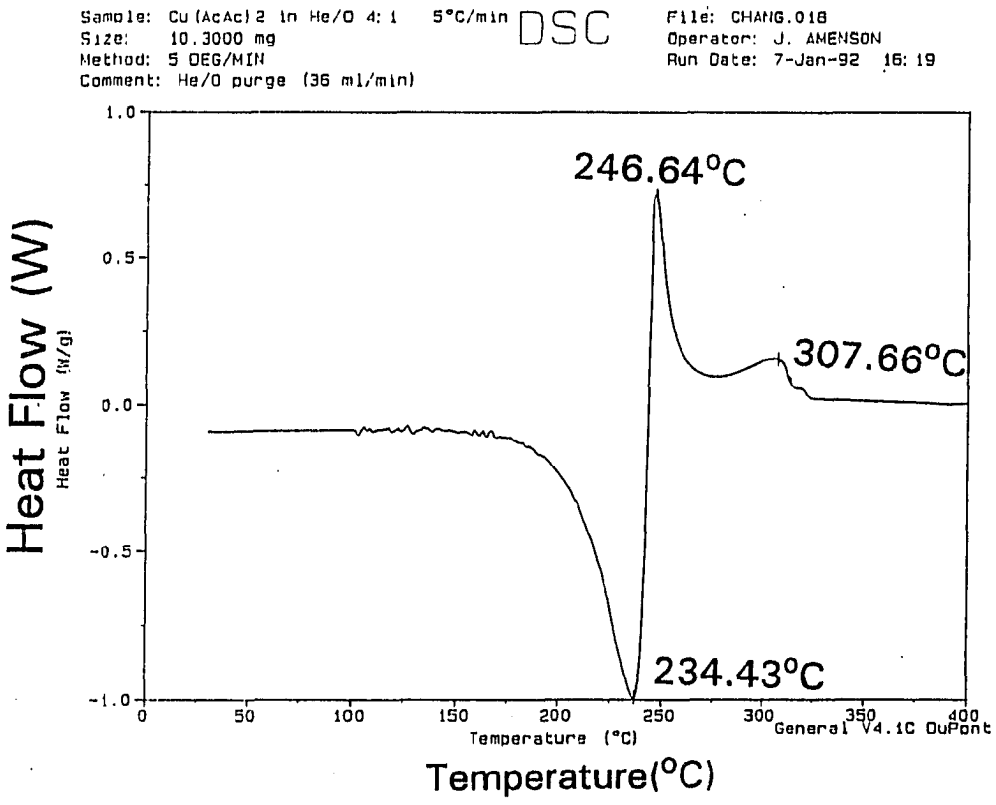

Fig. 4 DSC of $Cu(acac)_2$ pyrolyzed in He/O_2 (4:1) mixture

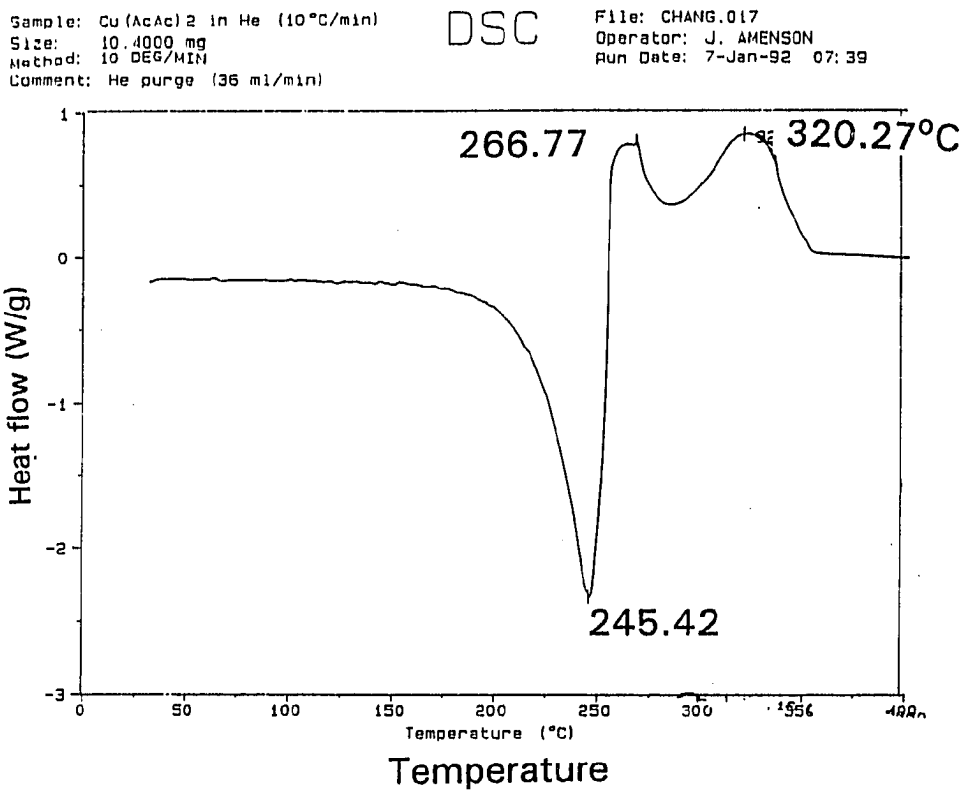

Fig. 5 · DSC of $Cu(acac)_2$ pyrolyzed in He (r=10^{o}C/min

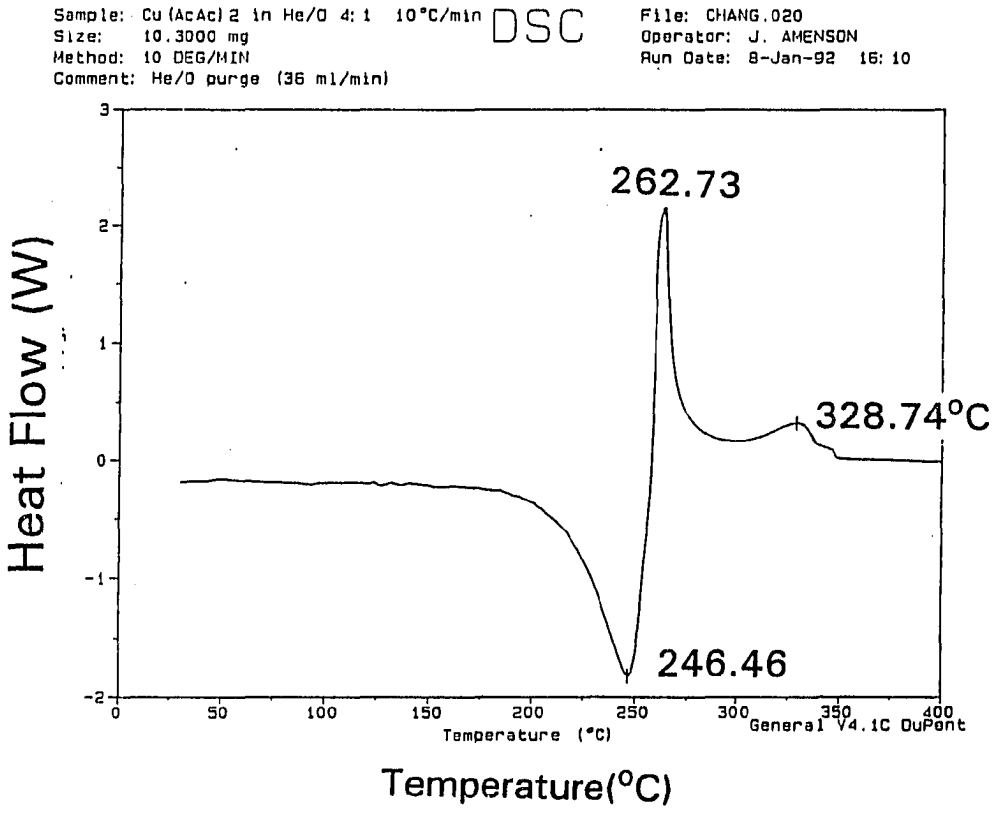

Fig. 6 DSC of $Cu(acac)_2$ pyrolyzed in He/O_2 (4:1)mixture (r=10°C/min

remained unchanged in all experiments, but the second exothermic peaks observed in all experiments, was strongly dependent on the specific oxygen concentration involved. In these DSC patterns, the most phenomenal effect for oxygen concentration increasing is the growth of the exothermic peak height. Fig. 8 shows the exothermic peak height increased from 56 mW to 98 mW as oxygen concentration changed from 20% to 50%. At the same time, there is no observed change for the endothermic peak corresponding to the variation in oxygen concentration. Fig. 9 demonstrates the DSC experimental results of another oxygen concentration study, which was conducted at various oxygen concentrations, but with a slower heating rate, 5^{o}C/min. These results again indicated that increasing Oxygen concentration increased the peak height of the exothermic step.

Effect of Molecular Weight of Ambient Gas on the $Cu(acac)_2$ Pyrolysis

In addition to He, N_2 has also been used as a transporting gas in MOCVD process. DSC was employed to monitor the energy absorption/liberation process during the decomposition of $Cu(acac)_2$. As observed in the DSC result (Figure 10A), there are three peaks for $Cu(acac)_2$ pyrolyzed in the mixture of 20% O_2 and 80% N_2. The first endothermic reaction occurs at 241^{o}C. This is followed immediately by an exothermic peak located at 255^{o}C. At 307^{o}C, a third feature has been found as a shoulder on the long tail of the second peak. In N_2 ambient, the DSC result also shows three peaks (Figure 10B). The first endothermic peak is located at 242^{o}C, which is almost the same as for air. The second exothermic peak (265^{o}C) is 10^{o} higher and much broader than the second peak for air. The third peak, at 338^{o}C, is located at nearly the same position as for air. Compared to DSC performed in

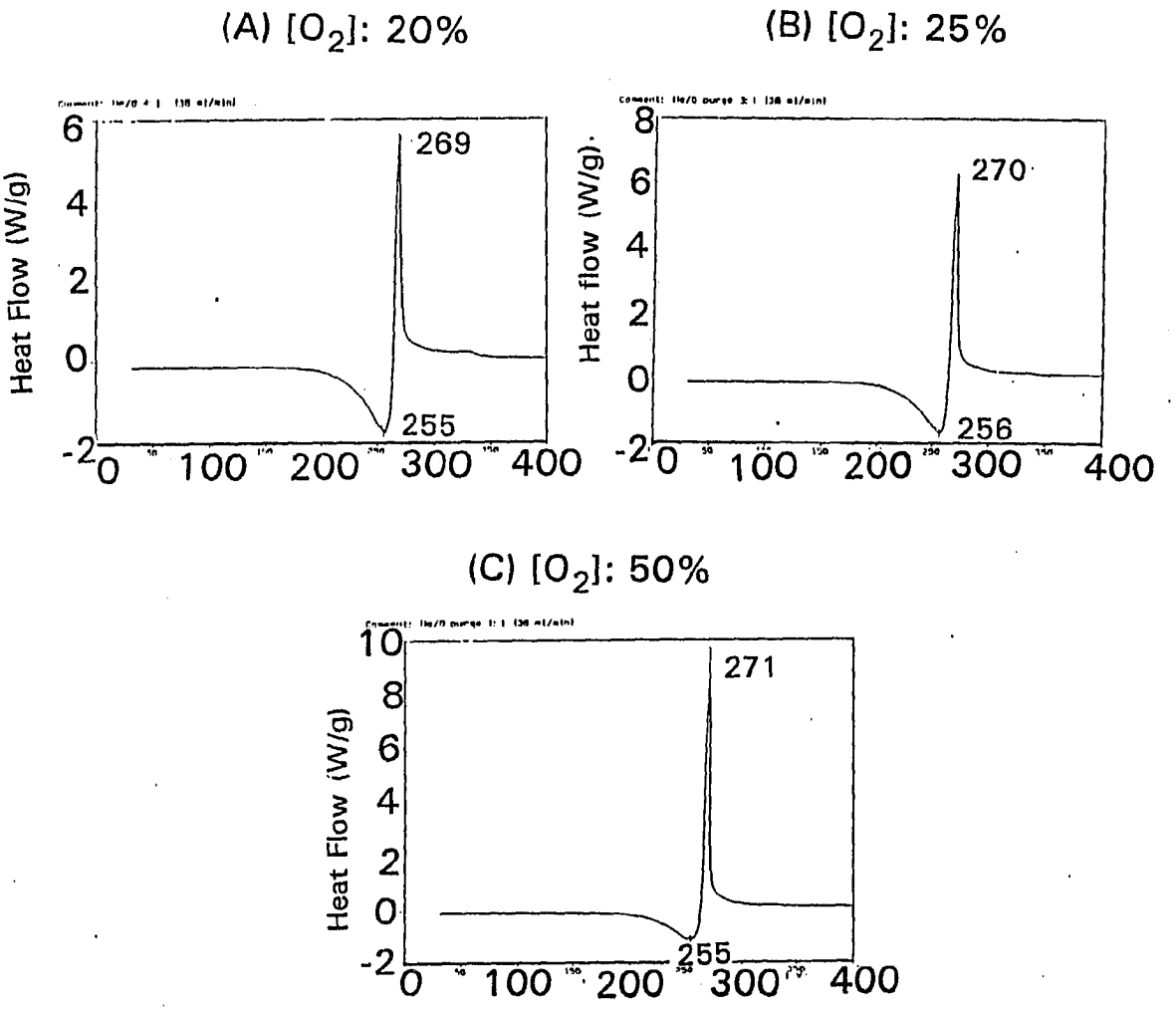

Fig. 7 The impact of oxygen concentration to the $Cu(acac)_2$ DSC pattern: with oxygen concentrations as (A) 20%, (B) 25%, and (C) 50%

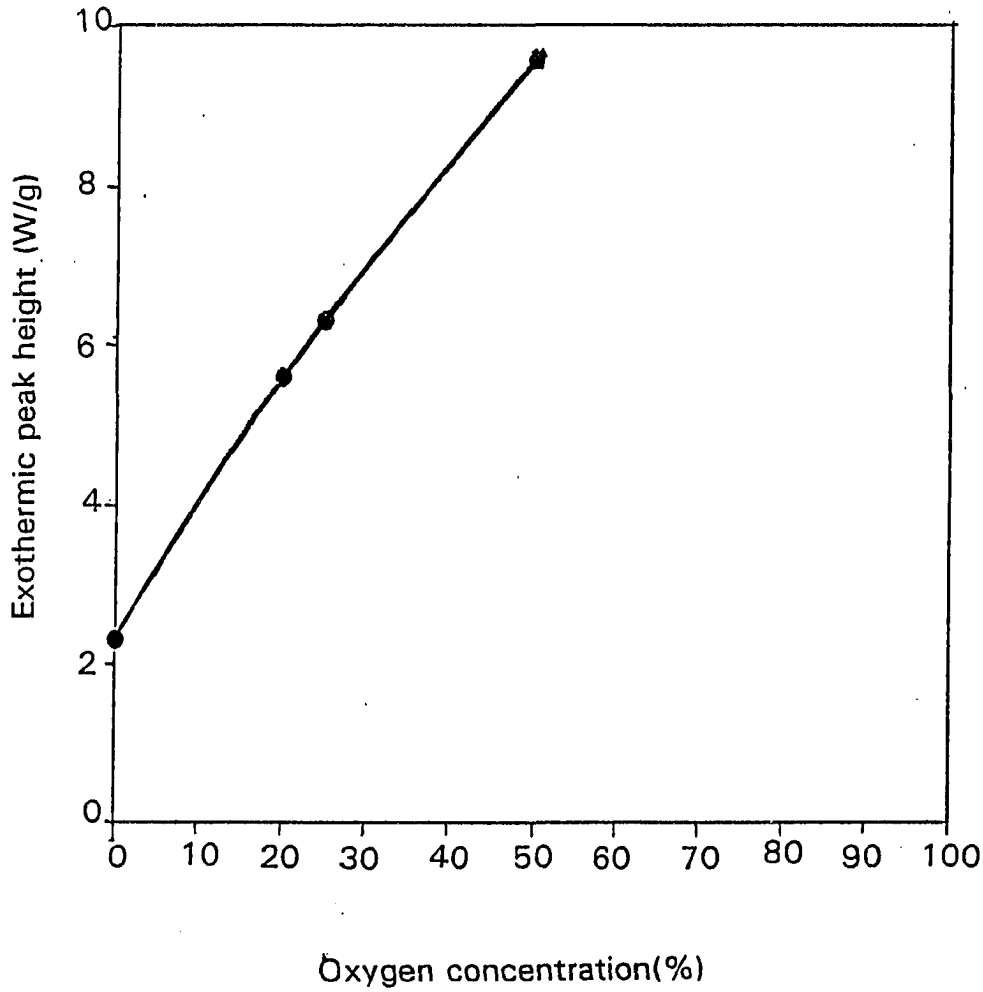

Fig. 8 The oxygen concentration impact on the exothermic peak height of $Cu(acac)_2$ DSC (r=10^oC/min)

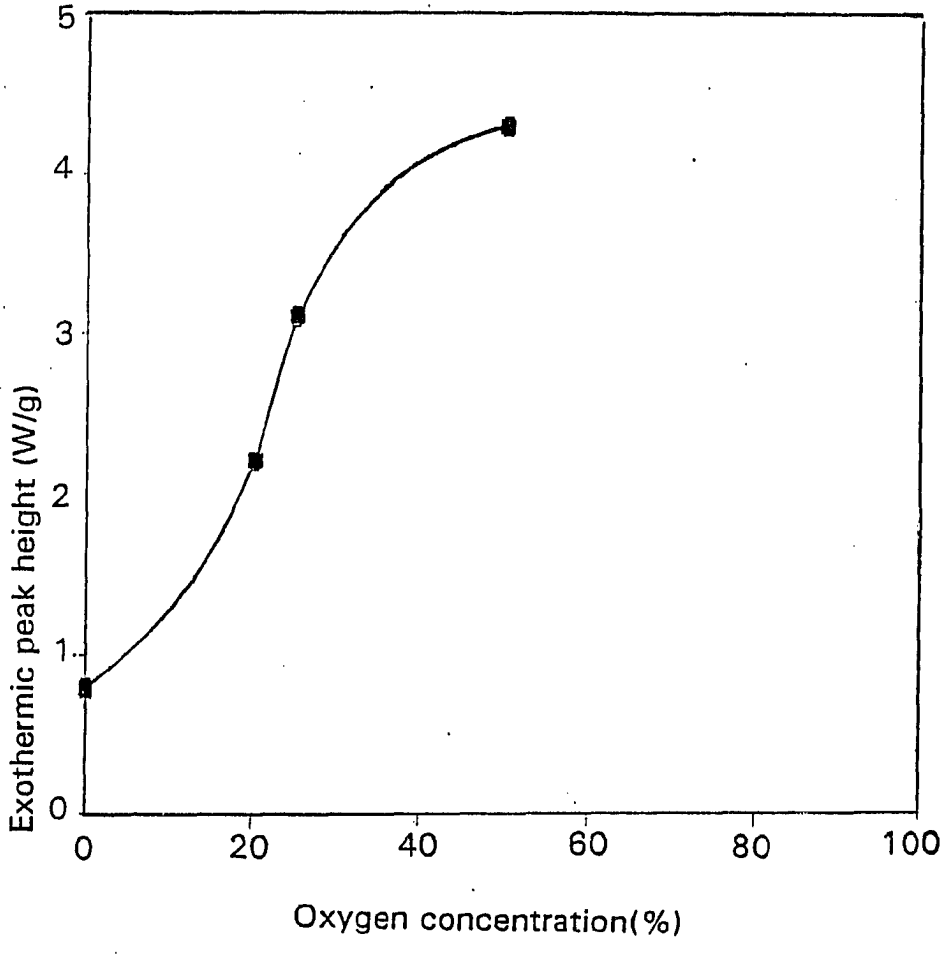

Fig. 9 The oxygen concentration impact on the exothermic peak height of $Cu(acac)_2$ DSC (r=5°C/min)

He and He/O_2 mixture, the DSC peaks all have temperature lags for N_2 ambient experiment.

As observed in Fig. 10A and 10B, by using purge gas with heavier molecular weight, N_2 instead of He, both the endothermic peak and the exothermic peak shift to a higher temperature position for 10^oC. It is observed as a universal phenomena that using a purge gas with heavier M.W. causes a temperature lag for the DSC peaks.

Effects of Heating Rate on DSC Pattern: He and O_2/He Mixture

The temperature profile in a real MOCVD reactor is always nonuniform. In an atmospheric pressure MOCVD reactor, when a precursor molecule diffuses from a cooler carrier gas stream, through the thermal boundary layer (usually with a thickness of several millimeters), and reaches onto the hotter substrate surface, the whole process may takes only 0.1 second. The temperature difference in the boundary layer may be as high as 100^oC. That is, the temperature variation rate that this molecule experiences during its diffusion process may be on the order of 1000^oC/sec. Therefore, the impact of the heating rate on the dissociation of $Cu(acac)_2$ may be of fundamental importance to the study of MOCVD.

In Fig. 11A, 11B and 11C, DSC performed at a constant He/O_2 ratio (3:1) but with different heating rates (10^oC/min, 15^oC/min, and 20^oC/min) were shown. In addition to the peak height growth, which was caused by the dynamic effect of a heating rate increase, the most obvious change in the DSC patterns was the shift in the DSC peak position. The exothermic DSC peak shifted from 271^oC, at a heating rate of 10^oC/min, to 289^oC, at a heating rate of 20^oC/min. This temperature

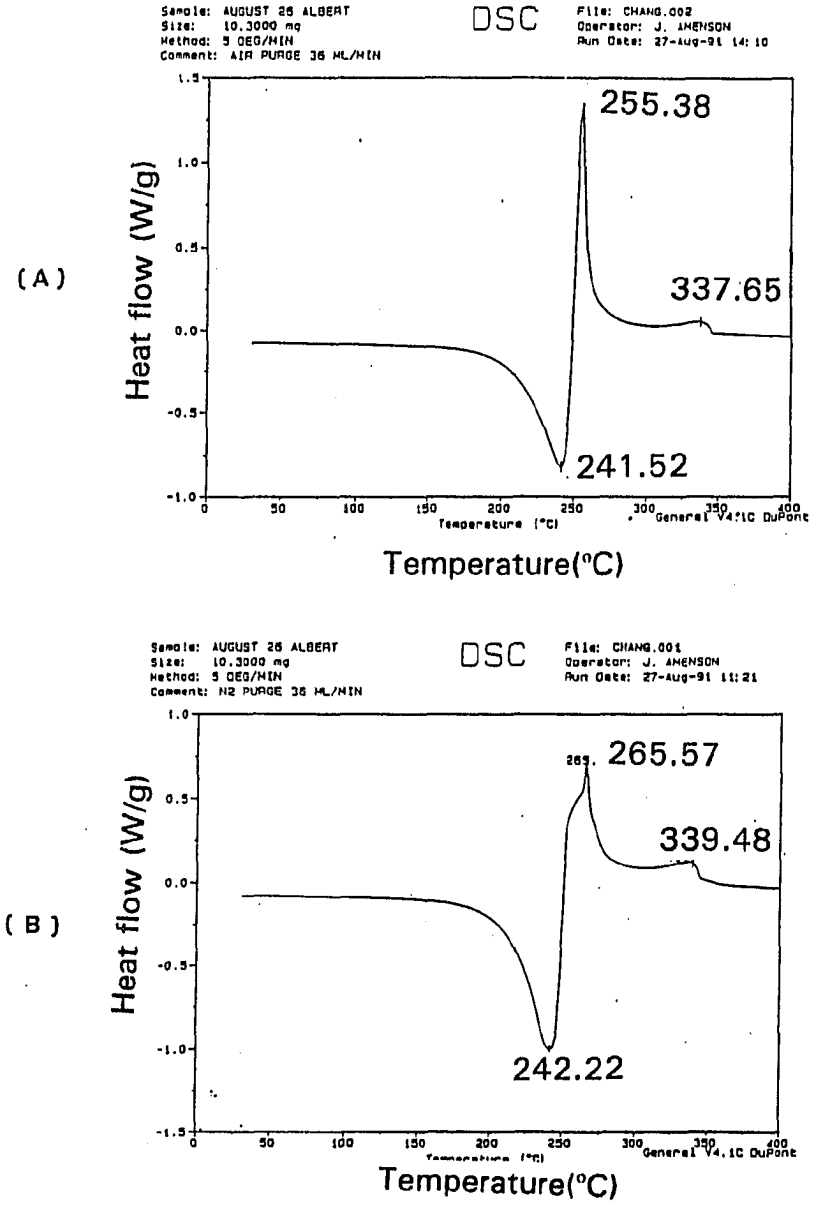

Fig. 10 DSC of $Cu(acac)_2$ pyrolyzed in (A) air and (B) N_2

shift is considered as principle evidence for the existence of an activation energy corresponding to such a specific phase transition.

Decomposition Activation Energy Estimation

The DSC data collected from Fig. 11A-11C was used to derive the activation energies for specific steps in He/O_2 (3:1) mixture. Table 1 listed the values of exothermic peak temperatures (Tp), heating rates (r), 1/Tp, and $\ln(r/Tp^2)$. $Ln(r/Tp^2)$ was plotted against 1/Tp in Fig. 12. The derived activation energies for the endothermic peak and the exothermic peak were 30.4 kcal/mol and 20 kcal/mol, respectively.

The second set of DSC was performed in a He/O_2 4:1 mixture, with heating rate as 5^oC/min, 10^oC/min, 20^oC/min, and 50^oC/min. The values of r, Tp, 1/Tp, and $\ln(r/Tp^2)$, were summarized on Table 2. From corresponding Kissinger plots (Fig. 13), the activation energies are 30.5 kcal/mol for the endothermic peak and 20.8 kcal/mol for the exothermic peak.

Following the same procedures, as shown on Table 3 and Table 4, the activation energies for $Cu(acac)_2$ pyrolyzed exothermically are 20.0 kcal/mol in N_2 and 20.3 kcal/mol in air.

In summary, the DSC results reflect the combination of several stages in the mechanism including: sublimation, decomposition, and oxidation. Overall, the experiments show that the activation energy of the first peak is 30 kcal/mol. The second peak's activation energy is around 20 kcal/mol.

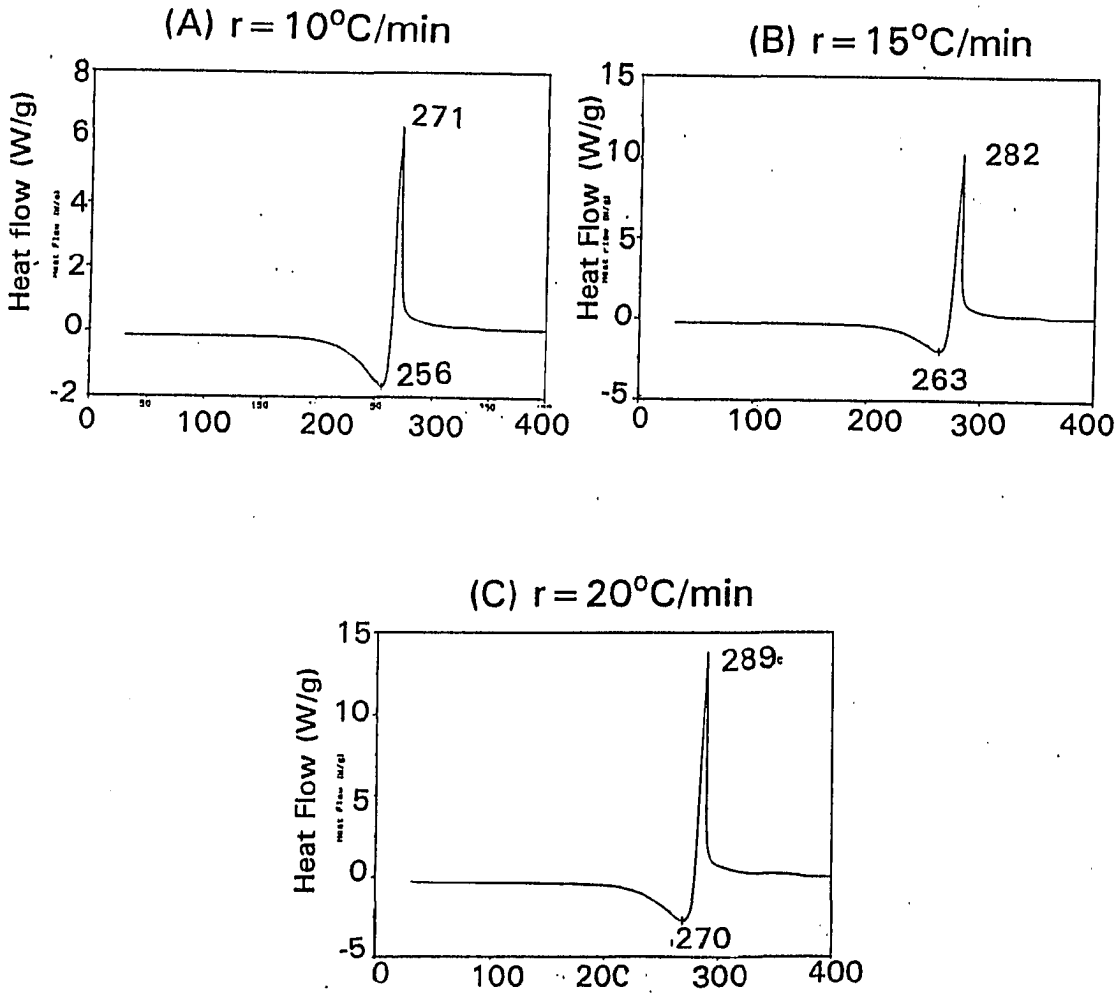

Fig. 11 DSC of $Cu(acac)_2$ pyrolyzed in He/O_2 (3:1) mixture with r= 10°C/min (A), 15°C/min (B), 20°C/min (C)

Table 1: DSC results for Kissinger analysis ($He:O_2$=3:1)

RUN #	$He:O_2$	r(^oC/min)	Tp^oC)	(1/Tp)X10^3	ln(r/Tp^2)
24	3:1	10	270.91	1.8380	-10.2955
34	3:1	15	281.98	1.8013	-9.93035
35	3:1	20	289.47	1.7773	-9.66947

Table 2: DSC result for Kissinger analysis ($He:O_2$=4:1)

RUN #	$He:O_2$	r(^oC/min)	Tp(^oC)	(1/Tp)X10^3	ln(r/Tp^2)
26	4:1	5	253.28	1.8993	-10.9227
25	4:1	10	269.30	1.8434	-10.2896
27	4:1	20	287.47	1.7852	-9.6606
28	4:1	50	314.20	1.7035	-8.8380

Table 3: DSC result for Kissinger analysis (ambient:air)

RUN#	purged gas	r(^oC/min)	Tp(^oC)	(1/Tp)X10^3	ln(r/Tp^2)
2	air	2.5	241.98	1.9418	-11.5712
3	air	5	255.33	1.8927	-10.9300
4	air	10	269.09	1.8447	-10.2882
5	air	20	289.97	1.7763	-9.6707

Table 4: DSC result for kissinger analysis (ambient: N_2)

RUN#	purged gas	r(^oC/min)	Tp(^oC)	(1/Tp)X10^3	ln(r/Tp^2)
41	N_2	2.5	247.88	1.8380	-10.2955
43	N_2	5	265.47	1.8013	-9.9303
44	N_2	10	279.14	1.7921	-9.7856
45	N_2	20	301.84	1.7773	-9.6694

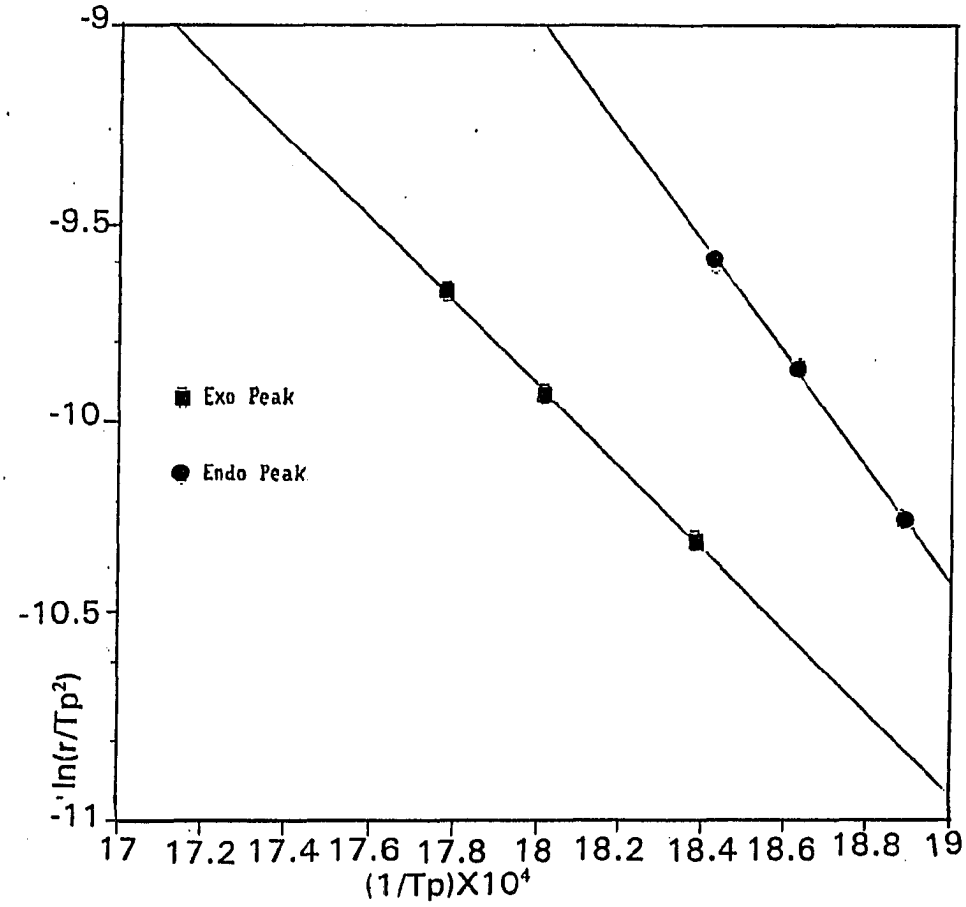

Fig. 12 Kissinger plot for $Cu(acac)_2$ DSC in $He:O_2$ = 3:1

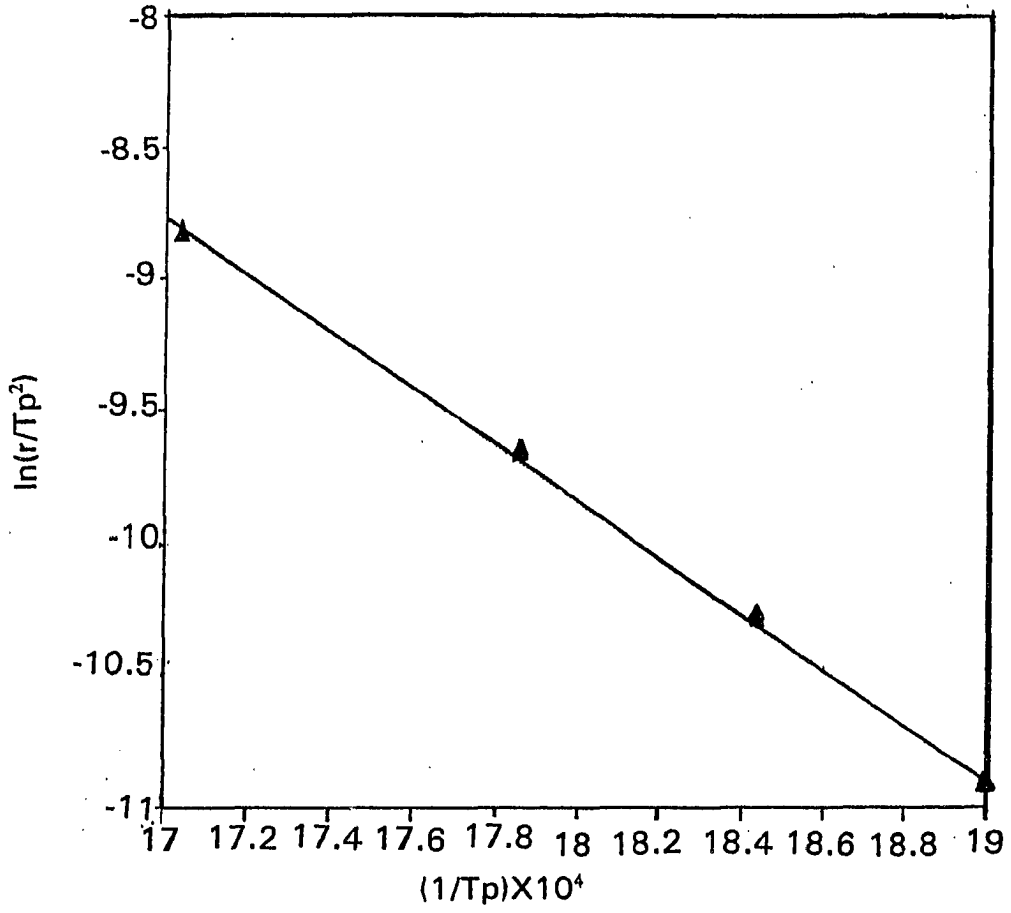

Fig. 13 Kissinger plot of $Cu(acac)_2$ DSC in $He:O_2$ =4:1

DISCUSSION

From all DSC results, it seems that the $Cu(acac)_2$ pyrolysis reaction proceeds more rapidly at higher temperatures. Below 150^oC, the DSC curves (Fig. 2-8) are smooth. Above 150^oC, some minor fluctuations were observed in the DSC curves with high heating rates. The temperature range for these fluctuations fell in the same temperature region where water vapor has been observed in the IR-MOCVD experiments [11]. For all DSC experiments performed in oxygen-containing ambient, there always is a critical temperature (Fig 2-4, 8A, 9), above which, the exothermic reaction begins with an exponential acceleration of the reaction rate.

The identity of the first endothermic peak found in DSC could be derived from the results of experiments comparing oxygen effect and purge gas molecular weights. Based on DSC results in Fig. 1 and Fig. 2, the height, position, and shape of this peak was unaffected by the presence or absence of oxygen. This endothermic peak seems to be unrelated to oxygen. Second, by varying the molecular weight of purge gas, from He to N_2, both the height and position of this endothermic peak changed (Fig. 1, 8). Because both He and N_2 are inert to $Cu(acac)_2$, when N_2 instead of He was used, the only factor changed was the molecular weight of ambient gas. This variation is supposed to alter primarily the gas phase mass transfer rate. Based on the experimental evidence (Fig. 1, 2, and 8), there must be a specific

gas phase specie, either as being a reactant or product, involved in this endothermic phase transformation. From this evidence, either decomposition of $Cu(acac)_2$ without oxygen involved or a simple evaporative step could be the possible cause. Third, the activation energy for this endothermic step was 30 kcal/mol, which is close to the literature value for the enthalpy change of $Cu(acac)_2$ sublimation [24-26]. Compared with sublimation study of $Cu(acac)_2$ in literatures [24-26], the peak position was also consistent with the peak rate temperature for the evaporation of $Cu(acac)_2$. Based on these data, the first endothermic peak is assigned to the evaporation of $Cu(acac)_2$.

The nature of the second exothermic peak was also identified through experimental results. From DSC results in Fig. 1-3, the shape and height of this exothermic peak are affected by the addition of oxygen. Actually, from the oxygen concentration experiment (Fig. 4), a reaction order more or less than one might even exist for the correlation between the oxygen concentration and the reaction rate (the peak height). One thing should be noted is that the peak position in every oxygen concentration DSC experiments (Fig. 4) was almost unaffected by the oxygen partial pressure. This evidence suggests that oxygen may accelerate the exothermic reaction rate. From the purge gas molecular weight experiments, the peak position was shifted by using purge gases with different molecular weights (Fig. 2, 8). This observation identifies that gas phase was involved in this reaction system.

Finally, according to the heating rate-Kissinger analysis, this exothermic reaction has an activation energy of 20 kcal/mol (Fig. 12, 13). For the mass transfer controlled reaction, the pseudo activation energy derived from reaction rate vs. temperature is around 3 to 4 kcal/mol [27]. For a homogeneous gas phase reaction, the activation energy should be at least on the same level as the bond breakage energy for the

reactant molecule. For $Cu(acac)_2$, the weakest Cu-O bond has a bond energy of 48 kcal/mol. Due to these reasons, it was presumed that this activation energy value, 20 kcal/mol, reflects a heterogeneous reaction controlled mechanism. The exothermic peak that occurred in the DSC pattern might correspond with an oxygen participating and gaseous products evolving reactive decomposition, which might be surface reaction controlled.

In summary, the pyrolysis of $Cu(acac)_2$ in inert or oxidizing environment could take entirely different pathways. By comparing these decomposition patterns, the value of oxygen in MOCVD process could also be identified. For the self decomposition of $Cu(acac)_2$ in an inert ambient, the exothermic reaction takes place in a prolonged period. This seemingly random decomposition of the precursor is too complex to manipulate and certainly unfavorable for MOCVD film composition control. On the other hand, $Cu(acac)_2$ pyrolyzed with a single-stage exothermic reaction in oxygen added ambient, is simple and could be beneficial for MOCVD film stoichiometry control.

As observed in Figure 10A and 10B, oxygen affects the second DSC peak for the pyrolysis of $Cu(acac)_2$. With the addition of O_2, the peak temperature is lowered by 10^oC, and the reaction rate is elevated. If DSC results are plotted according to heat flow(W/g) against time (t) rather than temperature(T) (by the constant heating rate: $\Delta T/\Delta t = 5^oC/min$), the sharper and higher exothermic peak observed for the air DSC result (Figure 10A) means that the thermal energy is liberated in a short time period at a high rate. From a comparison of DSC results, it appears that oxygen assists the exothermic step in $Cu(acac)_2$ pyrolysis. Considering a reactive radical mechanism, a primitive model of O_2-assisted $Cu(acac)_2$ pyrolysis process can be proposed. By

comparing the bond strengths in $Cu(acac)_2$ [which ranges from 48 kcal/mol (Cu-O bond) to 100 kcal/mol (C-H bond)] [28] to the bond strength of O_2 (which has a strong double bond, 119 kcal/mol), $Cu(acac)_2$ is more unstable thermally than O_2. It is suggested that the decomposition of $Cu(acac)_2$, which results in the formations of reactive radicals, initiated the MOCVD deposition reaction. The first reaction might be attributed to the ligand dissociation of $Cu(acac)_2$. Subsequently, O_2 reacts with these radicals. The oxidation of these organic fragments accounts for the exothermic step observed in DSC.

Comparing the DSC results with deposition results [10], the value of DSC data on MOCVD process development was also noted; it seems feasible to operate the MOCVD precursor sublimator at temperatures where the evaporative endothermic peak occurred, while operating the susceptor at temperatures where the exothermic decomposition of $Cu(acac)_2$ occurred.

Overall, the deposition and DSC results suggest that both thermal energy (a moderate deposition temperature) and oxygen are necessary for depositing Cu_2O films. Deposition temperatures above a critical value are needed to initiate $Cu(acac)_2$ pyrolysis.

CONCLUSION

Thermal decomposition of copper oxide MOCVD precursor, $Cu(acac)_2$, was studied by DSC. DSC results showed that, in the MOCVD operating temperature range, $Cu(acac)_2$ first undergoes an endothermic step, the sublimation of $Cu(acac)_2$, followed by a sharp exothermic step, the oxidative decomposition of $Cu(acac)_2$. This exothermic step should account for the initiation step for the copper oxide film deposition in the MOCVD process. The activation energy value of the first endothermic peak is 30 kcal/mol. The activation energy for the second exothermic peak is 20 kcal/mol. Through DSC results, He seems to be a better candidate as an MOCVD carrier gas than nitrogen because both $Cu(acac)_2$ sublimation and $Cu(acac)_2$ decomposition have lower onset temperatures in He ambient. In addition, the DSC results indicate that a minimum temperature of 280^oC is required to completely decompose $Cu(acac)_2$ and produce copper oxide films.

ACKNOWLEDGEMENTS

The author would like to thank Mr. Jerry Amenson for his assistance in the DSC measurements.

REFERENCES

1. W.M. Sears, and E. Fortin, Thin Solid Films, 103, 303 (1983).

2. H.J. Pauwels, and G. Vanhoutte, J. Phys., D11, 649 (1978).

3. S. Zhang, and H.C. Lu, Appl. Phys. Lett., 52, 1974 (1988).

4. D.N. Armitrage, N.I. Dunhill, R.H. West, and J.O. Williams, J. Cryst. Grow., 108, 683 (1991)

5. L. Brewer, and A. C. Loonam, J. Am. Chem. Soc., 72, 3038 (1950)

6. M.E. Gross, J. Electrochem. Soc., 138, 2422 (1991).

7. P.J. Gellings, MRS Fall meeting, 168, 125 (1990)

8. H. Holzschuh and H. Suhr, Appl. Phys. A 51, 486, (1990)

9. H. Suhr, and F. Schmaderer, Physica C, 151, 784

10. Y.N. Chang and G.L. Schrader, paper in prepn. (part I. of this dissertation)

11. Y.N. Chang and G.L. Schrader, paper in prepn. (part II. of this dissertation)

12. G.B. Stringfellow, J. Cryst. Growth, 65, 454 (1983)

13. M. J. Glavas and T. J. Ribar, Glanik Hemijskog Drustva, 32, 229 (1967).

14. I. Yoshida, H. Kobayashi, and K. Ueno, J. Inorg. Nuc. Chem., 35, 4061 (1973).

15. T.D. Radhakrishnan, P.Sherman, and N. Thankarajan, J. Indian. Chem. Soc., 59, 415, (1982).

16. S.K. Patnaik, P.K. Maharana, S.N. Sahu, and G.S.N. Murty, J. Radioanal. Nucl. Chem. Let., 128, 283 (1988)

17. R.W.J. Morrsinkhof, J. Fransen, and P.J. Gellings, MRS Proceedings, Vol. 168, 125 (1990)

18. S. Poston , and A. Resmian, J. Electronic Materials, 18, 553 (1989)

19. R.N. Rogers, and L.C. Smith, Thermochim. Acta, 1, 1 (1970)

20. W. WM. Wendlant, Thermal Analysis, 3rd ed., p.289, John Wiley & Sons, New York, (1986)

21. H.E. Kissinger, J. Anal. Chem., 29, 1702 (1959)

22. T. Ozawa, Bull. J. of Japan Chem. Soc., 38, 1881 (1965)

23. T. Ozawa, Thermal. Anal., 2, 301 (1970)

24. G. Beech, and R.M. Lintonbon, Thermochim. Acta. 3, 97 (1971)

25. S.J. Ashcroft, Thermochim. Acta, 2, 512 (1971)

26. J.P. Murry and J.O. Hill, Thermochim. Acta., 109, 383 (1987)

27. J. W. Shaw, Material Research Bull., 12, 37 (1988)

28. S.F. Ashcroft, and C.T. Mortimer, Thermochemistry of Transition Metal Complexes, p.136, Academis Press, London and New York, (1970)

GENERAL SUMMARY AND RECOMMENDATIONS

In this part, the MOCVD deposition results observed in part I, the complementary kinetics information gathered from FTIR gas phase study (part II) and DSC study (part III) were used to derive a comprehensive model describing the possible mechanism in the MOCVD process. Recommendations for future research were made with regarding the stereochemistry and thermochemistry of $Cu(acac)_2$. These discussions are organized in the following order:

1. MOCVD reaction mechanism
2. MOCVD process evaluation
3. recommendations for future study

MOCVD Reaction Mechanism

In paper I, it was observed that this $Cu(acac)_2$ using MOCVD process could deposit films with different compositions, depending on the specific deposition temperature and co-reactant (water vapor or O_2) was using. It was suggested that the pyrolysis behavior of $Cu(acac)_2$ determined this film composition distribution. As indicated by the ex-situ MOCVD/FTIR study (part II), the gas phase reaction in the MOCVD process is closely associated with the oxidative decomposition of the $Cu(acac)_2$ molecule in atmospheric pressure. It seems that at temperatures from

300^{o}C to 340^{o}C, Cu(acac)$_2$ decomposed into Cu(I)(acac) radical and acetylacetonyl (acac) radical. It is postulated that the acac radical may soon abstract H atoms from the gas phase water vapor and formed the acetylacetone molecule observed by IR. In this proposed mechanism, the oxidation state of copper in the Cu(acac) radical was +1. The Cu(acac) radical should have a stronger activity than the parent Cu(acac)$_2$ molecule because the Cu ion in Cu(acac) is not well coordinated. It seems, at 340^{o}C, the oxygen present in the MOCVD reactor can prevent the reduction of Cu in the Cu(acac) radical, when Cu(acac) radical decompose and leave Cu on the substrate surface.

From deposition result, the film deposited at 340^{o}C with oxygen pressure and precursor pressure being 150 torr and o,20 torr was Cu_2O, which contains Cu(I).

From IR results, the gas phase acetylacetone (Hacac) molecules achieved the maximum concentration at 340^{o}C. Above 350^{o}C, the concentration of acetylacetone dropped and the concentration of acetone, the decomposition product of acetylacetone, increased. As noted in the high temperature FTIR spectra, Cu(acac)$_2$ vapor was still observed in the gas phase at 400^{o}C. These overall results indicated that, at 340^{o}C, the liberation of acetylacetone from Cu(acac)$_2$ has reached the highest rate, and this reaction maintained a constant rate till higher temperatures in the MOCVD process. From 350^{o}C to 400^{o}C, the specific reaction rate of acetylacetone dissociating into acetone gradually increased. For the MOCVD process which was operated at 380^{o}C to 420^{o}C, there is almost no acetylacetone vapor observed in the IR spectrum. Acetone vapor became the primary heavy specie in the MOCVD gas phase and concentrations of CO_2 and H_2O vapor increased substantially.

It seems that, above 380^{o}C, oxygen reacted actively with Cu(acac) and acac rad-

icals, and produced acetone, CO_2, and H_2O as the oxidation products. From the IR results, it appeared that, at temperatures above 380^oC, the reactivity of oxygen with acac radicals seems to be much higher than the reactivity of oxygen with $Cu(acac)_2$ molecules, in the MOCVD reactor. From deposition results, CuO was deposited as the primary phase in this temperature range. It seems that oxygen has preserved the original oxidation state of copper in $Cu(acac)_2$ during its decomposition, or oxidized the Cu(I)(acac) radicals.

Supporting evidence was observed in DSC, above 350^oC, decomposition of $Cu(acac)_2$ was finished. The DSC curve returned to the base line, as the temperature increased[39]. These DSC results derived in part II implied that the presence of oxygen does not assist the initial decomposition of $Cu(acac)_2$. Oxygen rather alters subsequent pyrolysis mechanisms by readily oxidizing dissociated fragments.

From reviewing IR results, the reactivity of free $Cu(acac)_2$ molecules in the gas phase can be envisioned by the stereochemistry of coordinated complexes. In the $Cu(acac)_2$ molecule, as discussed in the General literature review section, the planar chelating acetylacetonyl ligands behave like an aromatic functional group, which is fairly stable at low temperature. The whole $Cu(acac)_2$ molecule, as a square planar charge transfer salt, is stabilized by the 6π electron resonating structure and reluctant to be oxidized. In the $Cu(acac)_2$, due their negative charges, the acetylacetonyl chelates are quite resistant to oxidation at low temperature. The possibility for reactions of the Cu(II) with oxygen ion is sterically hindered by these two bulky acac chelates, which make it difficult for oxygen molecules to approach.

From discussions about the molercular structure of $Cu(acac)_2$, all of these evidences indicate that the MOCVD reaction is a two-step process. First, the $Cu(acac)_2$

molecule has to be energetically activated and dissociated. Then, the copper containing fragment reacts with oxygen to produce copper oxide.

The first step, the thermal fragmentation of $Cu(acac)_2$ molecules, has been indicated by the observation of acetylacetone molecules in the MOCVD reactor gas phase. From the ex-situ IR/MOCVD results in part II, the liberation of acetylacetonyl ligand occurred in the same temperature range for depositing copper oxide. The liberation of acac from $Cu(acac)_2$ seems to be a principle initial step in the copper oxide deposition.

Subsequently, if there are any oxygen molecules near the decomposed fragments, oxygen may react readily with copper absent radicals and copper containing fragments to produce copper oxide and remove the oxidized radicals permanently.

A speculation can be made that when the deposition temperature increased to the range of 340-380^oC, the boundary layer temperature might also increase to the specific temperature, where the first acetylacetonyl chelates in $Cu(acac)_2$ molecules dissociated extensively . The copper containing intermediate is the Cu(I)(acac) fragment. Without complete protection by the acac ligand, this radical is very liable to react with surrounding oxygen, either on the surface or in the gas phase. Cu_2O is therefore the major product deposition in this temperature region. For deposition carried at temperatures above 380^oC, the remained acac ligands of $Cu(I)(acac)^{+1}$ radicals were also mostly dissociated, leaving primarily copper ions in the surface. If oxygen was used as the co-reactant, oxidation of copper is supposed to occur. CuO is the major product in that temperature region. If water vapor is used as the co-reactant, the H_2O vapor may provide the H atoms that acetylacetonyl ligands need to abstract and formed acetylacetone molecules. At the same time, the oxidation of

copper with water vapor might be of few chances. Cu metal film was deposited as discussed in paper I.

Evaluation of The Copper Oxide MOCVD Process

From the practical process aspect, due to its strong tendency of self reduction during decomposition, $Cu(acac)_2$ might not be a good precursor for depositing CuO film. Strong oxidation environment such as high temperature and high oxygen concentration are needed to deposit CuO film. During practical device processing, this processing condition can lead to some adverse effects to the deposited surface layer. From the milder deposition condition that Cu_2O MOCVD process required, $Cu(acac)_2$ might be a favorable precursor for depositing Cu_2O films. Because the cost of water vapor is much less than H_2, which is the primary chemical used in previous Cu MOCVD studies, the Cu MOCVD process, which used water vapor and $Cu(acac)_2$ as reactants, might have some practical advantages.

Recommendations for Future Work

The following areas are suggested for future studies:

1. To specify the oxidative decomposition process of $Cu(acac)_2$ in the MOCVD process, experiments should be performed to identify the origin of oxygen in the copper oxide film. One method is isotopic labelling technique. First, a specific concentration of $^{18}O_2$ will be dosed in the carrier gas stream during MOCVD process, which is operated in the standard condition yielding Cu_2O (or CuO). The deposited film can be analyzed by XRD to identify the composition. Then,

transmission IR will be used to reveal the IR band. The IR band position of Cu_2O depends on the masses of oscillating sublattices involved. If the gas phase $^{18}O_2$ reacted with $Cu(acac)_2$ and was incorporated into the copper oxide film, the IR band will shift to a lower wavenumber position, due to the higher mass of ^{18}O. If the IR band doesn't shift, it will suggest that the oxygen in copper oxide film is from the $Cu(acac)_2$ precursor.

2. To investigate the possible surface reaction in the MOCVD process, surface sensitive techniques such as infrared reflection-absorption spectroscopy (IRRAS) should be employed. The possible experiment topics can cover from the simplest one, the identification of surface oxidation states on MOCVD films by using IRRAS to study CO adsorption on MOCVD film, to the most complex but practical one, the investigation of surface reactions in the MOCVD system by using IRRAS to study in-situ MOCVD depositing substrate.

ADDITIONAL REFERENCES CITED

1. S.M. Sze, VLSI technology, p.1, McGraw-Hill book company, New York (1983)
2. S.K. Ghandhi, VLSI fabrication principles, p.2, McGraw-Hill book company, New York (1987)
3. J.W. Matthews, Epitaxial growth, p. 15, Academic press, New York (1980)
4. H.M. Manasevit, and W.I. Simpson, J. Electrochem. Soc., 12, 156 (1968)
5. G.B. Stringfellow, Reports on Progress in Physics, 45, 469 (1982)
6. C. Plass, H. Heinecke, and H. Luth, J. Cryst. Growth, 88, 455 (1988)
7. H. Krautle, and H. Beneking, J. Electron. Mater., 12, 215 (1983)
8. G.B. Stringfellow, Organometallic vapor-phase epitaxy: theory and practice, xii, Academic press, New York (1989)
9. W.M. Sears, and E. Fortin, Appl. Phys. Let., 64, 303 (1991)
10. O.B. Ajayi, M.S. Akanni, J.N. Lambi, Thin Solid Films, 185, 123 (1990)
11. A.B. Laurie and M.L. Norton, Mater. Res. Bull., 24, 2103 (1989)

12. H.R. Jen, M.J. Cherng, M.J. Jou, and G.B. Stringfellow, J. Cryst. Growth, 51, 2103 (1987)

13. H. Asai, J. Cryst. Growth, 80, 425 (1987)

14. K.E. Spear, J. Cryst. Growth, 82, 553 (1988)

15. C. Bernard, J. Cryst. Growth, 83, 127 (1988)

16. H.P. Vossen, J. Electrochem. Soc., 130, 675 (1983)

17. K.F. Jensen, and R.J. Jen, J. Electron. Mater., 17, 67 (1988)

18. K.F. Jensen, and R.J. Jen, J. Electochem. Soc., 130, 324 (1983)

19. (A) M.E. Bartram, T.A. Michalske, and T.M. Mayer, Chem. Mater., 3, 953 (1991); (B) N.H. Dryden, and P.R. Norton, Chem. Mater., 3, 667 (1991); (C) K. Inumaru, T. Okuhara, and M. Misono, J. Phys. Chem., 95, 4826 (1991)

20. K. Fujino, ,Y. Nishimoto, and K. Maeda, J. Electrochem. Soc., 138, 3727 (1991)

21. D.W. Shaw, and M.E. Jackson, J. Electochem. Soc., 115, 405 (1968)

22. D.W. Shaw, and B.G. Secrest, J. Cryst. Growth, 10, 251 (1971)

23. D.B. Beach, IBM. J. Res. Develop., 34, 795 (1990)

24. F.L. Brewer, and G.F. Raymond, J. Cryst. Growth, 87, 230 (1970)

25. H. Gillardeau and D.K. Johnson, Appl. Phys. Let.,14, 210 (1969)

26. V.G. Powell and M.N. Ryan, J.Electrochem. Soc., 32, 69 (1966)

27. Y.U. Zhang and C.E. Tracy, Appl. Phys. Let., 120, 4469 (1988)

28. K.E. Luo, P. R. Wall, and R.N. Duffitt, J. Cryst. Growth, 107, 242 (1990)

29. M.J. Underwood,,and F.K. Schwartz, Appl. Phys. Let., 119, 3032 (1990)

30. J.O. Carlsson, J. Electrochem. Soc. 132, 612 (1984)

31. D.N. Armtiage, N.I. Dunhill, R.H. West, and J.O. Williams, J. Cryst. Growth, 108, 683 (1991)

32. H. Holzschuh and H. Suhr, Appl. Phys., A 51, 486 (1990)

33. W. Kern, and R.K. Ban, J. Vac. Sci. Technol, 14, 32 (1972)

34. S.K. Ghandhi, and B.J. Baliga, J. Appl. Phys., 44, 990 (1973)

35. Y. K. Temple and G. L. Reisman, J..Electrochem. Soc., 138, 223 (1989)

36. A.D. Berry, R.T. Holm, M. Fatemiand, and D.K. Gaskill, J. Mater. Res., 5, 1169 (1990)

37. A. Combes, Ann. Chim., 12, 199, (1887)

38. K. Combes, Compt. Rend., 105, 869 (1887)

39. A. Werner, Ber. 34, 2584 (1901)

40. G.T. Morgan, and H.W. Moss, Proc. Chem. Soc., 29, 471 (1914)

41. A.N. Sarker, Phil. Mag., 2, 1153 (1926)

42. E.G. Cox and K.C. Webster, J.Chem. Soc., 126, 731 (1935)

43. A.E. Finn, G.C. Hampson, and L.E. Sutton, J. Chem. Soc., 129, 1255 (1938)

44. M. Calvin, and K.W. Wilson, J. Am. Chem. Soc., 67, 2003 (1945)

45. J.P. Collman, R.A. Moss, S.D. Goldby, and W.S. Trhanovsky, Chem. and Ind., 2, 1213 (1960)

46. G.T. Morgan, and H.W. Moss, J. Chem. Soc., 105, 189 (1914)

47. R.J. Irving, and M.A.V. Ribeiro da Silva, J. Chem. Soc. Dalton, 39, 798 (1975)

48. H.S. Jarrett, M.S. Sadler, and J.N. Shoolery, J. Chem. Phys., 21, 2092 (1953).

49. L.E. Marchi, Inorg. Synth., 2, 10 (1946)

50. H. Reihlen, R. Illing, and R. Wittig, Ber., 59, 1890 (1925)

51. C. Djordjevic, J. Lewis, and R.S. Nyholm, Chem. and Ind., 43, 122 (1959)

52. J.P. Collman, and E. T. Kittleman, Inorg. Chem., 1, 704 (1962)

53. J.P. Collman, R.A. Moss, H. Maltz, and C.C. Heindel, J. Am. Chem. Soc., 83, 531 (1961)

54. W.A. Pilskin, J Vac. Sci. Technol., 14, 1064 (1977)

55. W.J. Biermann, and H. Gesser, Anal. Chem. Soc., 32, 1525 (1960)

56. R. D. Hill, and H. Gesser, J. Gas Chromatography, 1, 11 (1963)

57. E. W. Berg, and J.T. Truemper, J. Phys. Chem., 64, 487 (1960)

58. (A) G. Beech, and R.M. Lintonbon, Thermochim. Acta. 3, 97 (1971) (B) S.J. Ashcroft, Thermochim. Acta, 2, 512 (1971) (C) J.P. Murry and J.O. Hill, Thermochim. Acta., 109, 383 (1987)

59. E. W. Berg, and J.T. Truemper, Anal. Chim. Acta., 32, 245 (1965)

60. R.A. Shulstad, Master's Thesis, Air Force Institute of Technology, Wright-Patterson Air Force Base, Ohio (1968)

ACKNOWLEDGMENTS

I would like to thank Professor Schrader for his guidance in this challenging area of research. His timely advice often provided the inspiration required to complete such an endeavor. I would also thank the NSF for providing me with personal financial support for the past years.

Additionally, I would like to thank the various coworkers that have put up with me over the past four years and ten months. I would like to thank Lucy, Mike, Jeff, Paul, Lu, Joe, and Kolan, for the funny good times. I am particularly indebted to Jef Cross for providing me good advice and keeping entropy production under control these last few months.

Behind all the research and technical work was a strong base on which my life has been built. I am forever indebted to my parents, Professor Ya-yun and Mrs. Chun-whai Chang for the support and encouragement they have given me these past five years.

Finally and most of all, I am proud of and give thanks to my friend Amanda. You help me gain the confidence I needed to achieve this and many other goals. Putting it simply, you are the best.